APPENDIX IX

MATES III

FINAL REPORT

Regional Modeling Analyses

Authors
Joe Cassmassi
Xinqiu Zhang
Satoru Mitsutomi
Sang-Mi Lee

Appendix IX
Regional Modeling Analyses

Introduction

The MATES III regional modeling analysis is presented in Chapter 4 of the main document. This Appendix provides the analyses to complement and support the regional modeling demonstration. These include: characterization and validation of the meteorological input data, development of the MATES III modeling emissions inventory, discussion of the development of the boundary conditions, model performance, and risk.

Several comments received from reviewers of the draft MATES III report were directed to the regional modeling analysis and evaluation. The key areas addressed follow:

- The need for a direct comparison between the regional modeling analyses generated for both MATES II and MATES III;
- The simulation performance of elemental carbon ($EC_{2.5}$) compared with observations measured during the MATES III monitoring program; and
- The adequacy of the comparison of simulated risk to risk calculated based on monitored data at the MATES III sites.

Several additional comments suggested modifications to the modeling assumptions including model configuration and specific emissions allocation. These included the following suggestions:

- Modify (increase) the number of layers in the model domain;
- Evaluate alternate methodologies to calculate vertical dispersion; and
- Review the emissions inventory, in particular the percentage apportionment of EC emissions released from ships.

The regional modeling analysis and evaluation presented in this report attempts to answer the key issues and suggestions identified through the review process. Most noteworthy, this Appendix presents a newly-generated recreation of the MATES II modeling analysis that is consistent in model application, inventory development and modeling assumptions to the MATES III analysis described in the following sections.

For MATES III, the Comprehensive Air Quality Model with Extensions enhanced with a reactive tracer modeling capability (CAMx RTRAC, Environ, 2006) provided the dispersion modeling platform and chemistry used to simulate annual impacts of both gaseous and aerosol toxic compounds in the Basin. The version of the RTRAC "probing tool" in CAMx used in the modeling simulations includes an air toxics chemistry module that is used to treat the formation and destruction of reactive air toxic compounds.

Modeling was conducted on a domain that encompassed the Basin and the coastal shipping lanes located in the Southern California Bight portions of the Basin using a grid size of two-squared kilometers. An updated version of the 2007 AQMP emissions inventory for model year 2005, which included detailed source profiles of air toxic sources, provided mobile and stationary source input for the MATES III CAMx RTRAC simulations. An additional back-cast of the 2007 AQMP emissions inventory was generated for 1998 to project emissions for use in the new simulation covering the MATES II monitoring period.

Grid-based, hourly meteorological fields generated from the MM5 (PSU/NCAR 2004) mesoscale meteorological model using four dimensional data assimilation, and National Weather Service model initializations for April 1998 through March 1999 and all days in 2005 provided the dispersion profile for the simulations.

Background

MATES III regional modeling analyses relied on the CAMx RTRAC model to simulate annual impacts of both gaseous and aerosol toxic compounds in the Basin. In the 2000 MATES II analysis, the Urban Airshed Model with TOX (UAMTOX) chemistry was used to simulate the advection and accumulation of toxic compound emissions throughout the Basin. UAMTOX was simulated for a two-squared kilometer grid domain that overlaid the Basin. The analysis relies on the 1997-98 emissions projection from the 1997 AQMP and meteorological data fields for 1997-98 generated from objective analysis using a diagnostic wind model. These tools were consistent with those used in both the 1997 and 2003 AQMP attainment demonstrations.

Peer review of the 2003 AQMP modeling strongly suggested that future AQMP attainment demonstrations utilize more state-of-the-sciences tools that utilize updated chemistry modules, improved dispersion algorithms, and mass consistent meteorological data. The recommendations were placed in action for the 2007 AQMP where the dispersion platform moved from UAM to CAMx and the diagnostic wind meteorological model was replaced by MM5 prognostic model. CAMx coupled with MM5 input using the “one atmosphere” gaseous and particulate chemistry was used to simulate both episodic ozone and annual concentrations of $PM_{2.5}$..

The original plan for MATES III was to replicate the analysis conducted for the 1998-99 field program using the UAMTOX model and diagnostic meteorological model. The theory was to enable a true apples-to-apples comparison of the current and previous modeling analyses. The plan was modified prior to adoption of the 2007 AQMP to take into account the advances in annual particulate modeling that was conducted as part of the 2007 $PM_{2.5}$ attainment demonstration. Given the extensive effort in the 2007 AQMP to simulate particulates, using the peer recommended state-of-the-science art modeling tools, it was decided that a better comparison linking the AQMP $PM_{2.5}$ projections to the base year toxics analysis would be more complementary and up-to-date. As such, the MATES III simulations were conducted using the CAMx – MM5 coupled with the RTRAC chemistry.

CAMx Modeling Domain

Modeling was conducted on a domain that encompassed the South Coast Air Basin and the coastal shipping lanes located in the Southern California Bight portions of the Basin using a grid size of two-squared kilometers. (Figure IX-1 depicts the MATES III modeling domain. The shaded portion of the grid area represents the extension of the domain beyond that used for MATES II). Concentrations simulated for a specific location in the domain consisted of nine-cell distance weighted average.

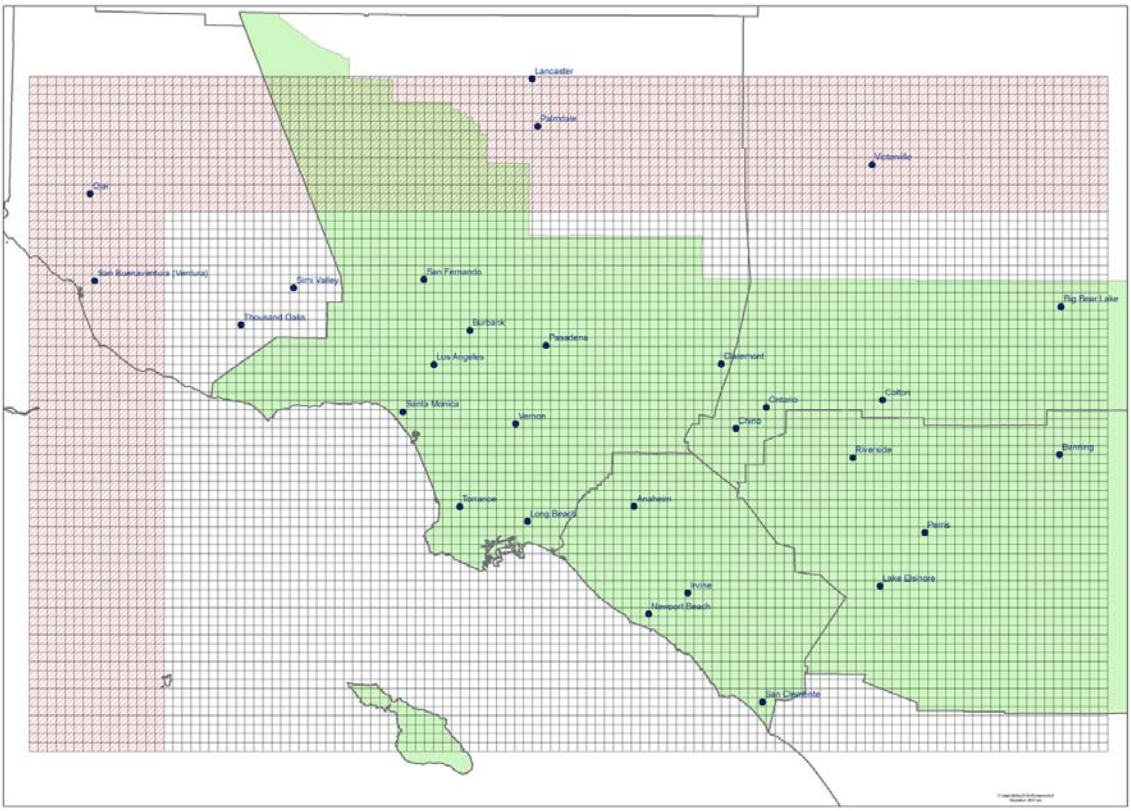

Figure IX-1
MATES III Modeling Domain
(Shaded area highlights the grid extension to the MATES II modeling domain).

Development of Meteorological Fields

The Penn State/National Center for Atmospheric Research Mesoscale Model 5 (MM5) was employed to produce meteorological fields for the CAMx RTRAC 2005 MATES III and 1998-99 back-cast of the MATES II regional modeling analyses.

MATES III air monitoring spanned a three-year calendar period from April 2004 through March of 2006. The regional toxic modeling analysis was conducted for data sampled during the one-year period including January 1, through December 31, 2005. The MATES II monitoring period included April 1, 1998 through March 31, 1999.

Meteorological Outlook of Year 2005

The beginning of year 2005 was characterized as anomalously above-average precipitation in Southern California. A pronounced split-flow configuration was evident over western North America, with one branch of the westerlies entering the continent over northern British Columbia and the other entering over the Baja Peninsula. These conditions were associated with a southward shift of the main jet stream and storm track across the western United States. These resulted in significantly above-average precipitation in Southern California, Southwest, and the western inter-mountain regions of the U.S. Southern California experienced above-average precipitation during the period of October 2004 to May 2005. During summer months – July and August, 500 hectopascal (hPa) geopotential heights were above-average level over the western U.S., which led to well above-average temperatures in the area, which was situated beneath a very persistent upper-level ridge. Fall and winter months returned close to climatology when North America generally experienced below average precipitation in the west and above average rainfall in the southeastern U.S.

When comparing the meteorology between 2005 to the MATES II monitoring period of April 1998-March 1999, two issues stand out. The MATES II period was drier than MATES III but over the course of the period experienced less stagnation. Using a statistical analysis developed for the 1997 AQMP that evaluates pollution dispersion potential based on the presence and strength of temperature inversions, 2005 was very close to average despite having greater rainfall than 1998-99. Using the same measure, 1998-1999 was slightly above average for dispersion potential but experienced a milder winter with less storm activity. This is borne out through Basin statistics of measurable rainfall, where 2005 experienced a greater frequency of days having measurable rainfall in Downtown Los Angeles by 30% (43 versus 33 days) and total rainfall measured at USC by 182% (26.0 versus 14.1 inches). The additional rainfall may have suppressed the amount of re-entrained or fugitive dust that contributes to concentration measurements of EC.

MM5 Numerical Model Configuration

Penn State/National Center for Atmospheric Research Mesoscale Model 5 (MM5) was employed to produce meteorological fields for CAMx RTRAC simulations. The MM5 simulations were comprised of three nested domains of which horizontal grid distances of 18, 6, and 2 km respectively. The relative sizes and locations of each domain are given in Figure IX-2. The innermost domain spans 254 km X 164 km in east-west and north-south directions, respectively, which overlaps the CAMx domain by two additional rows and columns in each lateral boundary. The initial guess field and lateral boundary values for the outermost domain were extracted from the operational NCEP Eta 218 grid (12km) grid analysis for the 2005 simulations and the 212 grid (40 km) analysis output for the 1998-99 simulation. Figure IX-3 depicts the grid specific terrain file used in the MM5 simulations.

The databases contain variables of air temperature, geopotential height, heat flux, humidity, precipitable water, sea level pressure, shortwave radiation, snow water equivalent, surface air temperature, surface winds, thermal infrared, upper level winds, vertical wind, and vorticity at each isobaric level of 1000, 975, 950, 925, 900, 875, 850, 800, 750, 700, 650, 600, 550, 500, 450, 400, 350, 300, 275, 250, 225, 200, 175, 150, 100, 50 hPa. (Refer to http://dss.ucar.edu/datasets/ds609.2 for further dataset information).

Four dimensional data assimilation (FDDA) was conducted by utilizing National Weather Service (NWS) twice-daily sounding data and hourly surface measurements taken within the domain. Each simulation was conducted for a 6-day period with the first 24 hours of spin up period. The detailed configuration and physical options used in the MM5 simulation are listed in Table IX-1.

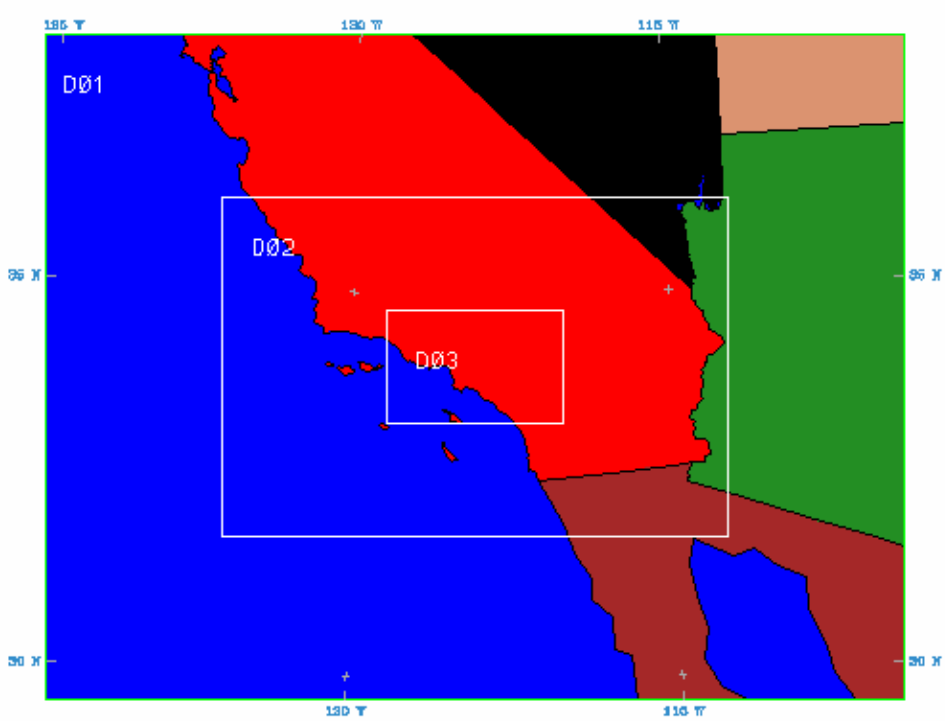

Figure IX-2.
The relative locations and sizes of three MM5 nested domains.

Table IX-1
MM5 configuration

Component	2005	1998-99
Number of grids	(127 X 82) in east-west and north-south respectively	(127 X 82) in east-west and north-south respectively
Number of vertical layers	29 layers with the lowest layer being approximately at 20 m agl.	29 layers with the lowest layer being approximately at 20 m agl.
Initial and boundary values	ETA 218 grid (12 km grid distance) analysis field	Eta 212 grid (40 kim grid distance) analysis field
Boundary layer scheme	Blackadar	Blackadar
Soil model	Five-layer soil model	Five-layer soil model
Cumulus parameterization	Explicit	Explicit
Micro physics	Simple ice	Simple ice
Radiation	Cloud radiation	Cloud radiation
Four dimensional data analysis	Analysis nudging with NWS surface and upper air measurements	Analysis nudging with NWS surface and upper air measurements

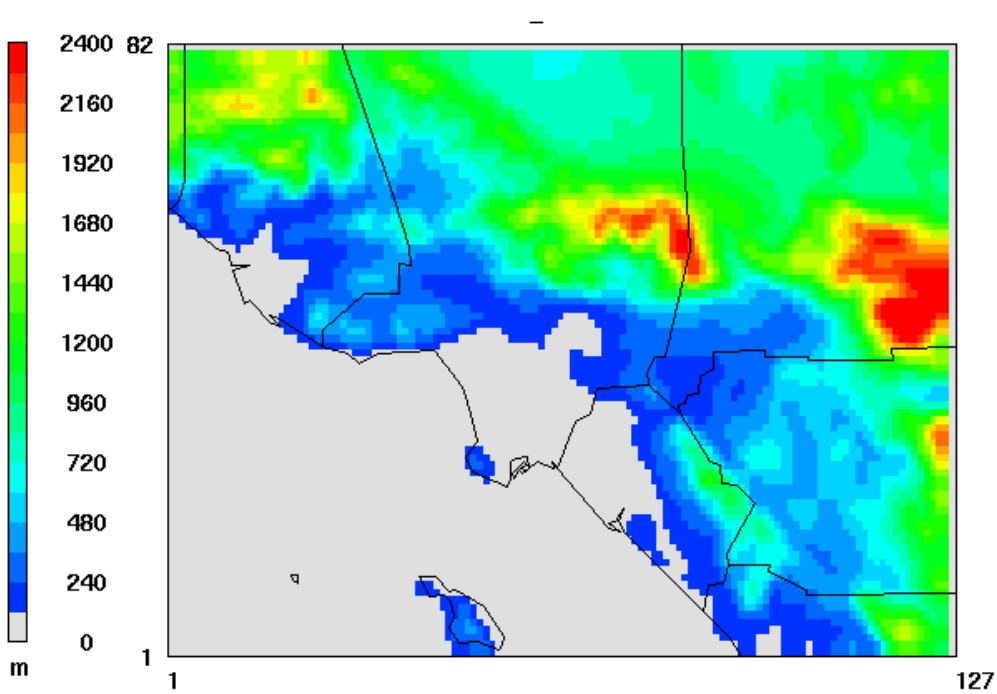

Figure IX-3
The topography and the county boundaries of the MM5 computational domain.

Meteorological Model Performance

The MM5 performance was extensively evaluated using NWS surface measurements and Environ's METSTAT (ENVIRON, 2001) statistical software to compute mean, bias, gross error, root mean square error (RMSE), and index of agreement.

Figure IX-4 shows the time series of hourly observed and predicted temperature at 2 m above ground level (agl) for September 2005. The model successfully resolved overall cooling and warming trend induced by synoptic scale motions, while daily maximum and minimum temperatures were slightly over and underpredicted, respectively. This can be partly attributed to inaccurate representation of surface characteristics such as soil moisture content and land use category.

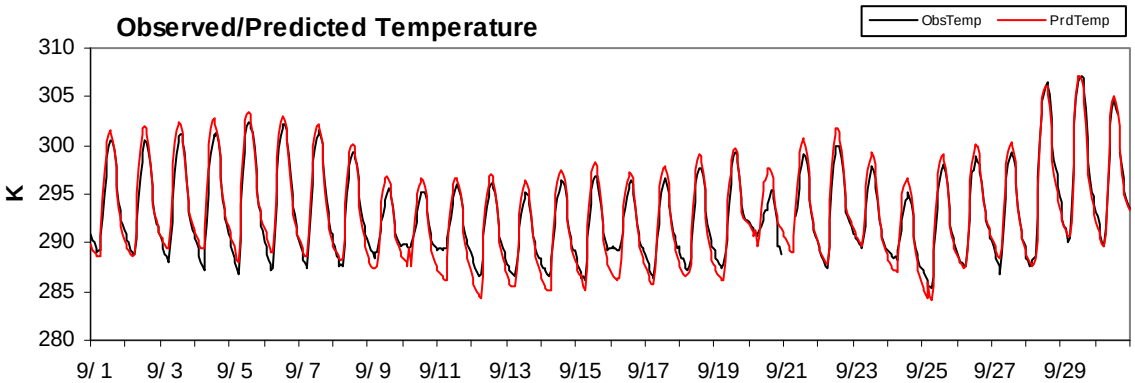

FIGURE IX-4

Time series of observed and predicted temperature at 2 m above ground level for September, 2005. The data are hourly average observations of all available measurements within the domain and the corresponding predictions.

In all, the model has less than 2 degrees of bias and gross error and approximately 2 degrees of RMSE, which are approximately equivalent to MM5 performance for 2007 Air Quality Management Plan (AQMP) modeling case (Figure IX-5). Wind speed turned out to be under-predicted by less than 1 m s^{-1}. In general, all conventional surface parameters including wind speed, direction, temperature and water vapor mixing ratio showed good agreement with the observations (Figures IX-6 and IX-7).

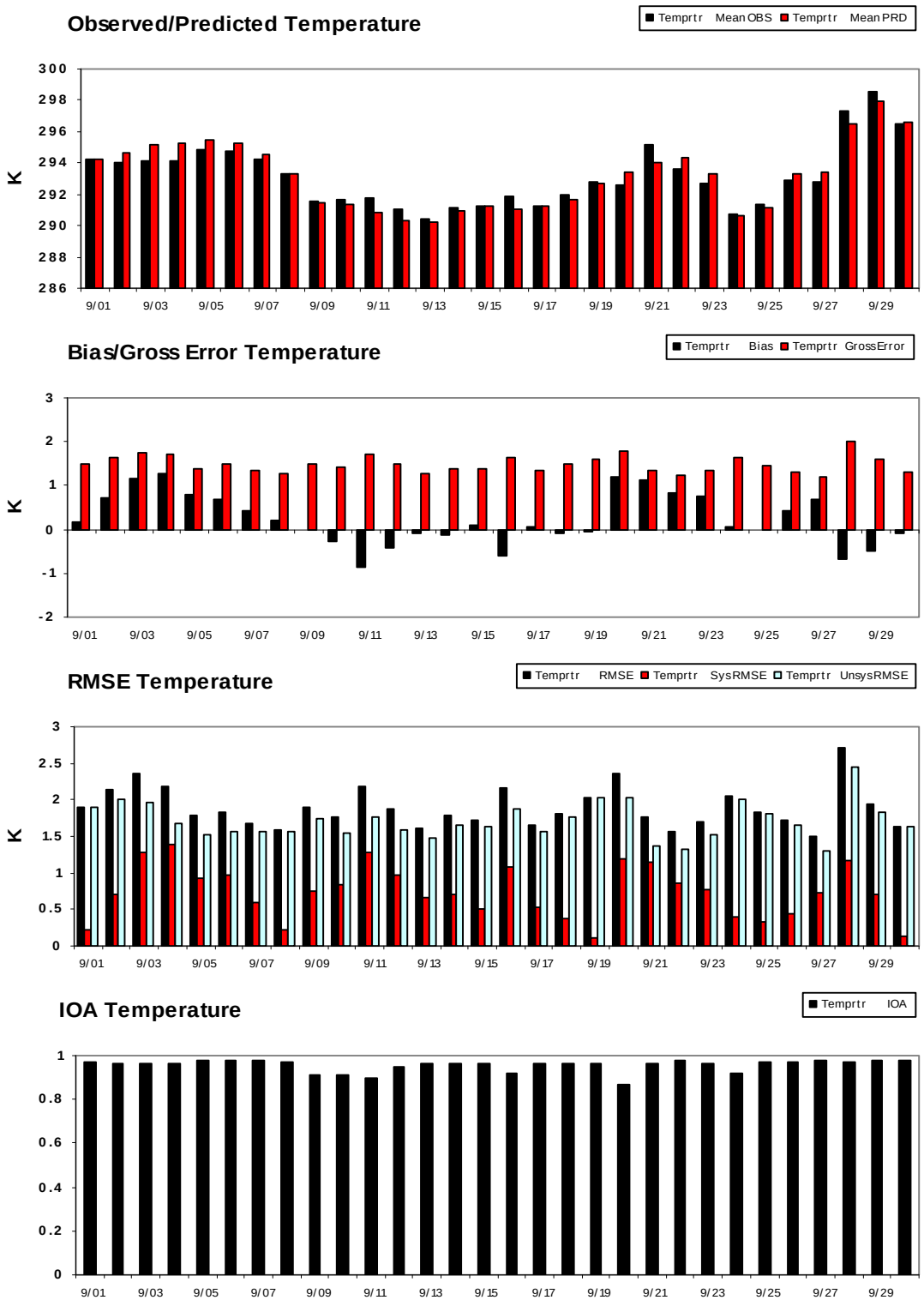

Figure IX-5

Daily averaged (a) mean, (b) bias and gross error, (c) root mean square error, and (d) index of agreement for observed and predicted temperature at 2 m agl.

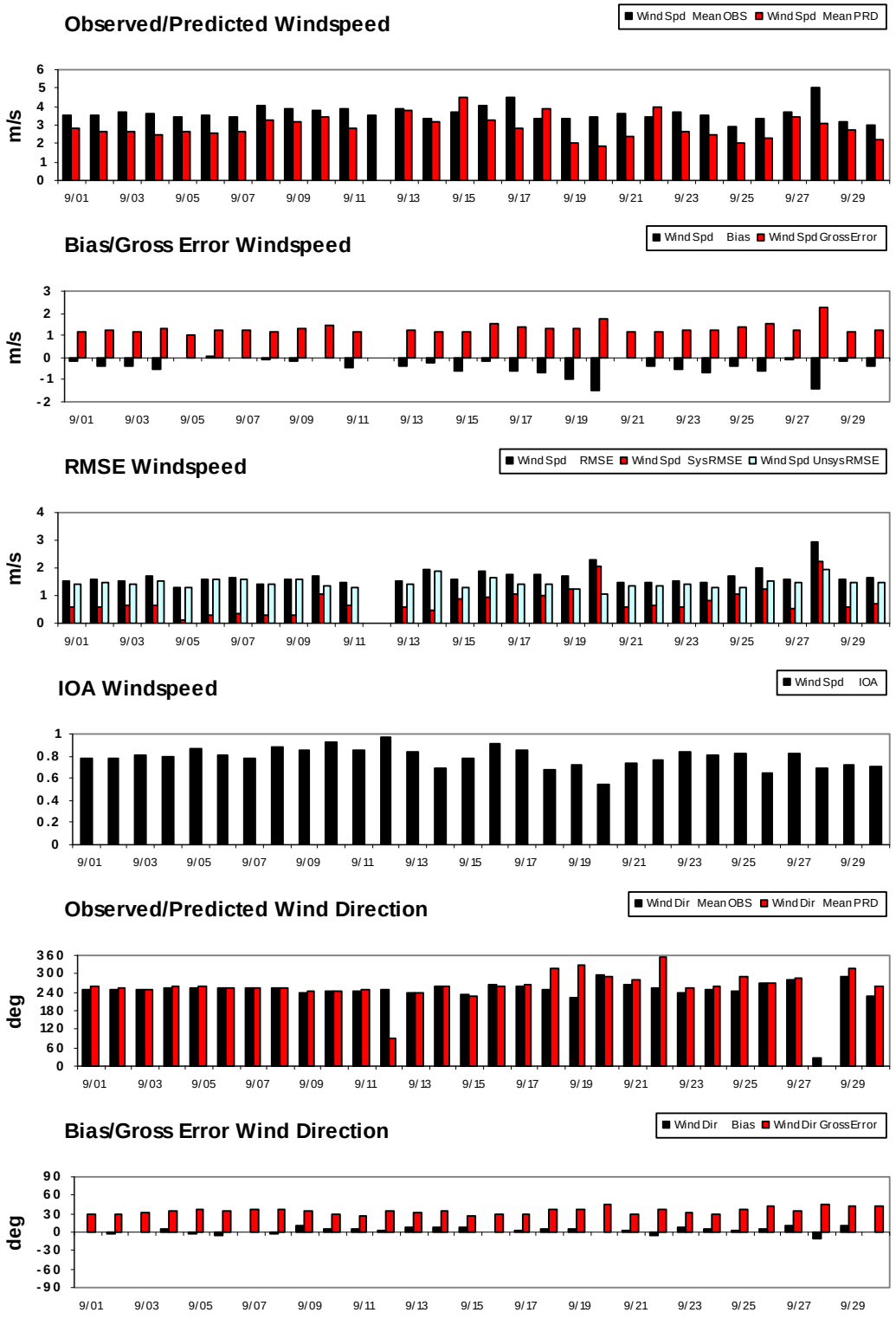

Figure IX-6

Daily averaged (a) mean, (b) bias and gross error, (c) root mean square error, and (d) index of agreement for observed and predicted wind speed. (e) Mean and (f) bias and gross error of wind direction are presented as well.

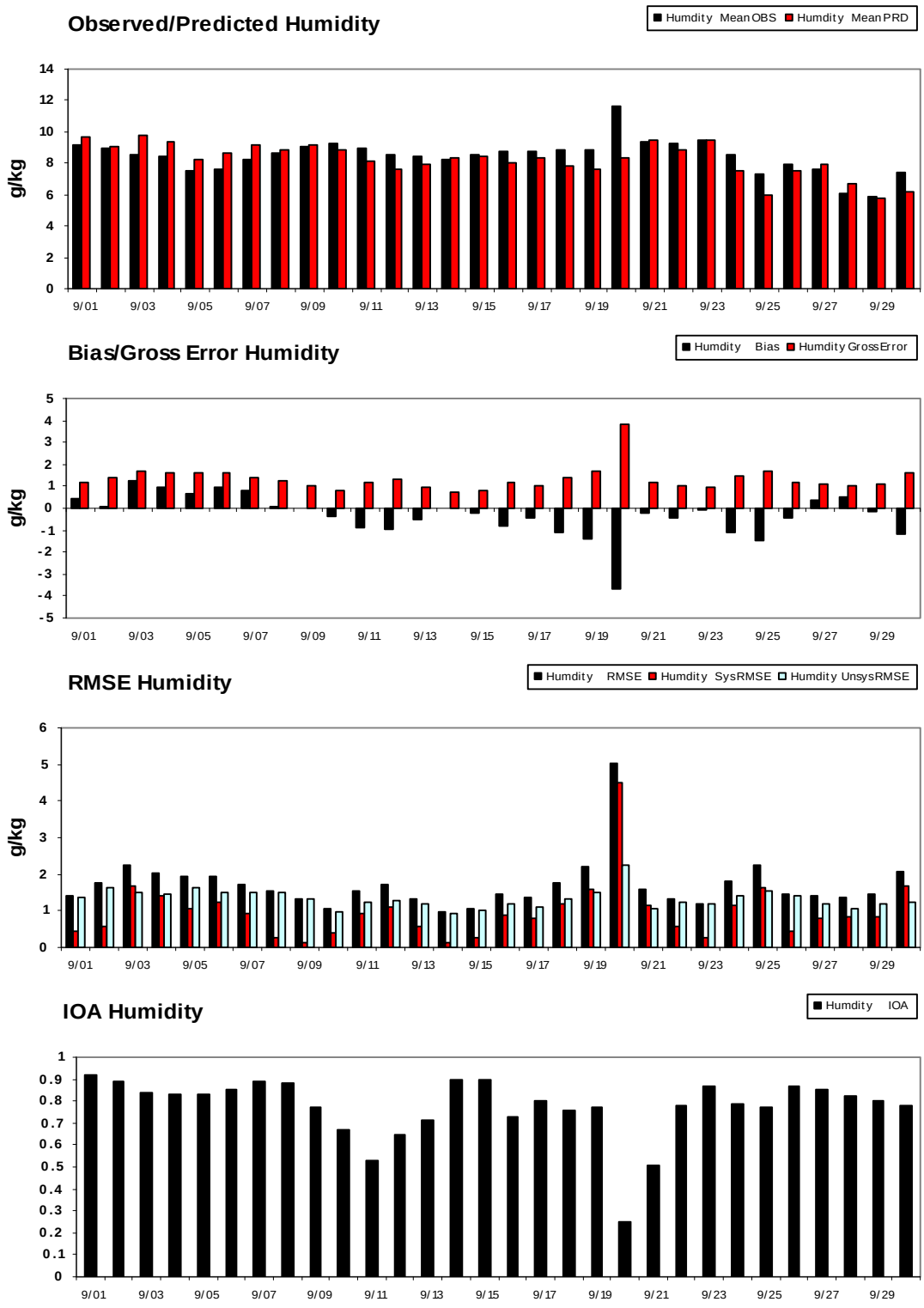

Figure IX-7

Daily averaged (a) mean, (b) bias and gross error, (c) root mean square error, and (d) index of agreement for observed and predicted wind speed. (e) Mean and (f) bias and gross error of wind direction are presented as well.

Wind Rose Comparison

While the METSTAT evaluation is a useful tool to assess the performance of the regional MM5 simulations, it is important to examine the capability to recreate observed annual local scale wind patterns. To assess the local scale flow, wind roses were generated from the hourly average 2005 MM5 model output for the 2 km-squared grid cell housing the MATES III monitoring sites and the monitoring data for those sites. An exact replication of the measured winds was not expected in the analysis. However, comparison of the modeled and measured annual average wind roses offers a visual comparison of the fit of the simulation to the local scale and assists in the evaluation of the CAMx RTRAC simulation performance.

Figures IX-8a through IX-8f depict the 2005 annual wind roses for Anaheim, Burbank, Inland Valley San Bernardino, North Long Beach, Central Los Angeles, and Rubidoux. (Figure IX-9 provides the 2005 MM5 generated wind roses for Compton and West Long Beach). Subtle nuances between the simulated and observed winds are observed at all stations. In general, wind speeds are slightly higher for the MM5 simulation. The directional frequencies are reasonably well-captured at most sites, with an offset in the primary wind vector of less than one sector (22.5 degrees). It is important to note that the local emissions sources (particularly ground level) directly upwind of the monitoring site have a significant impact to the measured concentration profile. As such, a minor one-sector difference in the simulated wind direction may impact the CAMx RTRAC performance. This is the case at Burbank, where the simulated winds are offset from the observed winds to the south by more than 45 degrees.

The Burbank monitoring station is located in the southeast corner of the San Fernando Valley. The thermally forced sea breeze that drives into the San Fernando Valley is channeled by the unique terrain features which cause the flow to back almost 90 degrees from a southwesterly trajectory in the coastal plain to south easterly at the monitoring station. While the MM5 simulation accomplishes the element of backing the wind flow in the Burbank area, the simulation is currently not capable of reversing the flow to the degree observed. As discussed in a following section, this feature does have an impact on the CAMx RTRAC simulation performance at Burbank. (Ongoing sensitivity analyses are currently being conducted to evaluate the MM5 simulation sensitivity to improved local land use and soil moisture characterization to overcome this shortfall. The results of these sensitivity analyses will be incorporated in future simulations).

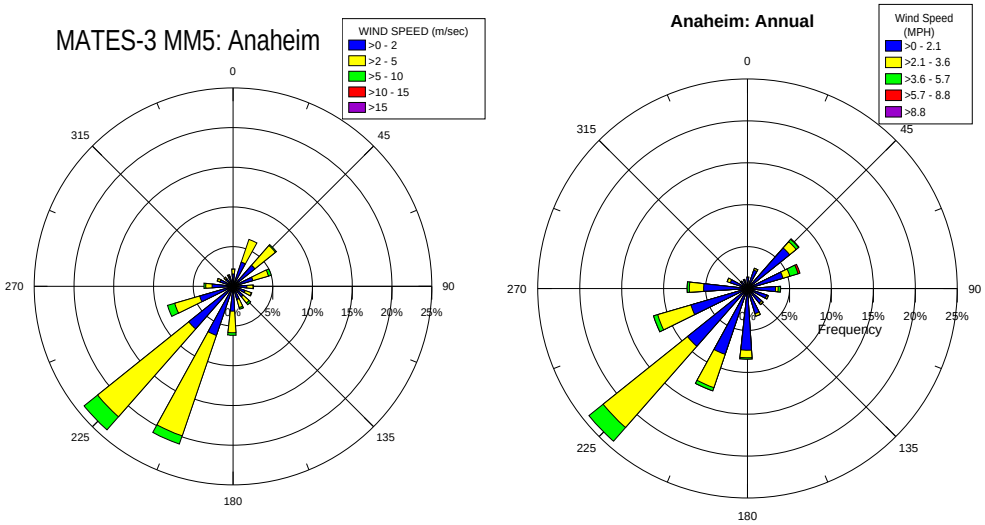

Figure IX-8a.
2005 MM5 Simulated and Observed Annual Hourly Averaged Wind Roses at Anaheim.

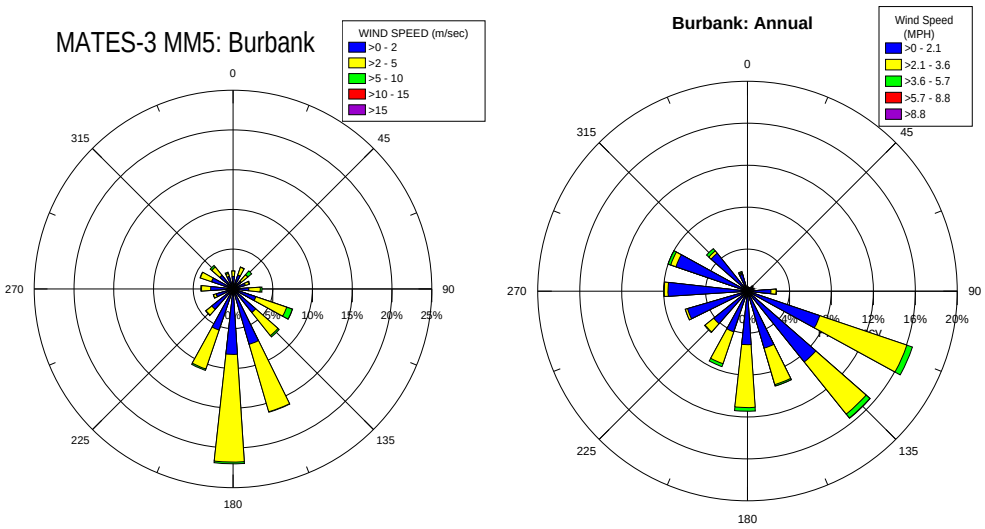

Figure IX-8b.
2005 MM5 Simulated and Observed Annual Hourly Averaged Wind Roses at Burbank.

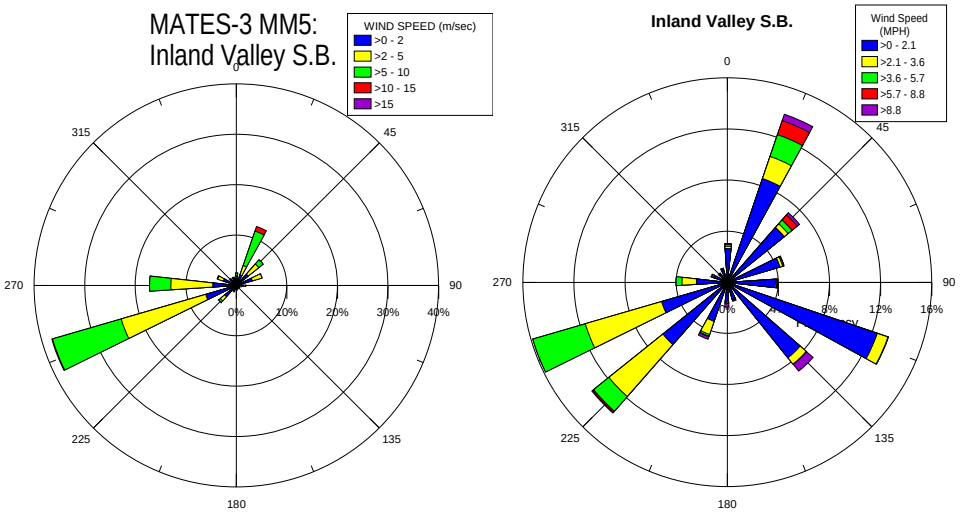

Figure IX-8c.
2005 MM5 Simulated and Observed Annual Hourly Averaged Wind Roses at Inland Valley S.B.

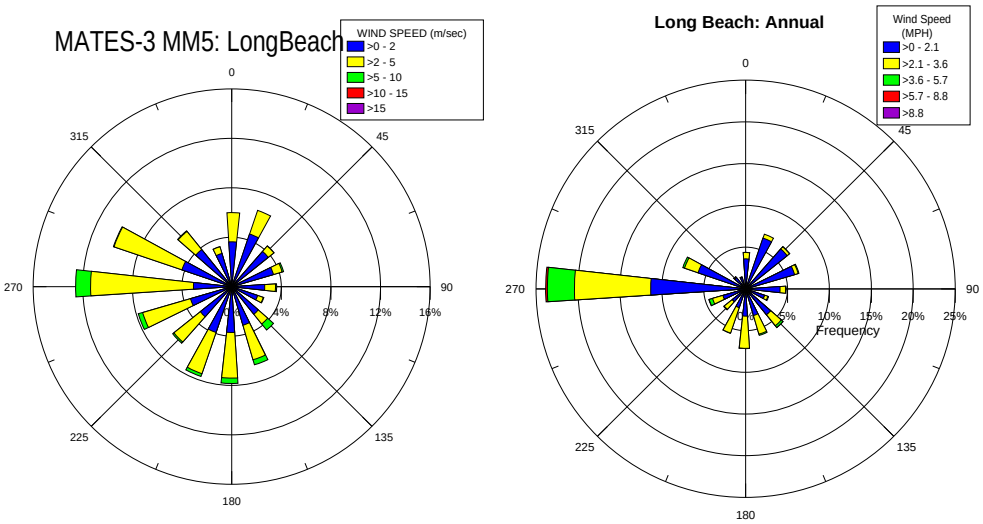

Figure IX-8d.
2005 MM5 Simulated and Observed Annual Hourly Averaged Wind Roses at North Long Beach.

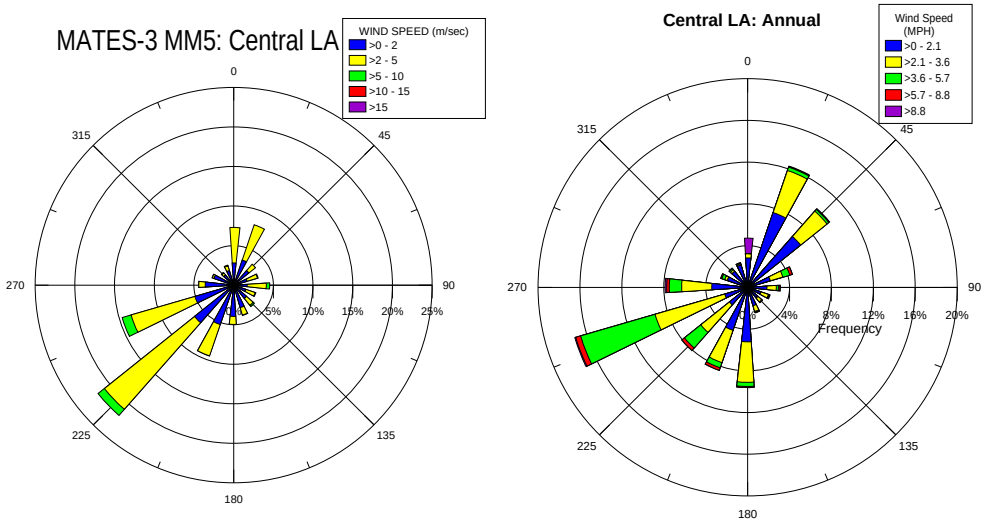

Figure IX-8e.
2005 MM5 Simulated and Observed Annual Hourly Averaged Wind Roses at Central Los Angeles.

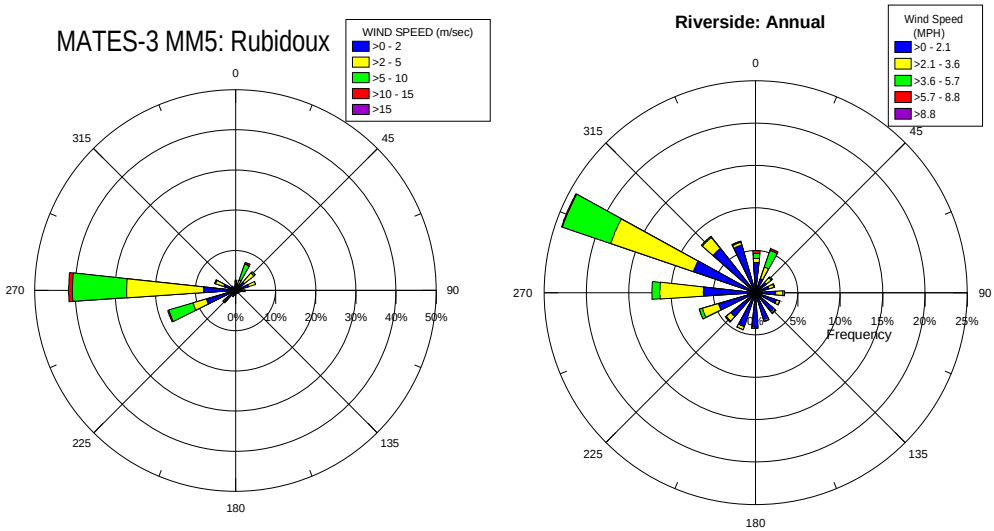

Figure IX-8f.
2005 MM5 Simulated and Observed Annual Hourly Averaged Wind Roses at Rubidoux.

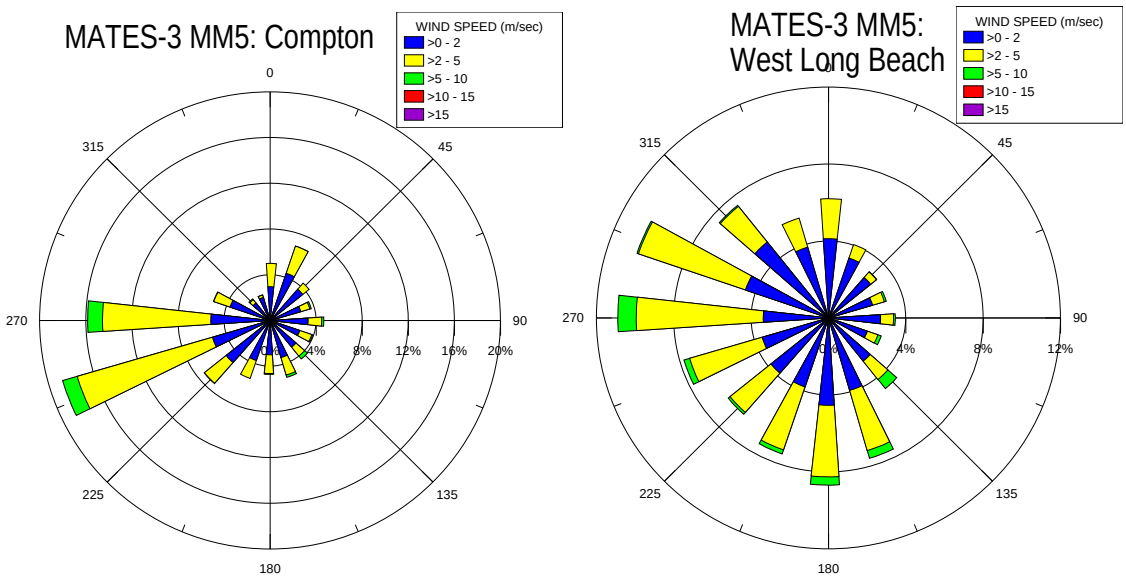

Figure IX-9.
2005 MM5 Simulated Annual Hourly Averaged Wind Roses at Compton and West Long Beach.

Vertical Dispersion

The initial CAMx RTRAC simulations were conducted using a vertical structure of eight layers, the CMAQ vertical stability parameterization, and a minimum value for vertical diffusivity (KV) of 1.0 m^2/sec. In the development phase of the meteorological data sets, the MM5 output was subjected to a variety of combinations of mixing schemes (CMAQ and the O'Brien 70 [OB70], O'Brien, 1970) using varying default minimum values of vertical diffusivity. The analysis evaluated CAMx RTRAC performance for $EC_{2.5}$ for both an eight and 16 vertical layer modeling structure. (Note: the MM5 simulations were conducted using a 29 layer vertical structure).

CAMx RTRAC $EC_{2.5}$ simulation performance was nearly identical for both layer structures using the CMAQ dispersion option using a minimum KV of 1.0 m^2/sec. The OB70 scheme resulted in overprediction at key sites (both layer structures) as did the CMAQ scheme using 16 layers and a minimum KV of 0.1 m^2/sec. All of the combinations, regardless of layer structure or minimum KV, resulted in overprediction at Long Beach and West Long Beach and underprediction to varying degrees at Rubidoux and Inland Valley San Bernardino. Since there was little difference between CMAQ dispersion option using a minimum KV of 1.0 m^2/sec for either the eight or 16 layer structures, the eight-layer structure using the CMAQ scheme and a minimum KV of 1.0 m^2/sec was selected to reduce computational demand.

Comments received from reviewers after release of the draft MATES III analysis focused on the underprediction of $EC_{2.5}$ in the eastern portion of the Basin. Additional sensitivity simulations using ENVIRON's KV-Patch software (Environ, 2006) were conducted to attempt to improve the simulation performance. Briefly, KV-Patch was used to assign a minimum value of KV (0.1

m^2/sec) to individual grid cells based on land use specification. The results of the application are summarized in Table IX-2 where the simulation performance is presented as a ratio of the observed $EC_{2.5}$ concentration measurement at each monitoring site.

The eight-layer simulation using the KV-Patch option and a minimum 0.1 m^2/sec value of KV labeled as interim improved the model performance in the east Basin while only having a nominal impact on the performance in the coastal zone. The 16-layer simulation using a 0.1 m^2/sec value of KV also resulted in improved performance in the east Basin but at the degradation of performance in the coastal plain. As a result of the additional sensitivity analyses, the vertical dispersion profile used in the final MATES III CAMx RTRAC simulations relied on an eight-layer structure using the CMAQ scheme overlaid with the KV-Patch option set at 0.1 m^2/sec value of KV.

MATES III Modeling Emissions

An updated version of the 2007 AQMP emissions inventory for model year 2005, which included detailed source profiles of AB2588 air toxic sources, provided mobile and stationary source input for the MATES III CAMx RTRAC simulations. Mobile source emissions were adjusted for time-of-day and day-of-week travel patterns based on CalTrans weigh-in-motion data profiles. Table IX-3 lists the January weekday daily diesel emissions projected for 2005 and back-cast for 1998. (A comprehensive breakdown of the planning VOC, NOx, CO, SO_2 and particulate emissions for 2005 used in the MATES III simulation is provided in Chapter 3 and Appendix XIII). Table IX-3 also includes the MATES II TSP diesel emissions for 1998 for comparison.

A comparison of the MATES III (2007 AQMP) 2005 projection of the weekday $PM_{2.5}$ diesel emissions shows a 4.8% reduction in emissions from the back-cast for 1998. The most significant area of diesel particulate matter emissions growth occurs in the shipping categories associated with goods movement. MATES III back-casts of the weekday 1998 TSP diesel inventory using the 2007 AQMP inventory were almost 21% higher than the corresponding MATES II values.

Figures IX-10a through IX-10x provides the grid based weekday modeling emissions for selected toxic pollutant and precursor emissions categories.

MATES III vs. MATES II: Key Emissions Modeling Assumptions

Three changes to emissions data preparation were implemented in the MATES III modeling. First, emissions from vessels in the shipping lanes were assumed emitted into the first two vertical modeling layers to better estimate plume rise from the hot stack emissions. Combined stack heights and plume rise for typical oceangoing (deep draft) vessels extend above 36 and below 73 meters (WRAP, 2007). MATES II held shipping emissions in the first vertical UAM layer.

TABLE IX-2

Simulated Annual Average $EC_{2.5}$ Using Selected Vertical Dispersion Profiles and Layer Structures

Dispersion Scheme	CMAQ						O'Brien 70			
Option/Location	Observed	Draft	Interim	Test	Test	Test	Test	Test	Test	Test
Layer Structure	Surface	8	8	16	16	16	8	8	16	16
Minimum KV (m^2/sec)	N/A	1.0	0.1	1.0	0.1	0.1	0.1	0.1	0.1	0.1
KV-Patch Used	N/A	No	Yes	No	No	Yes	Yes	No	No	Yes
Anaheim	1.00	1.03	1.07	1.01	1.57	1.10	1.21	1.77	1.66	1.24
Burbank	1.00	0.53	0.54	0.54	0.73	0.57	0.61	0.78	0.81	0.63
Compton	1.00	1.12	1.15	1.10	1.76	1.18	1.29	1.97	1.81	1.32
Inland Valley S.B.	1.00	0.72	0.88	0.73	1.12	0.88	1.00	1.28	1.17	0.98
Huntington Park	1.00	0.94	0.96	0.92	1.44	0.98	1.07	1.62	1.47	1.08
North Long Beach	1.00	1.42	1.47	1.41	2.13	1.51	1.63	2.38	2.17	1.67
Central Los Angeles	1.00	1.09	1.11	1.06	1.59	1.12	1.26	1.83	1.69	1.25
Pico Rivera	1.00	0.76	0.85	0.77	1.21	0.89	0.95	1.33	1.28	0.97
Rubidoux	1.00	0.60	0.84	0.64	0.98	0.89	0.93	1.00	1.02	0.94
West Long Beach	1.00	1.22	1.26	1.17	1.61	1.26	1.38	1.82	1.60	1.36

Table IX-3

January Weekday MATES III Diesel/EC Modeling Emissions (TPD)

Compound	MATES III				MATES II	
	2005		1998 (Back-cast)		1998	
	$PM_{2.5}$	TSP	$PM_{2.5}$	TSP	$PM_{2.5}$	TSP
Total Diesel	26.19	28.47	27.42	29.81	N/A	23.56
EC	14.12	18.9	14.68	19.89	N/A	25.87
DPM						
On-road	9.52	10.35	10.81	11.35	N/A	11.95
Off-road	11.02	11.97	12.29	11.36	N/A	8.08
Ships	4.28	4.65	2.75	2.99	N/A	2.59
Trains	0.86	0.94	0.79	0.86	N/A	0.53
Stationary	0.51	0.55	0.78	0.85	N/A	0.41

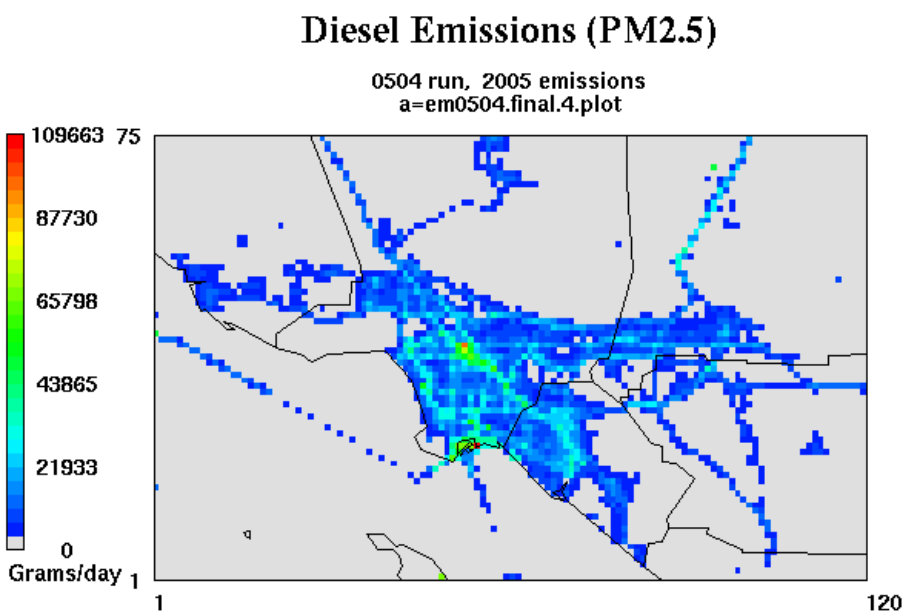

FIGURE IX-10a
Weekday average emissions pattern for Total Diesel $PM_{2.5}$.

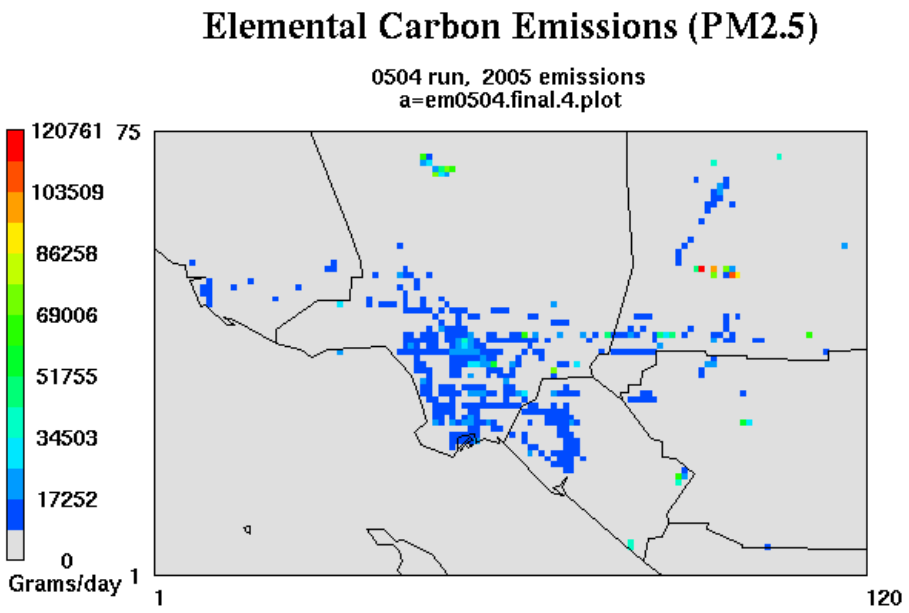

FIGURE IX-10b
Weekday average emissions pattern for Elemental Carbon.

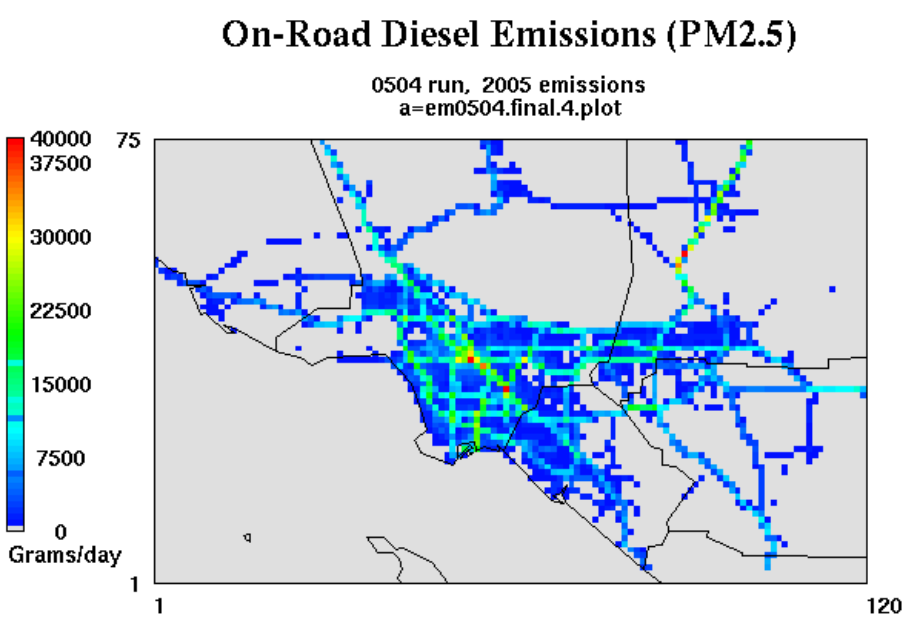

FIGURE IX-10c
Weekday average emissions pattern for On-Road Diesel $PM_{2.5}$.

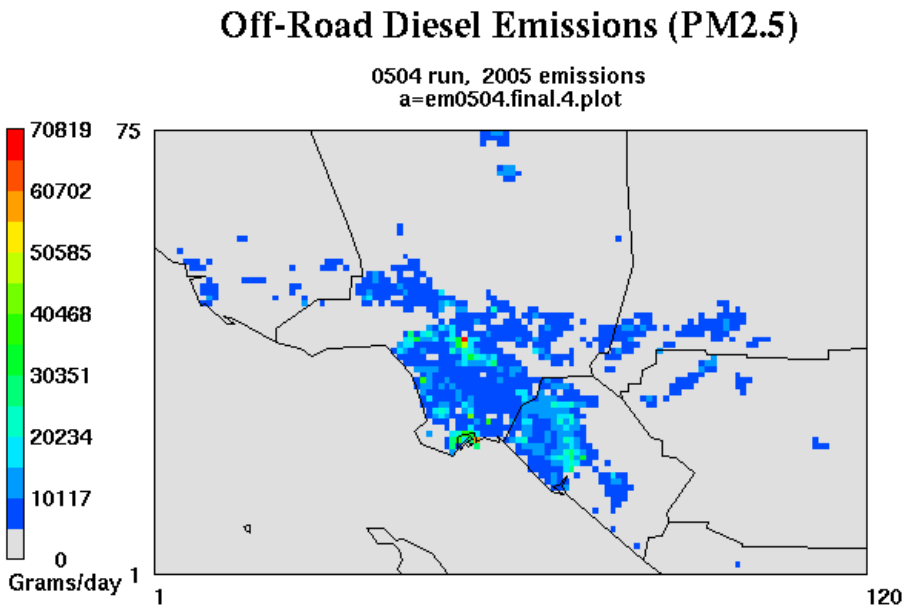

FIGURE IX-10d
Weekday average emissions pattern for Off-Road Diesel $PM_{2.5}$.

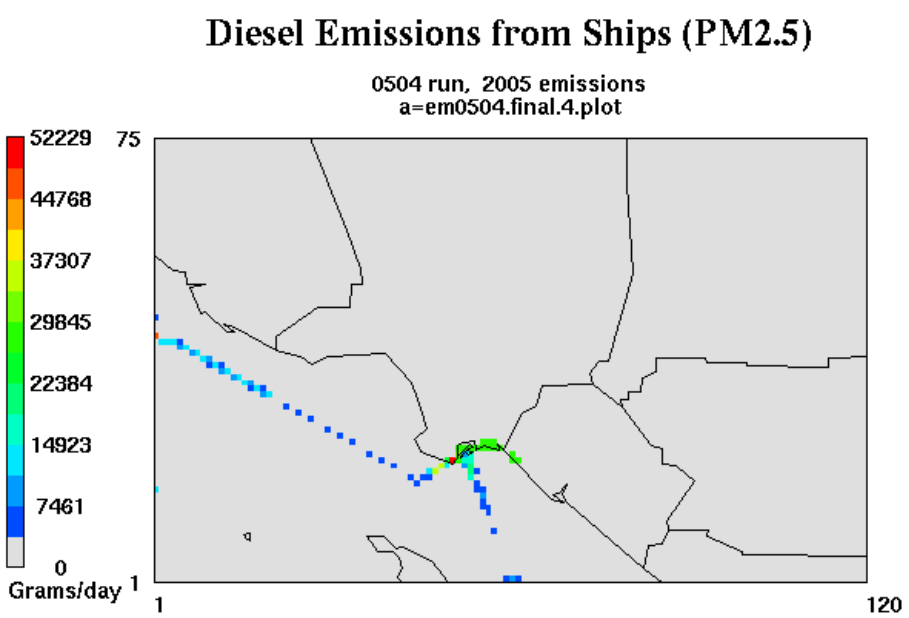

FIGURE IX-10e
Weekday average emissions pattern Diesel $PM_{2.5}$ from Ships.

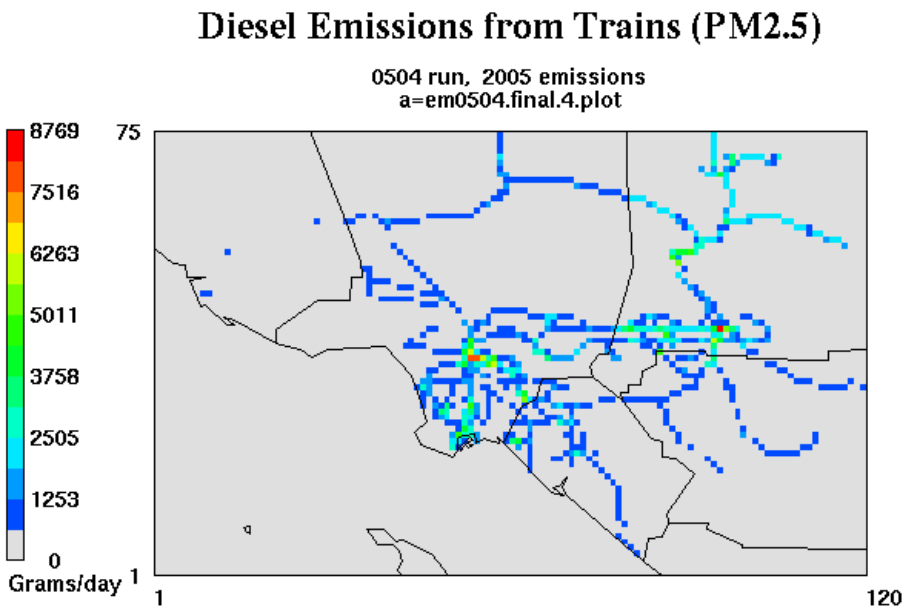

FIGURE IX-10f
Weekday average emissions pattern Diesel $PM_{2.5}$ from Trains.

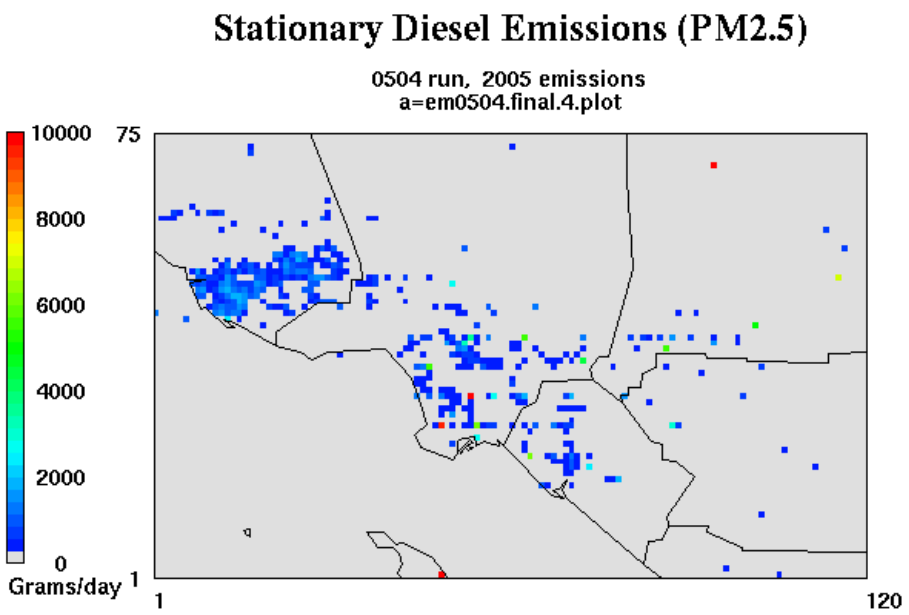

FIGURE IX-10g
Weekday average emissions pattern Diesel $PM_{2.5}$ from Stationary Sources.

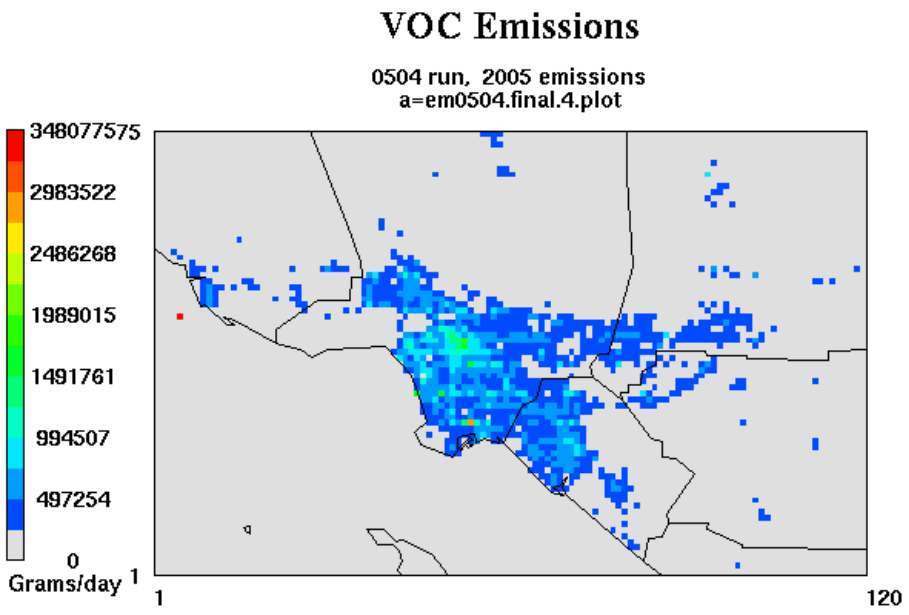

FIGURE IX-10h
Weekday average VOC emissions pattern.

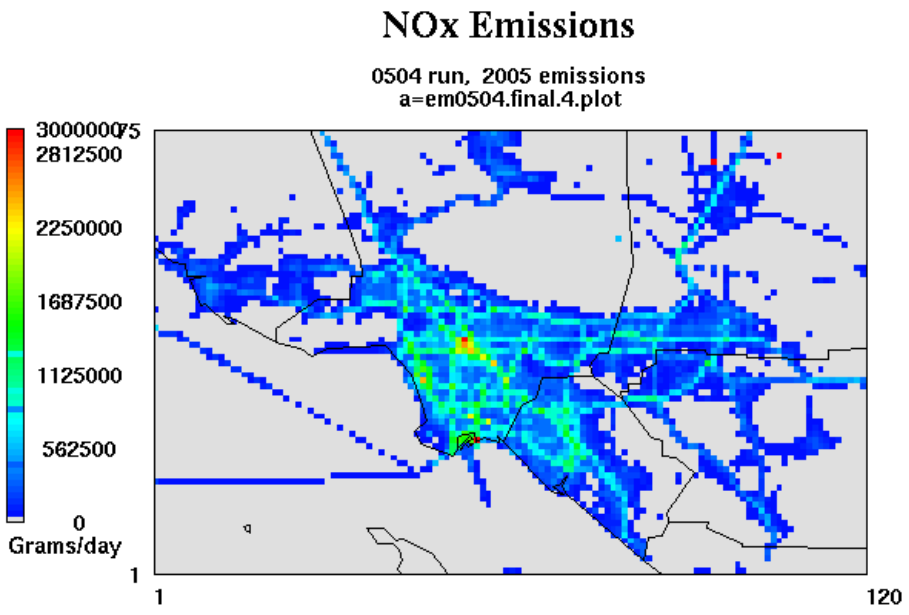

FIGURE IX-10i
Weekday average NOx emissions pattern.

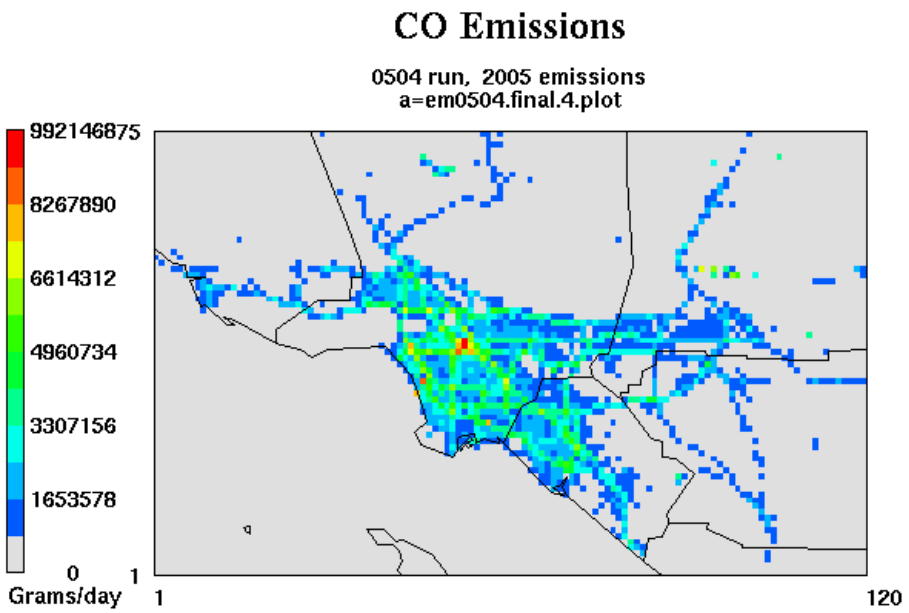

FIGURE IX-10j
Weekday average CO emissions pattern.

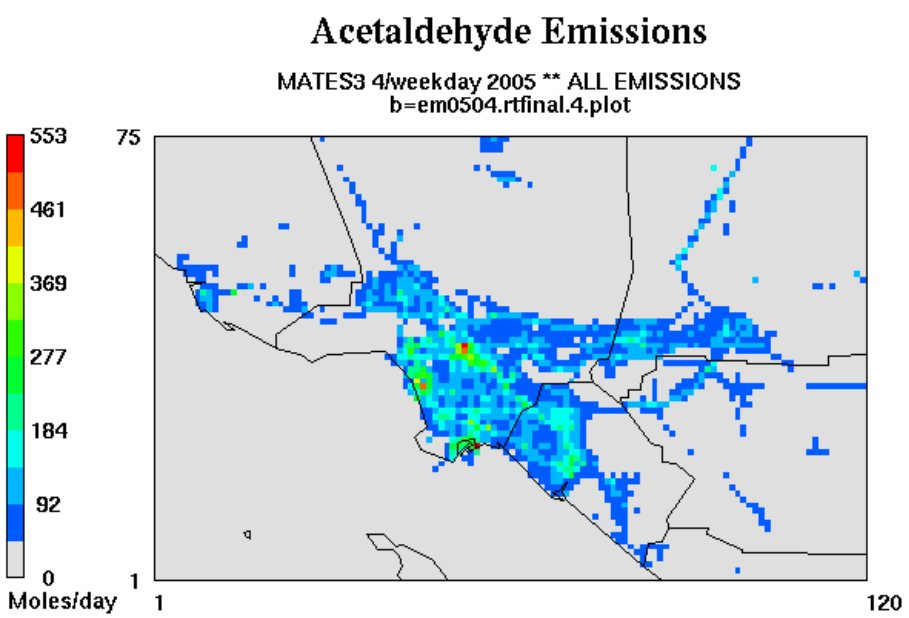

FIGURE IX-10k
Weekday average emissions pattern for Acetaldehyde.

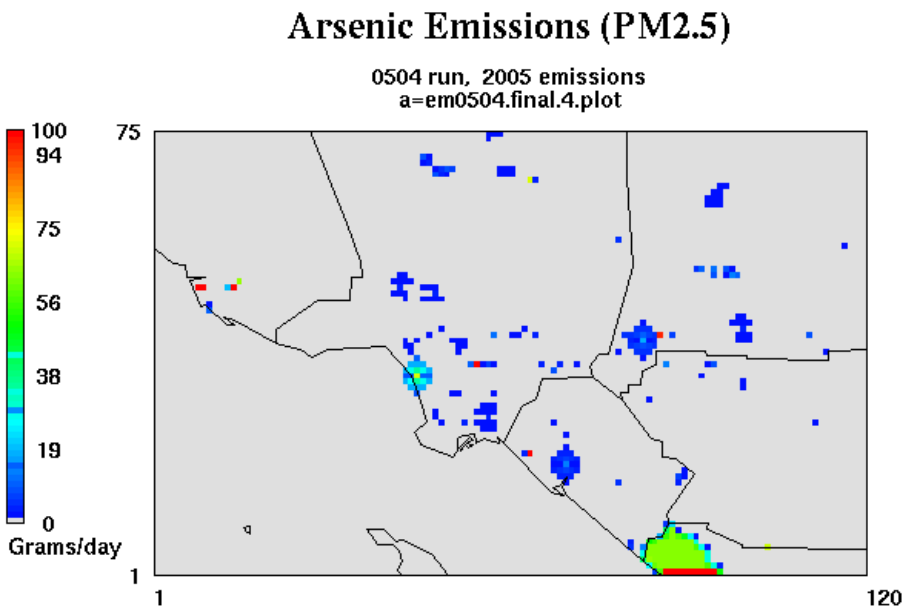

FIGURE IX-10l
Weekday average Arsenic emissions pattern.

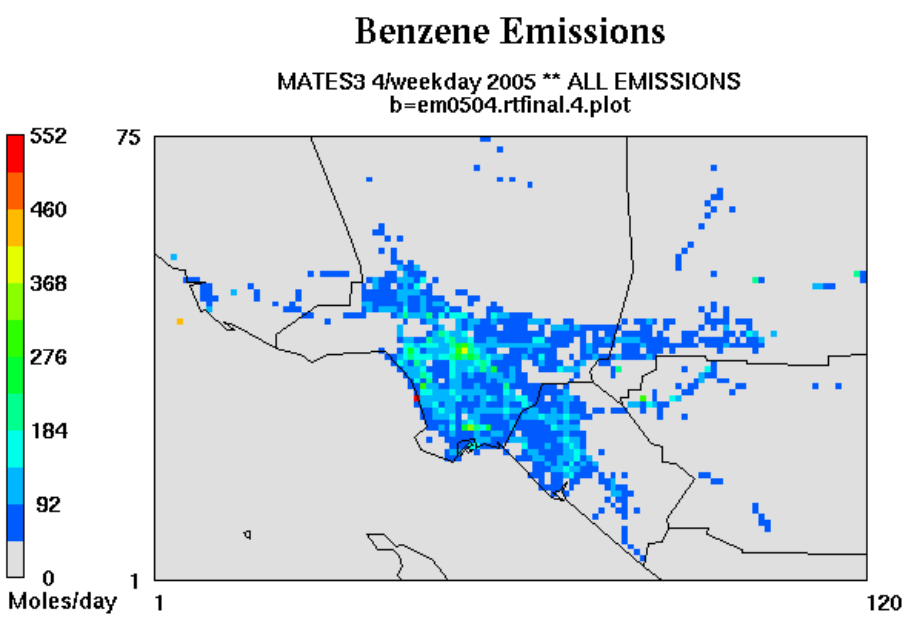

FIGURE IX-10m
Weekday average Benzene emissions pattern.

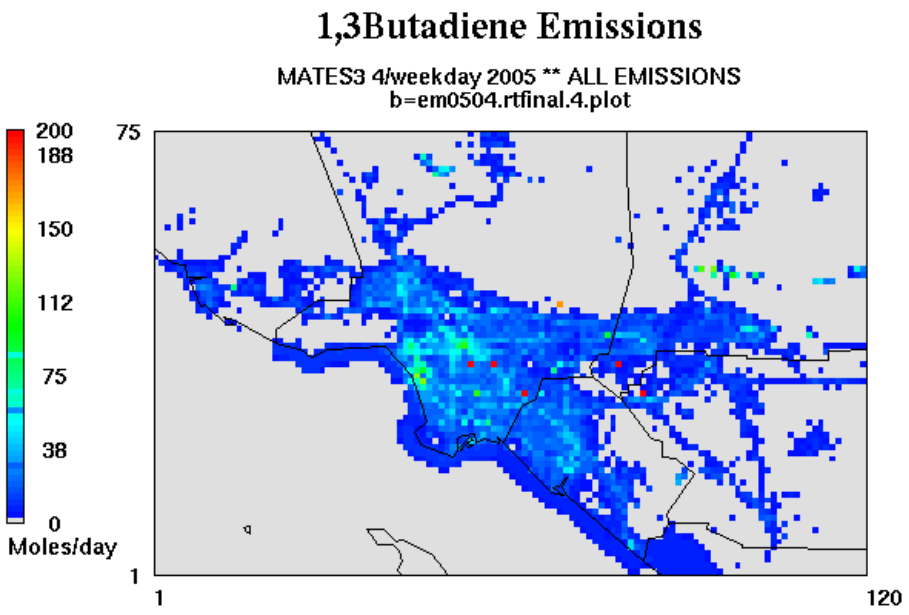

FIGURE IX-10n
Weekday average 1,3 Butadiene emissions pattern.

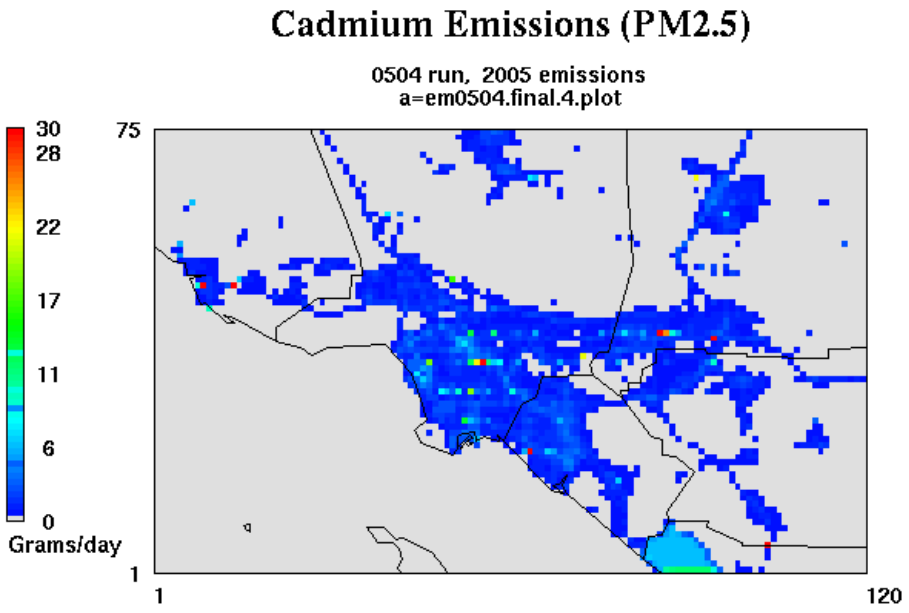

FIGURE IX-10o
Weekday average Cadmium $PM_{2.5}$ emissions pattern.

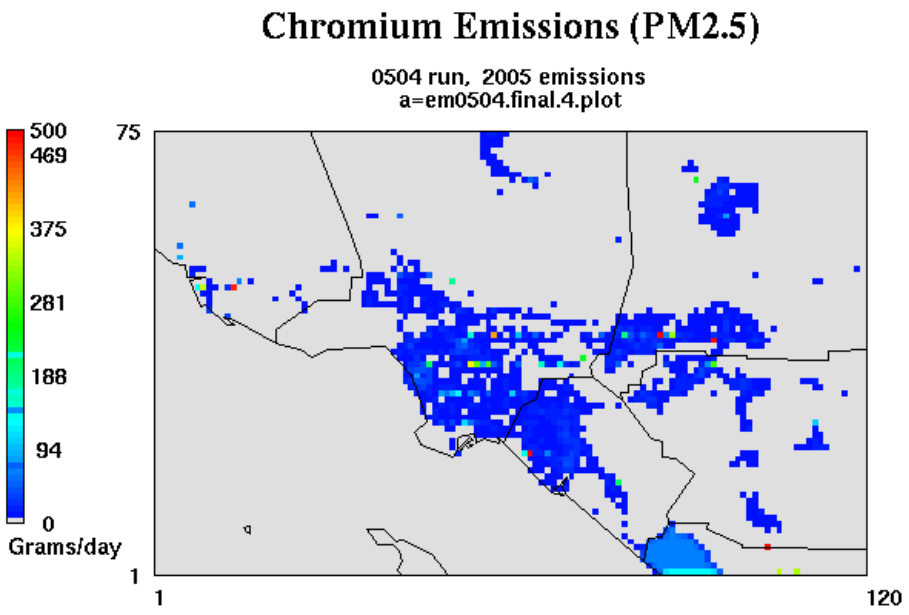

FIGURE IX-10p
Weekday average Chromium $PM_{2.5}$ emissions pattern.

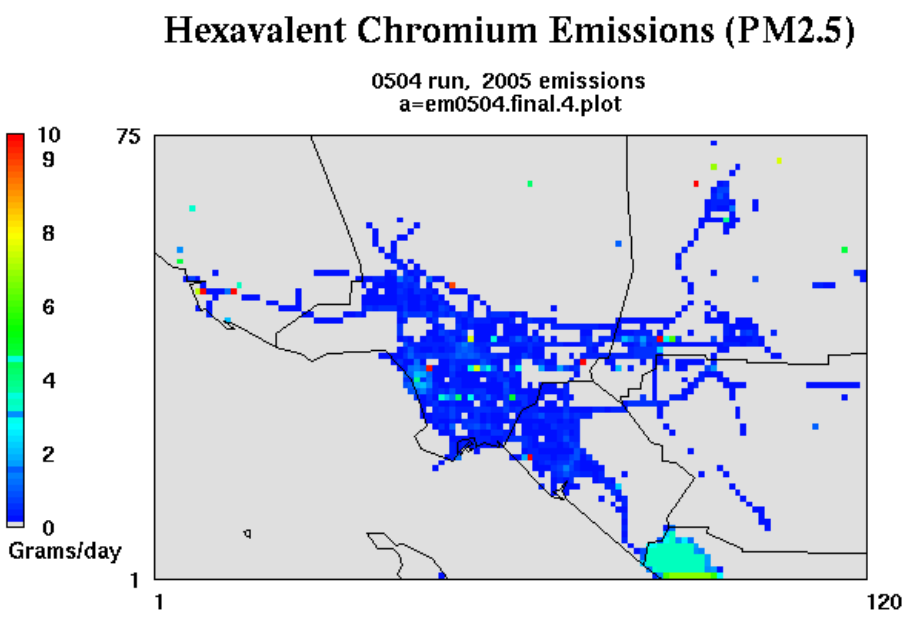

FIGURE IX-10q
Weekday average Hexavalent Chromium $PM_{2.5}$ emissions pattern.

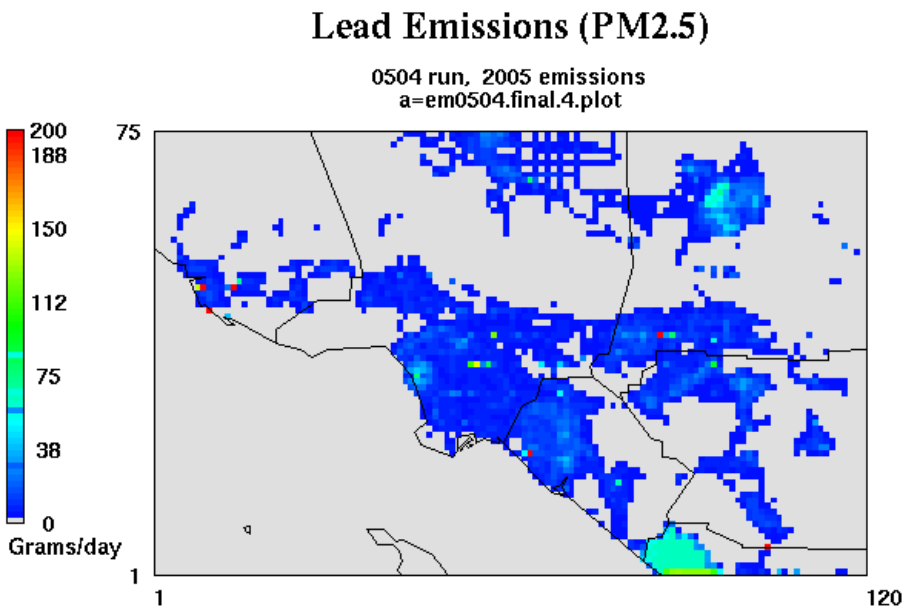

FIGURE IX-10r
Weekday average Lead $PM_{2.5}$ emissions pattern.

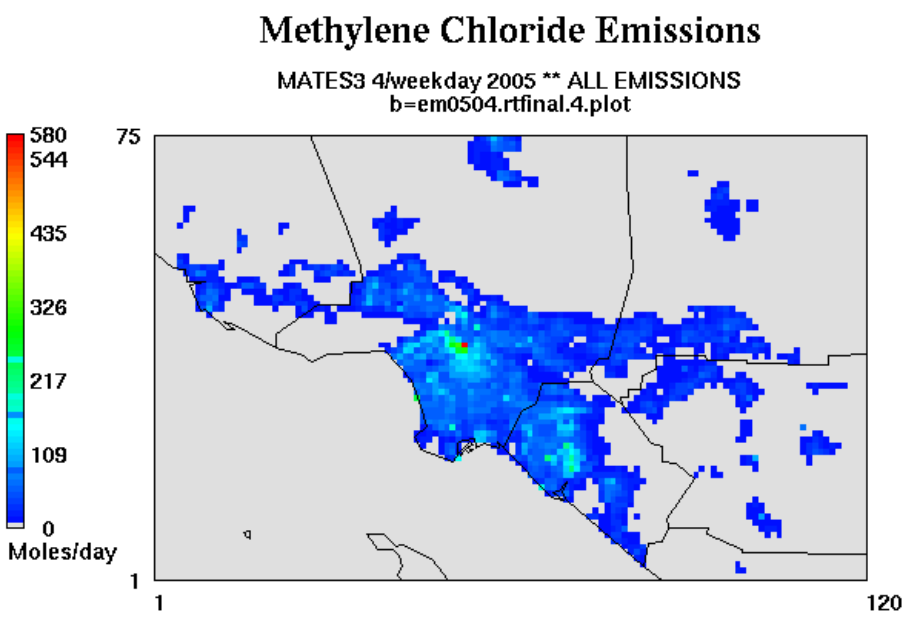

FIGURE IX-10s
Weekday average Methylene Chloride emissions pattern.

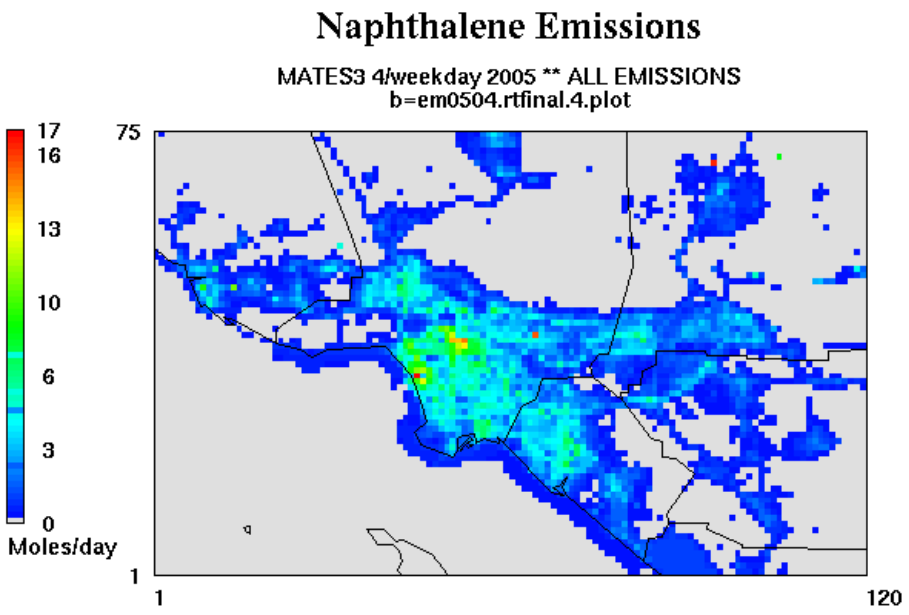

FIGURE IX-10t
Weekday average Naphthalene emissions pattern.

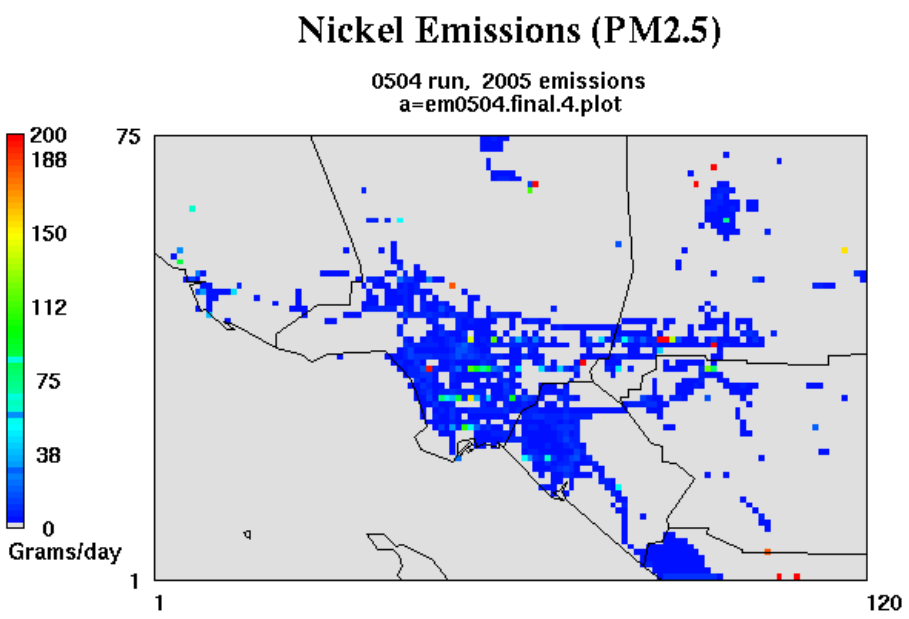

FIGURE IX-10u
Weekday average Nickel $PM_{2.5}$ emissions pattern.

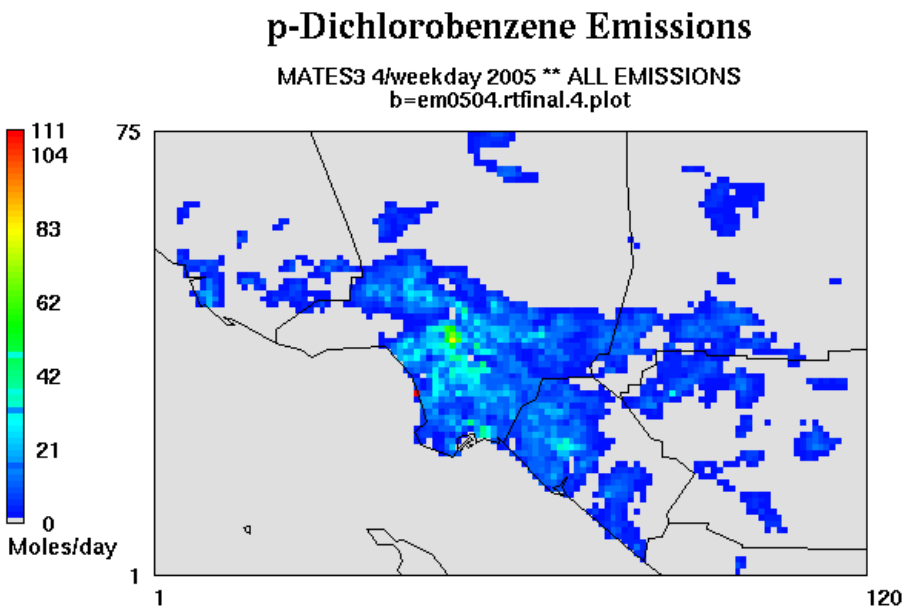

FIGURE IX-10v
Weekday average Nickel emissions pattern.

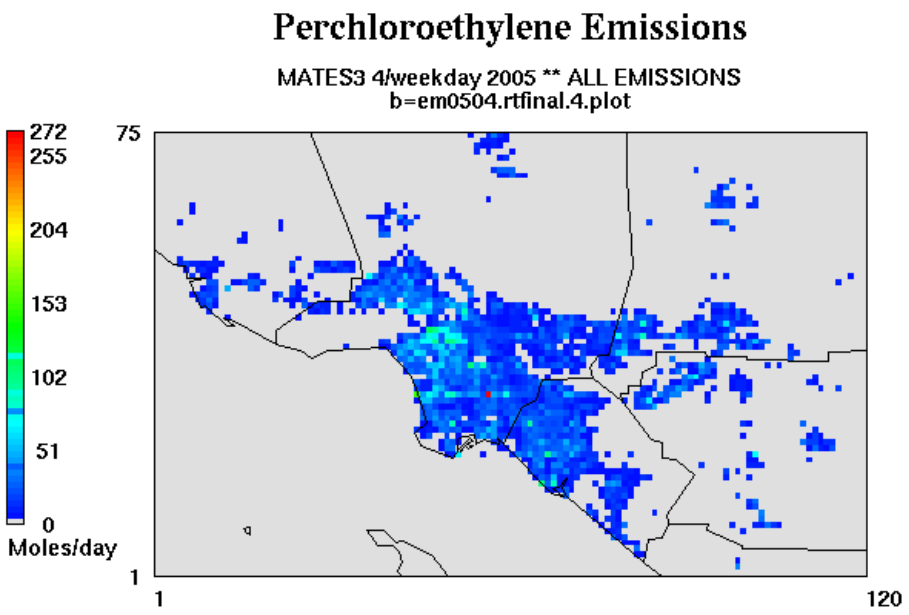

FIGURE IX-10w
Weekday average Perchloroethylene emissions pattern.

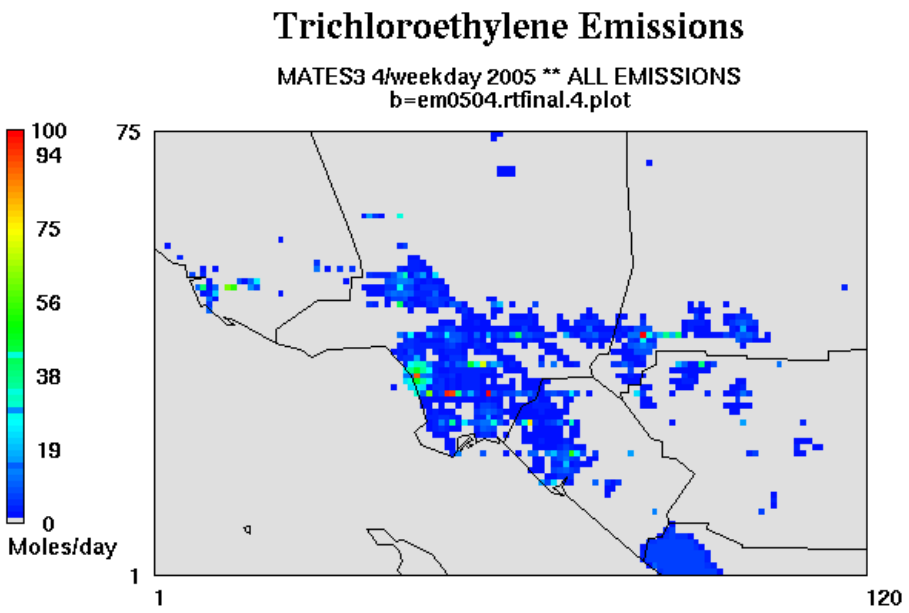

FIGURE IX-10x
Weekday average Trichloroethylene emissions pattern.

Table IX-4 summarizes the impact of using the revised emissions profile where CAMx RTRAC simulation overprediction of $EC_{2.5}$ at Long Beach, West Long Beach and Compton was lessened without adversely impacting performance at the remaining sites. The total diesel mass emissions from this source category were not impacted by the revision.

The third modification impacted the distribution of truck movement throughout the Basin. At the time of MATES II, no heavy-duty truck movement profile was available to characterize the truck distribution and travel on freeways, arterials, and major streets. Truck travel was assigned the travel model characteristics designated for light-duty passenger vehicle travel. MATES III directly incorporated the output of the heavy-duty truck demand model to provide a more realistic characterization of weekday travel. Weekend travel was assigned the same routes but at substantially lowered demand.

A brief assessment of the changes made to the modeling emissions from MATES II to MATES III showed that for diesel 97% of the grids exhibited net changes of 10 kg/ day or less. The maximum change in grid level emissions ranged from -81 kg/day to 120 kg/day. (A positive number indicates an increase in emissions from the MATES II inventory to MATES III). Overall, the shift in the emissions pattern from MATES II to MATES III reflects relatively small increments of emissions increase or decrease. Refinements to travel patterns and shipping result in more clearly defined offshore shipping routes and enhanced diesel emissions along Interstate 5 and 710. Reductions in diesel emissions are noted in southwestern San Bernardino and northwestern Riverside Counties.

TABLE IX-4
Simulated Impact of Revised Marine $EC_{2.5}$ Emissions Profile

Location	Observed	Initial*	Interim*	Final*
Anaheim	1.00	1.03	1.07	0.94
Burbank	1.00	0.53	0.54	0.50
Compton	1.00	1.12	1.15	1.04
Inland Valley San Bernardino	1.00	0.72	0.88	0.84
Huntington Park	1.00	0.94	0.96	0.91
North Long Beach	1.00	1.42	1.47	1.26
Central Los Angeles	1.00	1.09	1.11	1.06
Pico Rivera	1.00	0.76	0.85	0.80
Rubidoux	1.00	0.60	0.84	0.80
West Long Beach	1.00	1.22	1.26	1.04

* Ratio of Simulated to Observed $EC_{2.5}$ at Measurement Site

Boundary and Initial Conditions

The MATES III boundaries differed significantly from those used in MATES II. Overall, the concentrations were lower; and, unlike MATES II, the boundary conditions were not uniform. The boundaries along the eastern and western portions of the modeling domain were sectioned into thirds, and the north and south boundaries were apportioned into fifths. Each section of the four boundaries was assigned a unique value. Table IX-5 provides the boundary assignments. The western and southern boundaries were scaled to show a diminishing concentration as the southwest corner of the modeling domain was approached. The overland boundaries residing over populated areas or grid cells in major transportation corridors were assigned higher boundary concentrations compared with those cells over water or over mountains or desert areas.

The majority of the values of the boundary and initial conditions were extracted from the 2005 annual $PM_{2.5}$ simulations used for the 2007 AQMP compliance demonstration. Boundary conditions for EC and diesel particulate were generated from model simulations using the larger SCOS97 modeling grid and a clean boundary assumption. (The MATES III grid is a subset of the SCOS97 modeling grid which encompasses 550 km in the east-west direction and 370 km in the north-south direction).

TABLE IX-5

Boundary Conditions for Gaseous Compounds (PPM): North and East Boundaries

Compound	North					East		
	N1	N2	N3	N4	N5	E1	E2	E3
NO	0.00017	0.00022	0.0002	0.00022	0.0002	0.00016	0.00016	0.00016
NO2	0.0028	0.0038	0.0038	0.00431	0.00395	0.00298	0.00297	0.00298
O3	0.05	0.05	0.049	0.05	0.05	0.05	0.05	0.05
OLE	0.0007	0.00082	0.00106	0.00115	0.0012	0.001393	0.001393	0.001393
PAR	0.019	0.021	0.023	0.023	0.0239	0.02571	0.02571	0.02571
TOL	0.00023	0.0003	0.00033	0.00032	0.00036	0.00038	0.00038	0.00038
XYL	0.00009	0.000116	0.00011	0.00009	0.000109	0.000112	0.000112	0.000112
FORM	0.002	0.0021	0.0021	0.00203	0.00201	0.00238	0.00238	0.00238
ALD2	0.001	0.0012	0.00132	0.00136	0.0014	0.00163	0.00163	0.00163
ETH	0.00041	0.000542	0.000636	0.0006	0.00061	0.0006	0.0006	0.0006
CRES	0.000007	0.000007	0.000007	0.000007	0.000007	0.000009	0.000009	0.000009
MGLY	0.000001	0.000001	0.000001	0.000001	0.000001	0.000001	0.000001	0.000001
OPEN	0.000002	0.000002	0.000002	0.000002	0.000002	0.000003	0.000003	0.000003
PNA	0.00001	0.00001	0.000012	0.000011	0.000011	0.000008	0.000008	0.000008
NXOY	0.00007	0.00008	0.000095	0.000103	0.000115	0.00007	0.00007	0.00007
PAN	0.00059	0.00058	0.000565	0.00054	0.00054	0.0005	0.0005	0.0005
CO	0.2	0.2	0.2	0.2	0.2	0.2	0.2	0.2
HONO	0.000002	0.000003	0.000003	0.000003	0.000003	0.000004	0.000004	0.000004
H2O2	0.0018	0.0017	0.00165	0.0016	0.00165	0.00187	0.00187	0.00187
MEOH	0.0001	0.0001	0.0001	0.0001	0.0001	0.0001	0.0001	0.0001
ETOH	0.0001	0.0001	0.0001	0.0001	0.0001	0.0001	0.0001	0.0001
ISOP	0.0001	0.0001	0.0001	0.0001	0.0001	0.0001	0.0001	0.0001
BENZ	0.0002	0.0002	0.0002	0.0002	0.0002	0.0002	0.0002	0.0002
BUTA	0.0000037	0.0000037	0.0000037	0.0000037	0.0000037	0.0000037	0.0000037	0.0000037
PACET	0.0001	0.00012	0.000132	0.000136	0.00014	0.000163	0.000163	0.000163
HCHO	0.0002	0.00021	0.00021	0.000203	0.000201	0.000238	0.000238	0.000238
SACET	0.00045	0.00054	0.0006	0.00061	0.00063	0.000735	0.000735	0.000735
SFORM	0.0009	0.00095	0.00095	0.00092	0.000945	0.00107	0.00107	0.00107
PDIC	0.00001	0.00001	0.00001	0.00001	0.00001	0.00001	0.00001	0.00001
MCHL	0.00001	0.00001	0.00001	0.00001	0.00001	0.00001	0.00001	0.00001
PERC	0.00001	0.00001	0.00001	0.00001	0.00001	0.00001	0.00001	0.00001
TCE	0.00001	0.00001	0.00001	0.00001	0.00001	0.00001	0.00001	0.00001
NAPH	0.00001	0.00001	0.00001	0.00001	0.00001	0.00001	0.00001	0.00001

TABLE IX-5 (Continued)
Boundary Conditions for Gaseous Compounds (PPM): West and South Boundaries

Compound	West			South				
	W1	W2	W3	S1	S2	S3	S4	S5
NO	0.000128	0.00035	0.000325	0.00014	0.00028	0.00039	0.000585	0.00052
NO2	0.00103	0.00311	0.00317	0.00115	0.002	0.00426	0.0077	0.00664
O3	0.044	0.044	0.047	0.045	0.046	0.045	0.044	0.047
OLE	0.000069	0.000155	0.000389	0.00007	0.0001	0.000365	0.000928	0.001248
PAR	0.0108	0.0182	0.0204	0.011	0.015	0.0221	0.03485	0.0349
TOL	0.000096	0.000183	0.000213	0.00012	0.00017	0.00038	0.000855	0.0008
XYL	0.000031	0.000073	0.000081	0.00004	0.00007	0.000165	0.000381	0.000352
FORM	0.000637	0.00098	0.00167	0.00061	0.00073	0.00105	0.00173	0.00222
ALD2	0.000242	0.000422	0.000687	0.00024	0.0003	0.00058	0.00114	0.00139
ETH	0.000099	0.000175	0.000343	0.0001	0.00015	0.000349	0.000658	0.000827
CRES	0.000004	0.000006	0.000006	0.000004	0.000006	0.00001	0.000019	0.000019
MGLY	0.000001	0.000001	0.000001	0.000001	0.000001	0.000001	0.000001	0.000001
OPEN	0.000001	0.0000015	0.000001	0.000001	0.000002	0.000003	0.000005	0.000005
PNA	0.000004	0.000006	0.000009	0.000004	0.000004	0.000008	0.000013	0.000016
NXOY	0.00005	0.00006	0.000048	0.00005	0.0001	0.000125	0.000134	0.000112
PAN	0.0003	0.000413	0.00051	0.0003	0.00034	0.000427	0.000565	0.000657
CO	0.2	0.2	0.2	0.2	0.2	0.2	0.2	0.2
HONO	0.000002	0.000005	0.000004	0.000002	0.000003	0.000005	0.000007	0.000006
H2O2	0.00114	0.00127	0.00163	0.0011	0.0012	0.0013	0.00145	0.00168
MEOH	0.0001	0.0001	0.0001	0.0001	0.0001	0.0001	0.0001	0.0001
ETOH	0.0001	0.0001	0.0001	0.0001	0.0001	0.0001	0.0001	0.0001
ISOP	0.0001	0.0001	0.0001	0.0001	0.0001	0.0001	0.0001	0.0001
BENZ	0.0002	0.0002	0.0002	0.0002	0.0002	0.0002	0.0002	0.0002
BUTA	0.0000037	0.0000037	0.0000037	0.0000037	0.0000037	0.0000037	0.0000037	0.0000037
PACET	0.0000242	0.000042	0.0000687	0.000024	0.00003	0.000058	0.000114	0.000139
HCHO	0.0000637	0.000098	0.000167	0.000063	0.000073	0.000105	0.000173	0.000222
SACET	0.000109	0.00019	0.000618	0.000108	0.000135	0.00026	0.000501	0.000625
SFORM	0.000285	0.00044	0.0015	0.000275	0.00032	0.000475	0.00078	0.001
PDIC	0.00001	0.00001	0.00001	0.00001	0.00001	0.00001	0.00001	0.00001
MCHL	0.00001	0.00001	0.00001	0.00001	0.00001	0.00001	0.00001	0.00001
PERC	0.00001	0.00001	0.00001	0.00001	0.00001	0.00001	0.00001	0.00001
TCE	0.00001	0.00001	0.00001	0.00001	0.00001	0.00001	0.00001	0.00001
NAPH	0.00001	0.00001	0.00001	0.00001	0.00001	0.00001	0.00001	0.00001

TABLE IX-5 (Continued)
Boundary Conditions for Particulate Compounds (µg/m3): North and East Boundaries

Compound	North (Fine)					East (Fine)		
	N1	N2	N3	N4	N5	E1	E2	E3
AR	0.00004	0.0001	0.000144	0.0004	0.0004	0.00034	0.0002	0.000192
CD	0.000013	0.00003	0.0000425	0.000125	0.000125	0.000108	0.0000625	0.00006
CR	0.0001	0.00025	0.00034	0.001	0.001	0.00085	0.0005	0.00048
CR6	0.00001	0.00002	0.00002	0.00008	0.0001	0.00007	0.000045	0.000045
DPMa	0.078	0.117	0.085	0.3	0.29	0.104	0.075	0.084
DPMb	0.029	0.068	0.093	0.222	0.188	0.15	0.108	0.088
DPMc	0.0017	0.0041	0.005	0.0127	0.0123	0.0103	0.0055	0.00475
DPMd	0.0014	0.0034	0.0044	0.035	0.037	0.0075	0.0084	0.0123
DPMe	0.0088	0.01	0.011	0.0075	0.0055	0.005	0.0037	0.00246
DSL	0.119	0.2	0.2	0.58	0.503	0.278	0.201	0.192
EC	0.059	0.11	0.128	0.3	0.283	0.154	0.124	0.125
NI	0.000056	0.00014	0.00019	0.00056	0.00056	0.000476	0.00028	0.000269
OC	0.011	0.22	0.255	0.61	0.66	0.336	0.257	0.25
PB	0.00017	0.000425	0.00056	0.0017	0.0017	0.001445	0.00085	0.000817
	North (Coarse)					East (Coarse)		
	N1	N2	N3	N4	N5	E1	E2	E3
ARC	0.00005	0.00012	0.00022	0.0004	0.0004	0.000276	0.00016	0.000152
CDC	0.000014	0.00004	0.0000688	0.000125	0.000125	0.000086	0.00005	0.000048
CR6C	0.000001	0.000001	0.000001	0.00001	0.00001	0.000005	0.000005	0.000005
CRC	0.00012	0.0003	0.00055	0.001	0.001	0.00069	0.0004	0.00038
DPMaC	0.005	0.0072	0.005	0.017	0.016	0.0045	0.003	0.0034
DPMbC	0.0013	0.0027	0.006	0.0084	0.006	0.00625	0.00429	0.003
DPMcC	0.00003	0.00007	0.00011	0.00017	0.00016	0.000235	0.00011	0.00014
DPMdC	0.00006	0.00013	0.0005	0.0028	0.0023	0.00033	0.00037	0.0006
DPMeC	0.0005	0.00041	0.0004	0.00022	0.00018	0.00025	0.00016	0.0001
DSLC	0.008	0.01	0.0124	0.028	0.025	0.0116	0.008	0.0072
ECC	0.011	0.023	0.034	0.072	0.071	0.036	0.029	0.0319
NIC	0.000067	0.00017	0.00031	0.00056	0.00056	0.000386	0.000216	0.000213
OCC	0.07	0.15	0.25	0.36	0.29	0.261	0.154	0.135
PBC	0.0002	0.00051	0.00093	0.0017	0.0017	0.00117	0.00068	0.000646

TABLE IX-5 (Continued)

Boundary Conditions for Particulate Compounds (µg/m3): West and South Boundaries

	West (Fine)			South (Fine)				
	W1	W2	W3	S1	S2	S3	S4	S5
AR	0.000002	0.000022	0.000032	0.000004	0.00014	0.00016	0.00044	0.00056
CD	6.3E-07	6.88E-06	0.00001	0.0000013	0.000043	0.00005	0.0001375	0.0002
CR	0.000005	0.000055	0.00008	0.00001	0.00034	0.0004	0.0011	0.0016
CR6	0.0000005	0.00001	0.00001	0.000001	0.00006	0.00007	0.00017	0.0002
DPMa	0.00016	0.00494	0.0078	0.00025	0.0013	0.003	0.096	0.143
DPMb	0.00034	0.0048	0.012	0.00055	0.0025	0.005	0.097	0.165
DPMc	0.015	0.0211	0.02	0.0245	0.0185	0.0216	0.025	0.0166
DPMd	0.000125	0.00125	0.00142	0.00014	0.00032	0.0005	0.00327	0.006
DPMe	0.0001	0.0015	0.0058	0.00013	0.00036	0.00058	0.0031	0.0055
DSL	0.0155	0.033	0.047	0.0255	0.023	0.031	0.219	0.335
EC	0.006	0.043	0.05	0.0097	0.019	0.028	0.134	0.196
NI	0.0000028	0.0000308	0.000045	0.0000056	0.00019	0.000226	0.000616	0.000896
OC	0.011	0.026	0.043	0.018	0.0175	0.025	0.223	0.377
PB	0.0000085	0.0000935	0.000126	0.000017	0.000578	0.00068	0.00187	0.00272
	West (Coarse)			South (Coarse)				
	W1	W2	W3	S1	S2	S3	S4	S5
ARC	0.0000006	0.000006	0.000026	0.0000004	0.000002	0.000008	0.00016	0.00028
CDC	0.0000002	1.88E-06	0.000008	1.3E-07	0.0000006	0.0000025	0.00005	0.0001
CR6C	1E-08	0.0000001	0.0000005	0.000001	0.000001	0.000001	0.000001	0.000005
CRC	0.0000015	0.000015	0.000065	0.000001	0.000005	0.00002	0.0004	0.0008
DPMaC	0.00001	0.00039	0.00055	0.000015	0.00007	0.00017	0.0065	0.0086
DPMbC	0.00002	0.00034	0.00082	0.00003	0.00013	0.00027	0.0065	0.0094
DPMcC	0.001	0.0015	0.00139	0.0015	0.00096	0.0011	0.00125	0.00063
DPMdC	0.00001	0.00009	0.0001	0.00001	0.00002	0.00003	0.00021	0.00032
DPMeC	0.000005	0.0001	0.00042	0.00001	0.00002	0.00003	0.0002	0.00018
DSLC	0.001	0.0024	0.0032	0.0015	0.0012	0.0016	0.0146	0.019
ECC	0.00036	0.0036	0.0065	0.0005	0.0011	0.0022	0.036	0.055
NIC	8.4E-07	0.0000084	0.000036	5.6E-07	0.0000028	0.0000112	0.000224	0.000448
OCC	0.0014	0.011	0.035	0.0019	0.0041	0.0079	0.236	0.392
PBC	2.55E-06	0.0000255	0.00011	0.0000017	0.0000085	0.000034	0.00068	0.00136

Modeling Results

The performance of the CAMx regional modeling simulation for the 2005 emissions and meteorology is summarized through model performance statistics and graphically through time series displays and bivariate plots of key projected pollutant concentrations. Summarized in Table IX-6 are the toxic components observed and simulated concentrations and the prediction accuracy (PA) measured as the percentage difference between the mean annual observed and simulated concentrations.

2005 CAMx RTRAC Simulation

Simulated annual average $EC_{2.5}$ was the compound used to assess overall model performance for the 2005 MATES III period at the eight sites having a full year's sampling. The analysis used annual average $EC_{2.5}$ model performance to provide consistency with the 2007 AQMP annual average $PM_{2.5}$ attainment demonstration modeling assessment. While the 2007 $EC_{2.5}$ AQMP modeling was conducted on a coarser grid (5 kilometer squared), it was expected that the summary performance of the CAMx RTRAC 2005 MATES III simulation should be consistent, but not identical.

In general, $EC_{2.5}$ performs well in the simulation. The $EC_{2.5}$ performance is comparable to that observed in the 2007 AQMP annual $PM_{2.5}$ attainment demonstration. Performance for several of the minor toxic components varies. This in part can be attributed to very low measured concentrations nearing levels of detection, uncertainties in the emissions inventory and model performance in recreating dispersion patterns. Adding to the uncertainty is the nine-cell distance weighted averaging to recreate a measurement made at a discreet location.

EPA guidance (U.S. EPA, 2006) recommends evaluating gaseous and particulate modeling performance using measures of prediction bias and error. PA goals of ±20% for ozone and ±30% for individual components of $PM_{2.5}$ or PM_{10} have been used to assess simulation performance in previous modeling attainment demonstrations.

Table IX-7 provides the CAMx performance for $EC_{2.5}$ at the eight MATES III monitoring sites that have complete monitoring records for 2005. Three of the eight sites (Burbank, Inland Valley San Bernardino, and Rubidoux) underpredict the annual average $EC_{2.5}$ concentration. The greatest tendency for overprediction is at North Long Beach. The mean error of the simulated versus measured concentrations ranges from 0.54 $\mu g/m^3$ to 1.11 $\mu g/m^3$. PA at seven of the eight MATES III sites meets the particulate goal with only Burbank exhibiting a large degree (50%) of underprediction of the annual average concentration. Of the remaining sites, Inland Valley San Bernardino, and Rubidoux are underpredicted by 19 and 22%, respectively and Long Beach is overpredicted by 22%. All other sites PA falls within ±10% of observations.

Table IX-8 provides the CAMx RTRAC performance for Benzene at the eight MATES III monitoring sites that have complete monitoring records for 2005. Benzene model performance is included in the evaluation because of the confidence in the benzene measurement data based on the long-term monitoring conducted in the Basin and throughout California. With the exceptions of Burbank and Compton, the remaining sites achieve a PA of less than 20%. The simulation bias is mixed and is generally less than 0.1 ppb (with the exceptions of Burbank and Compton).

The time series fit of the simulated $EC_{2.5}$ concentrations to measurements for each station is depicted in Figures IX-11a through IX-11h and in the cumulative eight-site combined bivariate plot shown in Figure IX-12. The time series depiction of the measured and simulated $EC_{2.5}$ echo the statistical evaluation whereby concentrations are underpredicted throughout the year at Burbank and Riverside, with the greatest margin occurring in the fall and early winter periods. Similarly, $EC_{2.5}$ at Inland Valley San Bernardino is underpredicted in the second half of the year. The time series for the other sites show a general tendency to nominally overpredict in the summer but capture the trend in the fall and winter.

In Figure IX-12, the $EC_{2.5}$ predictions for the eight sites combined show an overall tendency towards underprediction. However a large percent of the predictions are within 30% of the measured concentrations.

1998-99 CAMx RTRAC Simulation

Table IX-9 and Table IX-10 provide a comparison of the 2005 and 1998-99 model performance for $EC_{2.5}$ and benzene, respectively. The tables provide comparisons of the performance of the mean annual CAMx RTRAC simulated $EC_{2.5}$ and benzene and the annual average concentrations based on the monitoring data. Performance solely for days when observations were conducted was not calculated for the 1998-99 simulation. Listed in each table are PA, mean error, and absolute error. The 1998-99 CAMx RTRAC evaluation includes simulation performance at Huntington Park and Pico Rivera in the assessment.

The 1998-99 CAMx RTRAC model simulations were developed using the same procedures and methodologies as the 2005 simulation. Overall, the 1998-99 simulated annual average concentrations tended to underpredict observed mean concentrations.

As presented in Table IX-8, the $EC_{2.5}$ 1998-99 simulation depicts a systematic bias towards underprediction. In addition, prediction accuracy degrades compared to the 2005 simulation with only three of eight stations meeting the ±30% goal. The ratio of the 1998-99 average absolute error to the average observed concentration was over 36% compared to a similar ratio for 2005 valued at 17%. (Note: the mix of stations is different for the two periods).

The 1998-99 simulation performance for benzene, (depicted in Table IX-9), is also degraded compared to the 2005 simulations, however, to a lesser degree than for $EC_{2.5}$. While the average bias for the 1998-99 simulation trends towards underprediction, several coastal metropolitan sites are well-simulated. The poorest performing site for PA and bias in both simulations 1998-99 and 2005 is Compton. The ratio of the 1998-99 average absolute error to the average observed concentration was 29% compared to a similar ratio for 2005, valued at 17%.

Discussion of Simulation Uncertainties

It is difficult to assign incremental degrees of uncertainty to the model simulations. Both simulation periods required emissions projections from the 2002 base-year inventory. A significant amount of effort was taken in the development of the 2002 to 2005 emissions projections, particularly for the mobile source inventory as a component in the development of the 2007 AQMP. The 1998-99 back-cast of the emissions data used the same projection

protocol as the forward projection from 2002 to 2005. The simulation used the 1998 reported point source emissions and mobile source emissions based on EMFAC 2007.

There are several areas where incremental uncertainty in the back-cast of the emissions can take place. Traffic patterns, spatial vehicle age distributions and marine vessel activities all changed from 1998 to 2005. Weigh-in-motion (WIM) traffic count data has been used in the 2003 and 2007 AQMPs to help better define weekday and weekend traffic patterns. The WIM data used in the analysis is more contemporary with the 2002-2005 time frames and was not changed in the development of the 1998-99 diurnal traffic patterns. Also, the greater number of older, higher emitting cars and their distribution throughout the Basin may have added to the uncertainty in the 1998 mobile source emissions estimate. Finally, detailed shipping surveys, including port calls and route assignment for oceangoing vessels and marine craft, were conducted for the development of the 2003 and 2007 AQMPs. Uncertainties arise in the back-casts of the 1998 activities contributing to the estimation of these emissions.

As previously discussed, a general assessment of the meteorological profiles of the two monitoring periods suggests that the dispersion potentials were comparable but not identical. The meteorological input fields generated from the MM5 simulations followed the same protocol with the exceptions of the grid resolution of the analysis initialization simulations and the day specific data used in the FDDA analysis. Finally, both simulations use the same initial and boundary conditions.

Simulation Evaluation Averaged Over the Monitoring Network

For this comparison, the monitored data for six stations are combined to provide an estimate of average basin-wide conditions for the two sampling periods: 2005 and 1998-99. Table IX-11 summarizes the network average measured and predicted pollutant concentrations at the six sites. Two stations in 2005, Huntington Park and Pico Rivera, did not have complete measurement records for the full 12 months and were excluded from the analysis. Similarly, complete measurements for Compton and West Long Beach were not available for 1998-99. CAMx RTRAC simulated pollutant concentrations for the six stations that have complete data for the two measurement periods were calculated from the grid data using the distance weighted nine-cell average. No direct measurements of $PM_{2.5}$ diesel were available for comparison to simulate annual average concentrations. However, estimates of diesel concentrations based on Chemical Mass Balance (CMB) analysis using ambient measured elemental carbon concentrations are discussed later. Measured concentrations of naphthalene were available for Central Los Angeles and Riverside. Each of the four counties is represented by at least one station. The six stations' average measured and simulated concentrations provide an estimate of the regional profile but with a bias towards impacts to the coastal communities in the heavily transited areas of the Basin. Moreover, the assessment provides a direct comparison for model performance evaluation.

In general, 2005 model simulated particulate $EC_{2.5}$, EC_{10}, hexavalent chromium and $PM_{2.5}$ nickel average annual toxic compound concentrations compared well with the measured annual average values. The majority of gaseous components were well-simulated with the sole exception of acetaldehyde which is underpredicted. Arsenic and TSP lead exhibit the greatest tendency for

overprediction. Cadmium, and $PM_{2.5}$ lead concentrations tend to be underpredicted. In general, the concentrations of the gaseous compounds are closely recreated.

For 1998-99, there exists a general tendency for underprediction. Hexavalent chromium and nickel average annual toxic compound concentrations are exceptions that are closely matched to observations. Aside from the uncertainties associated with the modeling analyses, some uncertainty in prediction accuracy is introduced into the analysis through the measurement and analysis programs. The 1998-99 data samples were measured and analyzed by different agencies (AQMD and ARB) and their laboratories. In addition, to the substitution of one-half level of detection for data measured below the detection limit also adds to the uncertainty in the analysis.

Simulation Estimated Spatial Concentration Fields

Figures IX-13a through IX-13u depict the CAMx projected annual average concentration distributions of selected toxic compounds as well as the impacts of five emissions categories of diesel particulates in the Basin. In general, the distribution of diesel particulates follows the major arterials. However, localized hot spots with annual average concentrations to 4.8 $\mu g/m^3$ are observed in the Central Los Angeles area and 8.5 $\mu g/m^3$ at the Ports of Los Angeles and North Long Beach. Figures IX-13h and IX-13i provide the distributions of benzene and 1,3-butadiene, respectively, whereby the toxic compounds are almost uniformly distributed throughout the Basin (reflecting patterns of light-duty vehicle fuel consumption). The formaldehyde profile (Figure IX-13j) depicts higher concentrations in the heavily-traveled western and central Basin, with additional hot spots in the downwind areas of the Basin that are impacted by higher levels of ozone formation (Santa Clarita and Crestline).

Table IX-6
2005 Station Observed and CAMx Simulated MATES III Annual Average Concentrations

Compound	Units	Anaheim			Burbank			Compton			Inland Valley San Bernardino		
		Obs	Model	PA	Obs	Model	PA	Obs	Model	PA	Obs	Model	PA
1,3 Butadiene	ppb	0.09	0.09	9	0.15	0.07	56	0.19	0.15	19	0.07	0.07	11
Acetaldehyde	ppb	1.28	1.04	19	1.94	1.02	47	1.57	1.04	34	1.90	1.10	42
As (TSP)	$\eta g/m^3$	0.44	1.91	333	0.74	1.49	102	0.66	3.41	417	0.75	2.94	294
As (2.5)	$\eta g/m^3$	0.50	0.76	52	0.52	0.51	2	0.46	2.14	363	0.54	1.15	115
Benzene	ppb	0.44	0.50	15	0.71	0.47	34	0.80	0.57	29	0.49	0.44	11
Cd (TSP)	$\eta g/m^3$	1.58	0.59	63	1.49	0.38	74	1.42	0.98	31	1.67	1.32	21
Cd (2.5)	$\eta g/m^3$	1.63	0.32	80	1.30	0.21	84	1.70	0.71	58	1.73	0.87	50
Cr6 (TSP)	$\eta g/m^3$	0.16	0.17	2	0.18	0.11	35	0.31	0.19	38	0.20	0.41	104
EC_{10}	$\mu g/m^3$	1.60	1.82	13	2.35	1.35	42	1.84	2.34	27	2.40	2.30	4
$EC_{2.5}$	$\mu g/m^3$	1.41	1.35	4	2.04	1.03	50	1.76	1.88	7	2.18	1.77	19
Formaldehyde	ppb	2.96	2.97	0	3.84	2.85	26	3.14	3.18	1	3.70	3.08	17
Methylene Chloride	ppb	0.24	0.36	54	0.34	0.27	20	0.29	0.39	33	0.18	0.18	2
Naphthalene	ppb												
Ni (TSP)	$\eta g/m^3$	3.93	3.13	20	3.75	2.05	45	6.02	7.97	32	3.72	11.87	219
Ni (2.5)	$\eta g/m^3$	4.31	1.71	60	3.72	1.12	70	4.50	5.87	30	3.50	7.89	126
Pb (TSP)	$\eta g/m^3$	3.06	8.80	188	3.12	5.49	76	3.06	8.14	166	3.11	12.71	308
Pb (2.5)	$\eta g/m^3$	3.57	1.96	45	4.66	1.17	75	5.84	2.40	59	8.67	6.16	29
p-Dichlorobenzene	ppb	0.03	0.09	174	0.04	0.07	95	0.07	0.11	62	0.03	0.05	96
Perchloroethylene	ppb	0.06	0.10	60	0.10	0.10	1	0.12	0.13	11	0.05	0.07	34
Trichloroethylene	ppb	0.03	0.03	17	0.05	0.02	53	0.03	0.06	87	0.03	0.04	44

Table IX-6 (Continued)
2005 Station Observed and CAMx Simulated MATES III Annual Average Concentrations

Compound	Units	Huntington Park (Less than 12 Months)			North Long Beach			Central Los Angeles			Pico Rivera (Less than 12 Months)		
		Obs	Model	PA	Obs	Model	PA	Obs	Model	PA	Obs	Model	PA
1,3 Butadiene	ppb	0.21	0.25	21	0.10	0.10	2	0.12	0.13	5	0.14	0.13	3
Acetaldehyde	ppb	1.58	1.13	28	1.26	1.11	12	1.78	1.31	26	1.73	1.27	26
As (2.5)	$\eta g/m^3$	1.46	10.67	629	0.65	2.21	241	0.66	3.95	496	1.03	4.04	294
As (TSP)	$\eta g/m^3$	1.27	8.79	593	0.51	0.90	77	0.51	1.52	197	1.34	2.14	59
Benzene	ppb	0.83	0.62	25	0.50	0.57	13	0.59	0.69	16	0.70	0.66	5
Cd (2.5)	$\eta g/m^3$	1.46	1.04	28	1.65	0.88	46	1.43	0.82	43	1.38	0.79	43
Cd (TSP)	$\eta g/m^3$	2.18	0.67	69	1.27	0.65	49	1.39	0.47	66	1.21	0.45	63
Cr6 (TSP)	$\eta g/m^3$	0.23	0.38	62	0.18	0.18	4	0.18	0.26	42	0.17	0.24	37
EC_{10}	$\mu g/m^3$	2.54	3.03	19	1.81	2.25	24	2.05	2.67	30	2.63	2.77	5
$EC_{2.5}$	$\mu g/m^3$	2.28	2.29	0	1.40	1.71	21	1.93	2.04	6	2.33	2.03	13
Formaldehyde	ppb	3.70	3.69	0	3.50	3.36	4	4.23	4.10	3	3.54	3.70	5
Methylene Chloride	ppb	0.39	0.51	31	0.62	0.34	45	0.38	0.58	53	0.31	0.37	17
Naphthalene	ppb							205.33	149.51	27			
Ni (2.5))	$\eta g/m^3$	5.54	6.59	19	6.64	8.77	32	4.87	4.91	1	4.93	4.41	10
Ni (TSP)	$\eta g/m^3$	2.59	4.11	59	4.15	5.83	40	4.33	2.99	31	3.34	2.51	25
Pb (2.5)	$\eta g/m^3$	3.14	13.07	316	3.26	7.67	135	3.04	10.09	232	3.16	9.66	206
Pb (TSP)	$\eta g/m^3$	7.74	5.48	29	4.32	1.87	57	4.67	2.14	54	6.02	2.37	61
p-Dichlorobenzene	ppb	0.08	0.13	68	0.03	0.09	184	0.04	0.12	234	0.04	0.09	150
Perchloroethylene	ppb	0.11	0.16	48	0.05	0.10	110	0.06	0.13	125	0.07	0.11	56
Trichloroethylene	ppb	0.04	0.06	67	0.03	0.05	88	0.03	0.03	0	0.04	0.03	29

Table IX-6 (Continued)
2005 Station Observed and CAMx Simulated MATES III Annual Average Concentrations

Compound	Units	Rubidoux			West Long Beach		
		Obs	Model	PA	Obs	Model	PA
1,3 Butadiene	Ppb	0.09	0.09	5	0.12	0.09	22
Acetaldehyde	Ppb	1.67	1.09	35	1.41	1.08	23
As (2.5)	ηg/m^3	0.82	1.96	139	0.71	2.33	227
As (TSP)	ηg/m^3	0.45	0.56	26	0.47	0.99	113
Benzene	Ppb	0.44	0.44	2	0.53	0.60	14
Cd (2.5)	ηg/m^3	1.54	0.57	63	1.46	1.32	9
Cd (TSP)	ηg/m^3	1.46	0.32	78	1.47	1.08	27
Cr6 (TSP)	ηg/m^3	0.39	0.14	65	0.26	0.17	34
EC_{10}	μg/m^3	2.06	1.74	15	2.30	2.57	12
$EC_{2.5}$	μg/m^3	1.69	1.32	22	2.07	2.14	3
Formaldehyde	Ppb	3.44	3.01	13	3.34	3.25	3
Methylene Chloride	Ppb	0.33	0.21	37	0.20	0.29	43
Naphthalene	Ppb	151.73	81.42	46	188.68	96.08	49
Ni (2.5))	ηg/m^3	3.73	3.31	11	10.55	17.36	65
Ni (TSP)	ηg/m^3	3.57	2.17	39	7.45	10.96	47
Pb (2.5)	ηg/m^3	3.12	7.26	132	3.17	7.17	126
Pb (TSP)	ηg/m^3	6.31	1.78	72	4.50	2.36	47
p-Dichlorobenzene	Ppb	0.04	0.06	58	0.03	0.10	191
Perchloroethylene	Ppb	0.03	0.08	130	0.05	0.09	100
Trichloroethylene	Ppb	0.02	0.03	38	0.04	0.04	0

Table IX-7
2005 Simulation Performance Statistics for $PM_{2.5}$ Elemental Carbon

Location	Observed ($\mu g/m^3$)	Samples	Predicted ($\mu g/m^3$)	PA	Mean Bias ($\mu g/m^3$)	Mean Error ($\mu g/m^3$)	Normalized Mean Bias ($\mu g/m^3$)	Normalized Mean Error ($\mu g/m^3$)
Anaheim	1.41	120	1.35	4	-0.06	0.54	0.39	0.61
Burbank	2.04	119	1.03	50	-1.02	1.11	-0.31	0.48
Compton	1.76	115	1.88	7	0.12	0.61	0.39	0.52
Inland Valley S.B.	2.18	117	1.77	19	-0.41	0.91	0.09	0.56
North Long Beach	1.40	107	1.71	21	0.30	0.61	0.55	0.65
Central L.A.	1.93	117	2.04	6	0.11	0.76	0.39	0.58
Rubidoux	1.69	119	1.32	22	-0.38	0.74	0.09	0.58
West Long Beach	2.07	114	2.14	3	0.07	0.79	0.33	0.53

Table IX-8
2005 Simulation Performance Statistics for Benzene

Location	Observed ($\mu g/m^3$)	Samples	Predicted ($\mu g/m^3$)	PA	Mean Bias ($\mu g/m^3$)	Mean Error ($\mu g/m^3$)	Normalized Mean Bias ($\mu g/m^3$)	Normalized Mean Error ($\mu g/m^3$)
Anaheim	0.439	115	0.504	15	0.064	0.213	0.597	0.735
Burbank	0.709	121	0.466	34	-0.243	0.344	-0.072	0.428
Compton	0.796	117	0.567	29	-0.229	0.388	0.105	0.498
Inland Valley S.B.	0.492	117	0.438	11	-0.054	0.169	0.092	0.398
North Long Beach	0.504	118	0.571	13	0.066	0.213	0.485	0.621
Central L.A.	0.588	119	0.685	16	0.097	0.249	0.469	0.614
Rubidoux	0.435	119	0.442	2	0.007	0.16	0.267	0.464
West Long Beach	0.525	119	0.598	14	0.073	0.214	0.603	0.725

Table IX-9
Comparative Simulation Performance Statistics for EC

	1998-99					2005				
Location	Observed Days ($\mu g/m^3$)	Modeled All Days ($\mu g/m^3$)	PA	Bias ($\mu g/m^3$)	Absolute Error ($\mu g/m^3$)	Observed Days ($\mu g/m^3$)	Modeled All Days ($\mu g/m^3$)	PA	Bias ($\mu g/m^3$)	Absolute Error ($\mu g/m^3$)
Anaheim	2.30	2.12	8	-0.18	0.18	1.41	1.35	4	-0.06	0.06
Burbank	3.19	1.59	50	-1.6	1.6	2.04	1.05	49	-0.99	0.99
Compton						1.76	1.87	6	0.11	0.11
Inland Valley S.B.	3.10	1.84	41	-1.26	1.26	2.18	1.82	17	-0.36	0.36
Huntington Park	4.35	2.73	37	-1.62	1.62					
North Long Beach	2.54	2.41	5	-0.13	0.13	1.4	1.82	30	0.42	0.42
Central L.A.	3.53	2.74	22	-0.79	0.79	1.93	2.08	8	0.15	0.15
Pico Rivera	4.35	2.14	51	-2.21	2.21					
Rubidoux	3.39	1.39	59	-2.00	2.00	1.69	1.36	20	-0.33	0.33
West Long Beach						2.07	2.16	4	0.09	0.09
Average	3.34	2.12	34	-1.22	1.22	1.81	1.69	17	-0.12	0.31

Table IX-10
Comparative Simulation Performance Statistics for Benzene

	1998-99					2005				
Location	Observed Days (ppb)	Modeled All Days (ppb)	PA	Bias (ppb)	Absolute Error (ppb)	Observed Days (ppb)	Modeled All Days (ppb)	PA	Bias (ppb)	Absolute Error (ppb)
Anaheim	1.05	0.81	23	-0.24	0.24	0.44	0.51	15	0.07	0.07
Burbank	1.26	0.52	59	-0.74	0.74	0.71	0.47	33	-0.24	0.24
Compton	1.8	0.84	53	-0.96	0.96	0.8	0.57	29	-0.23	0.23
Inland Valley S.B.	0.74	0.56	24	-0.18	0.18	0.49	0.45	9	-0.04	0.04
Huntington Park	1.65	1.05	36	-0.6	0.6		0.63			
North Long Beach	0.83	0.85	2	0.02	0.02	0.5	0.57	15	0.07	0.07
Central L.A.	1.01	1.07	6	0.06	0.06	0.59	0.69	17	0.10	0.10
Pico Rivera	0.89	0.88	1	-0.01	0.01		0.60			
Rubidoux	0.87	0.52	40	-0.35	0.35	0.44	0.45	2	0.01	0.01
West Long Beach	1.27	1.15	9	-0.12	0.12	0.53	0.60	12	0.07	0.07
Average	1.14	0.83	25	-0.31	0.33	0.56	0.55	17	-0.02	0.10

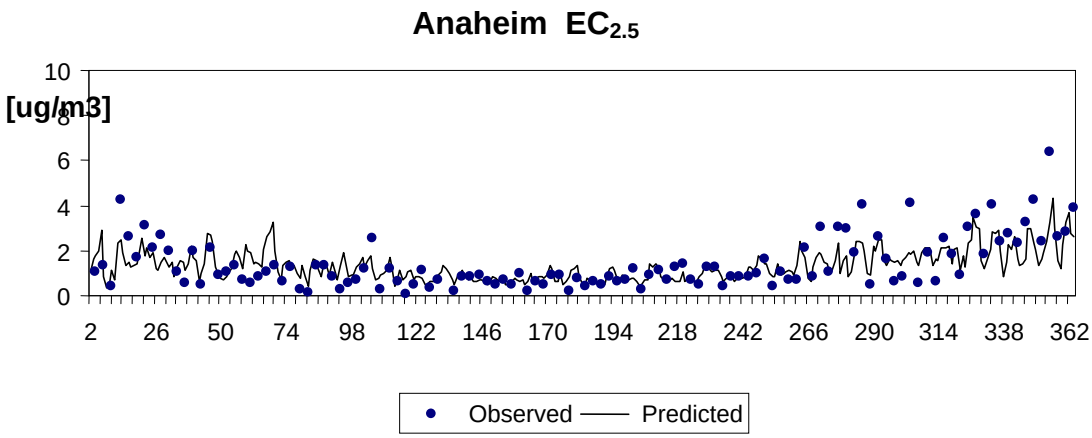

Figure IX-11a
$EC_{2.5}$ Time Series: Simulated Vs. Measured at Anaheim.

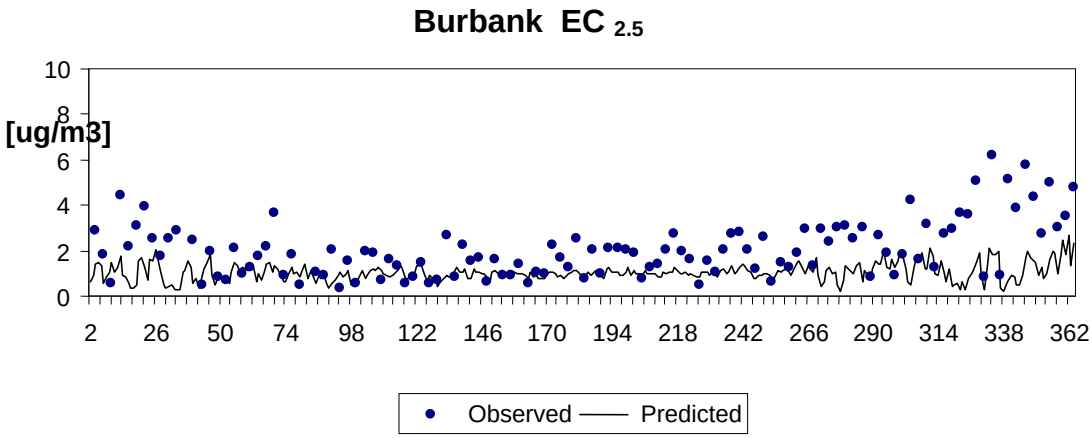

Figure IX-11b
$EC_{2.5}$ Time Series: Simulated Vs. Measured at Burbank.

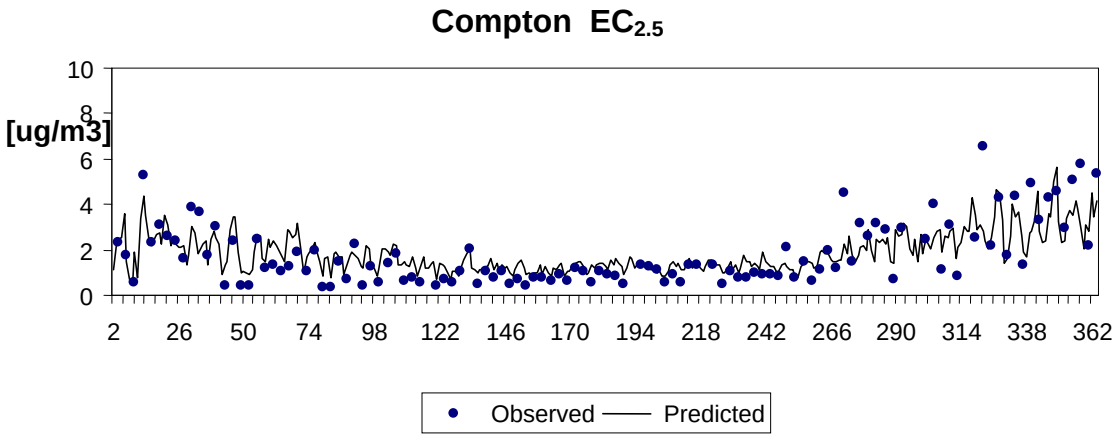

Figure IX-11c
$EC_{2.5}$ Time Series: Simulated Vs. Measured at Compton.

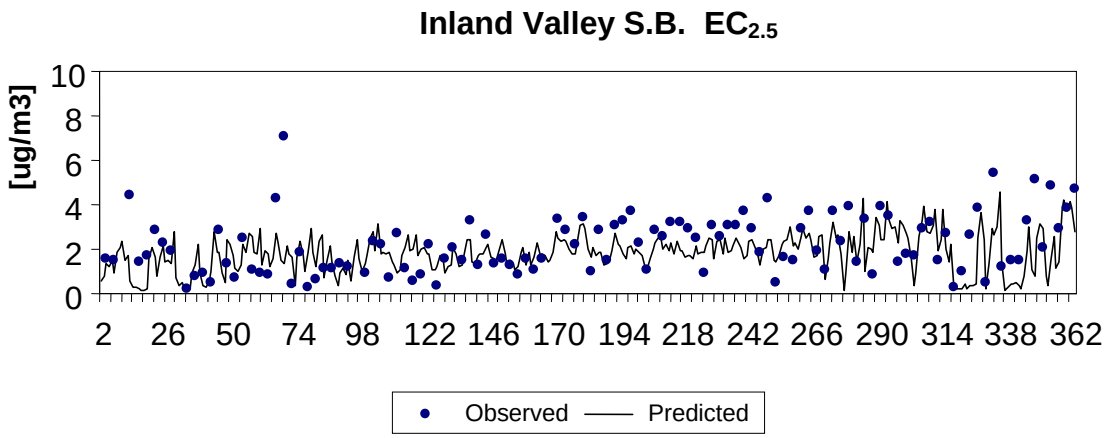

Figure IX-11d
$EC_{2.5}$ Time Series: Simulated Vs. Measured at Inland Valley San Bernardino.

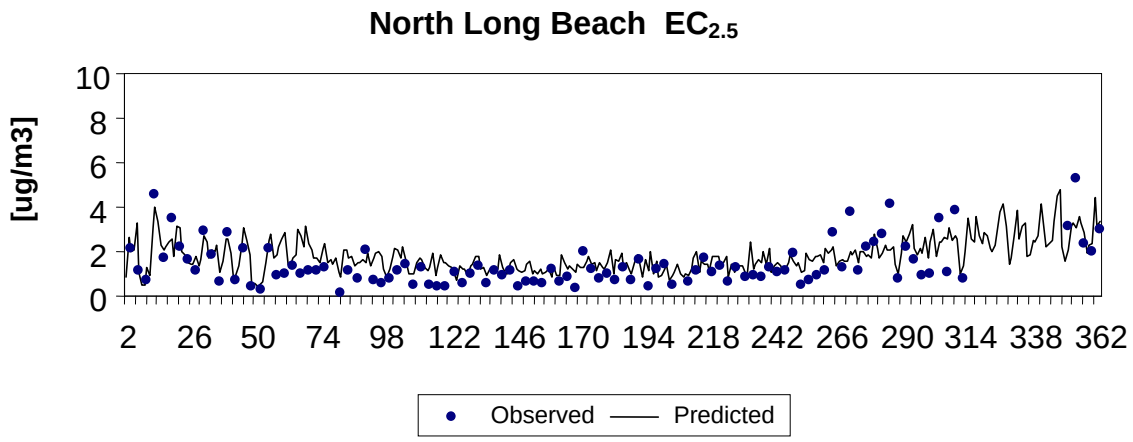

Figure IX-11e
$EC_{2.5}$ Time Series: Simulated Vs. Measured at North Long Beach.

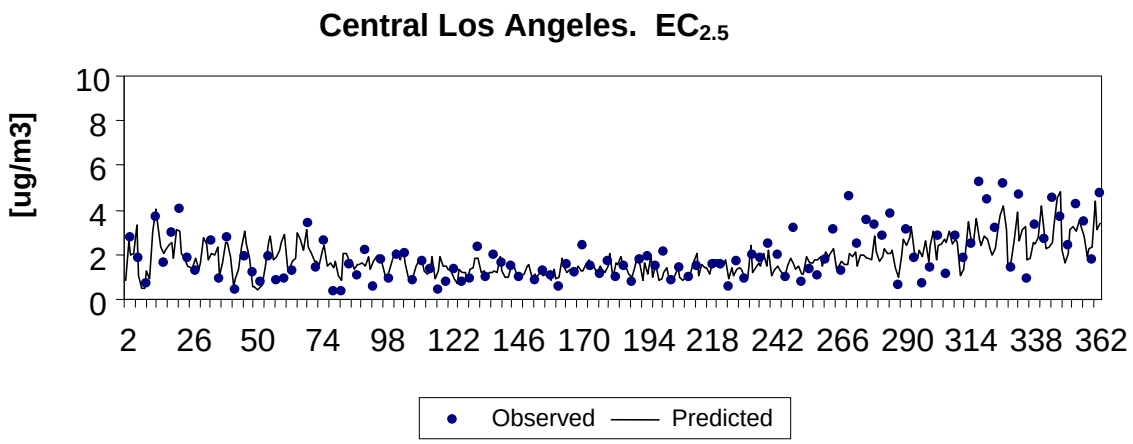

Figure IX-11f
$EC_{2.5}$ Time Series: Simulated Vs. Measured at Central Los Angeles.

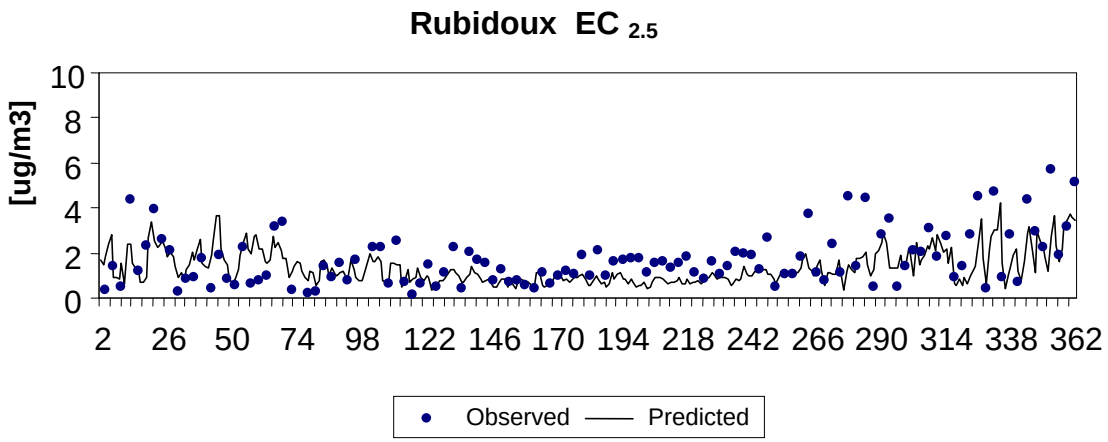

Figure IX-11g
$EC_{2.5}$ Time Series: Simulated Vs. Measured at Rubidoux.

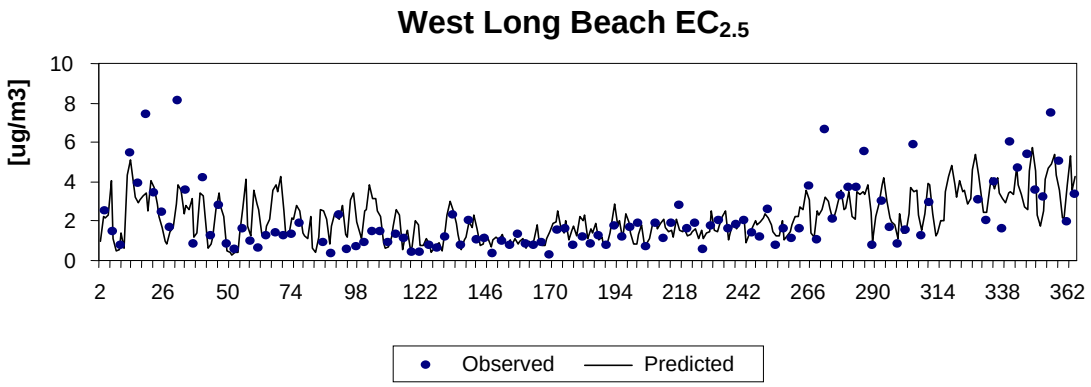

Figure IX-11h
$EC_{2.5}$ Time Series: Simulated Vs. Measured at West Long Beach.

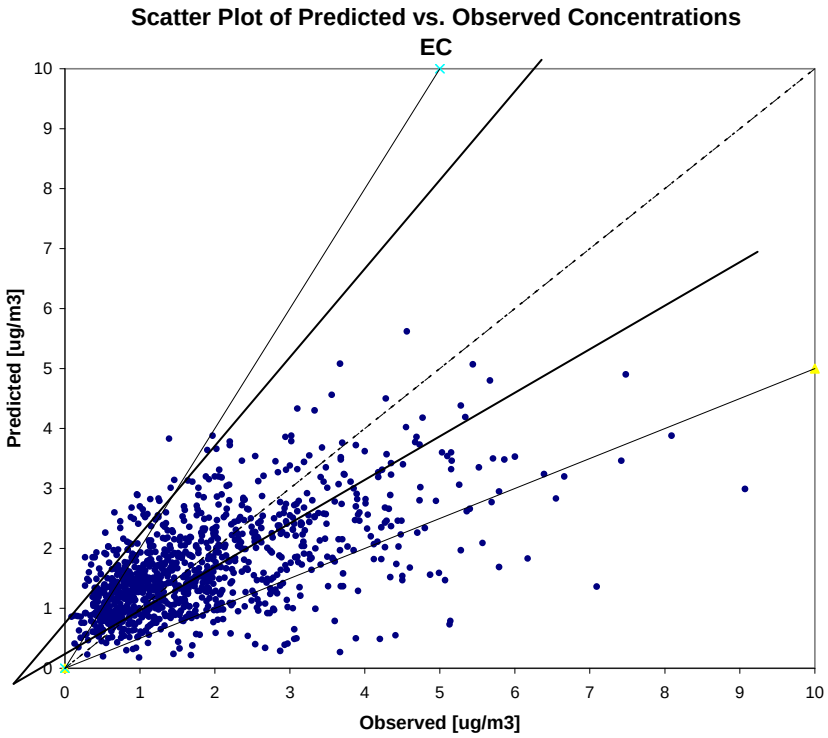

Figure IX-12
$EC_{2.5}$ Bivariate Scatter Plot Simulated Vs. Measured All Stations.

Table IX-11
Toxic Compounds Simulated and Measured:
Six-Station Annual Average Concentrations
2005 MATES III and 1998-99 CAMx RTRAC Analyses

Toxic Compound	Units	2005 MATES III		1998-99 MATES II (CAMx RTRAC Simulation)	
		Measured Annual Average	Simulated Annual Average	Measured Annual Average	Simulated Annual Average
$EC_{2.5}$	$\mu g/m^3$	1.78	1.58	N/A	N/A
EC_{10}	$\mu g/m^3$	2.04	2.05	3.01	2.03
Cr6 (TSP)	$\eta g/m^3$	0.22	0.21	0.18	0.17
As (2.5)	$\eta g/m^3$	0.5	0.92	N/A	N/A
As (TSP)	$\eta g/m^3$	0.68	2.46	1.79	3.00
Cd (2.5)	$\eta g/m^3$	1.46	0.49	N/A	N/A
Cd (TSP)	$\eta g/m^3$	1.56	0.78	6.57	1.00
Ni (2.5))	$\eta g/m^3$	3.93	3.65	N/A	N/A
Ni (TSP)	$\eta g/m^3$	4.44	5.82	7.51	6.83
Pb (2.5)	$\eta g/m^3$	5.41	2.60	N/A	N/A
Pb (TSP)	$\eta g/m^3$	10.64	8.68	22.72	10.00
Benzene	Ppb	0.53	0.52	0.97	0.75
Perchloroethylene	Ppb	0.06	0.09	0.27	0.18
p-Dichlorobenzene	Ppb	0.03	0.08	0.12	0.06
Methylene Chloride	Ppb	0.35	0.32	0.70	0.54
Trichloroethylene	Ppb	0.03	0.03	0.10	0.05
1,3Butadiene	Ppb	0.1	0.09	0.29	0.13
Formaldehyde	Ppb	3.61	3.26	4.00	3.75
Acetaldehyde	Ppb	1.64	1.12	1.81	1.26
Naphthalene	Ppb	0.02*	0.01	N/A	0.02

* Two station average

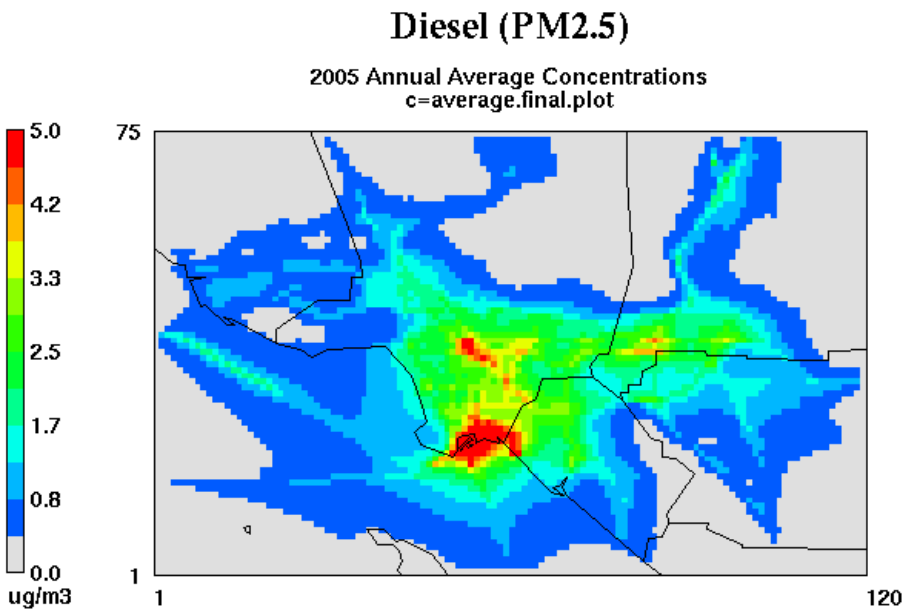

FIGURE IX-13a
CAMx simulated 2005 annual average Diesel $PM_{2.5}$.

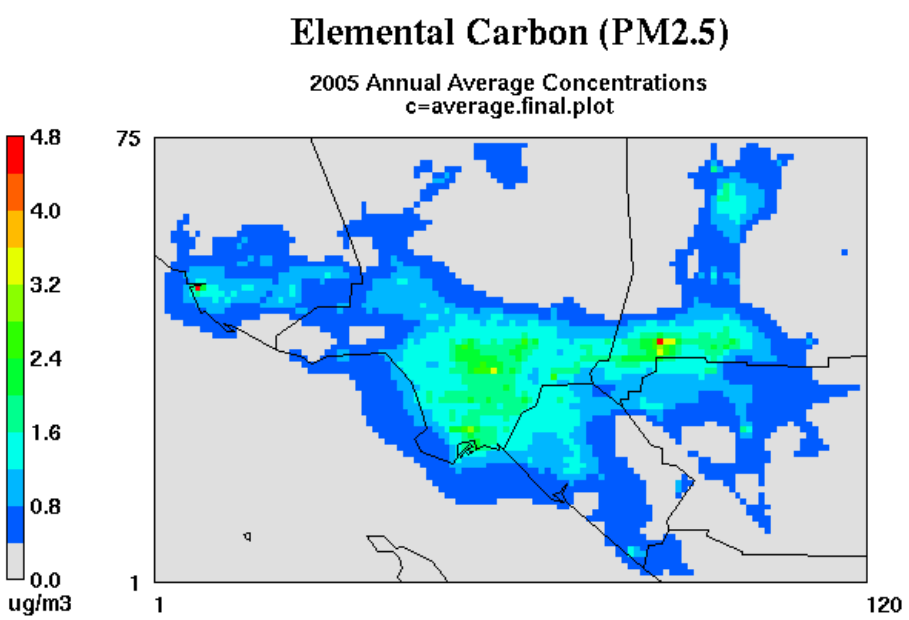

FIGURE IX-13b
CAMx simulated 2005 annual average Elemental Carbon $PM_{2.5}$.

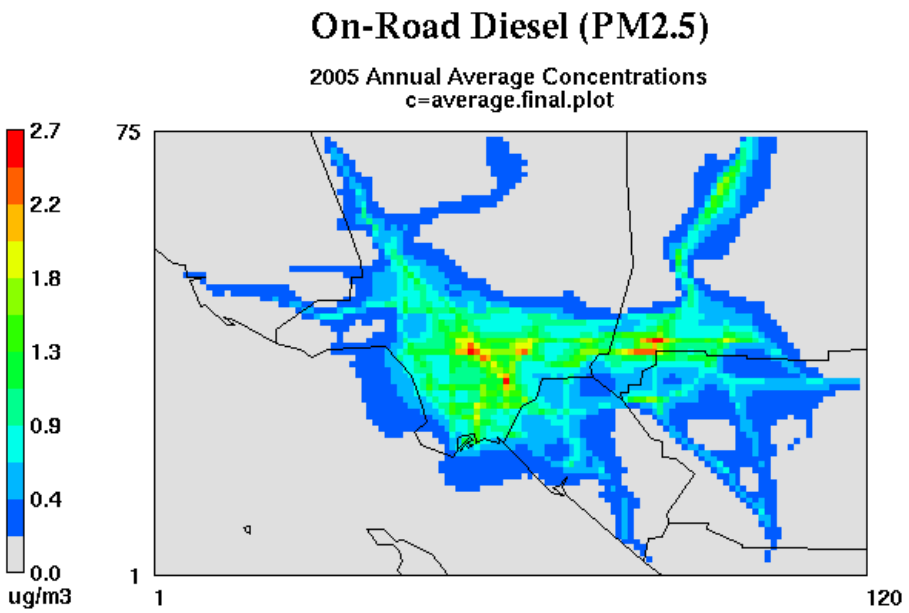

FIGURE IX-13c
CAMx simulated 2005 annual average On-Road Diesel $PM_{2.5}$.

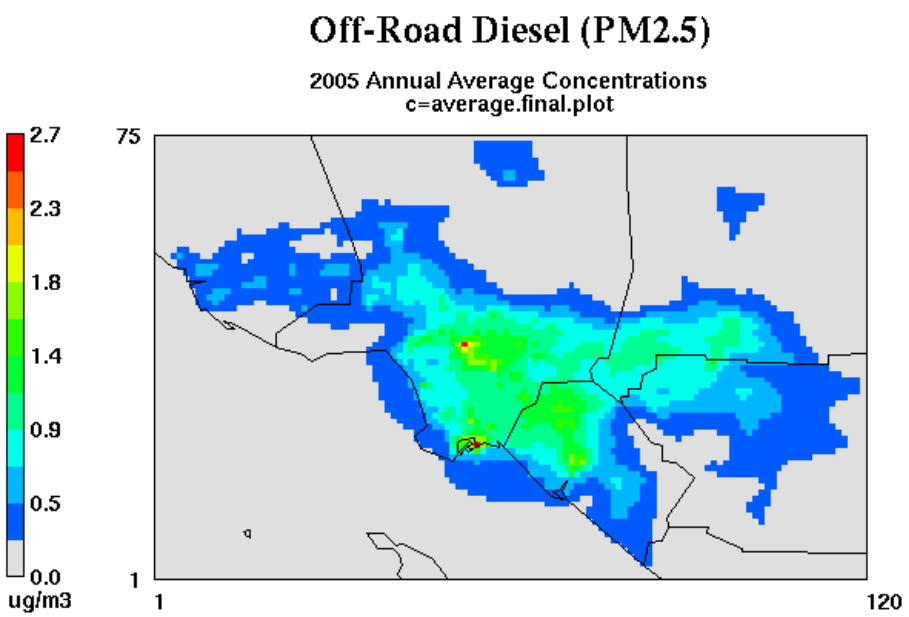

FIGURE IX-13d
CAMx simulated 2005 annual average Off-Road Diesel $PM_{2.5}$.

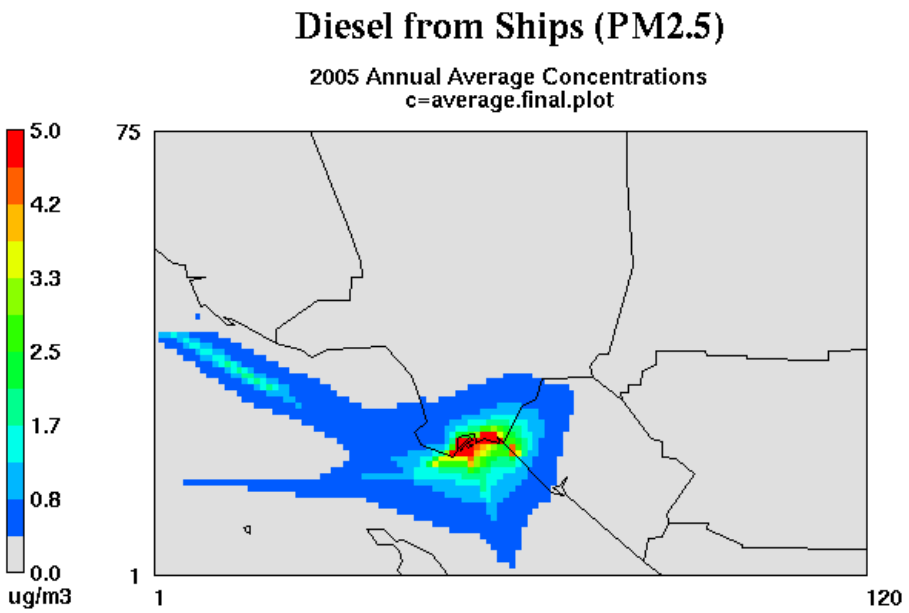

FIGURE IX-13e
CAMx simulated 2005 annual average Diesel from Ships $PM_{2.5}$.

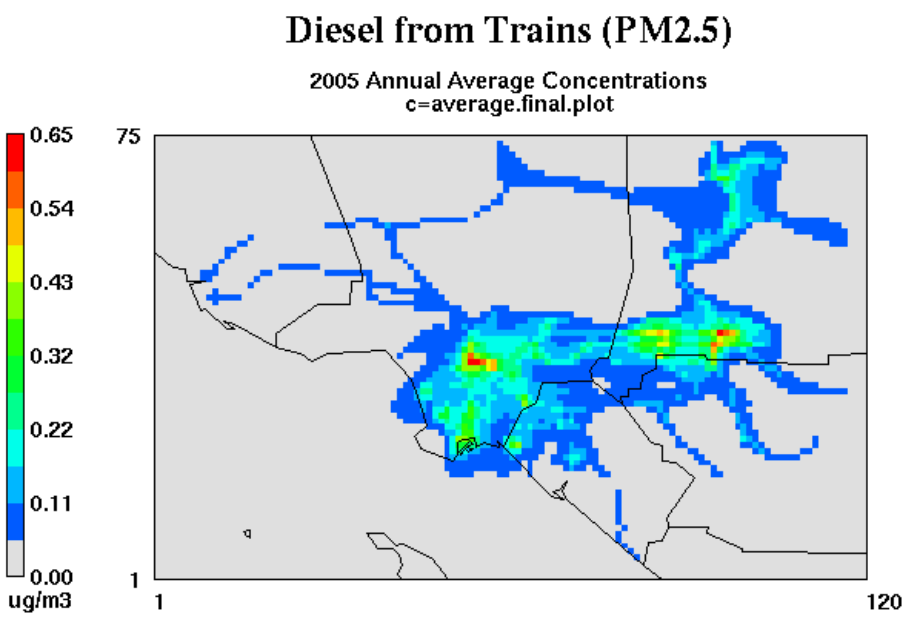

FIGURE IX-13f
CAMx simulated 2005 annual average Diesel from Trains $PM_{2.5}$.

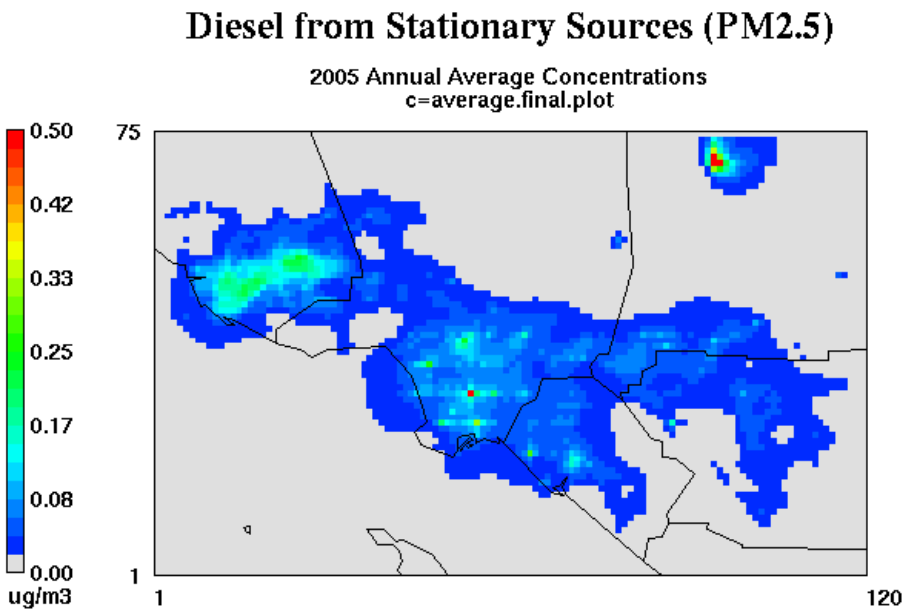

FIGURE IX-13g
CAMx simulated 2005 annual average Diesel from Stationary Sources $PM_{2.5}$.

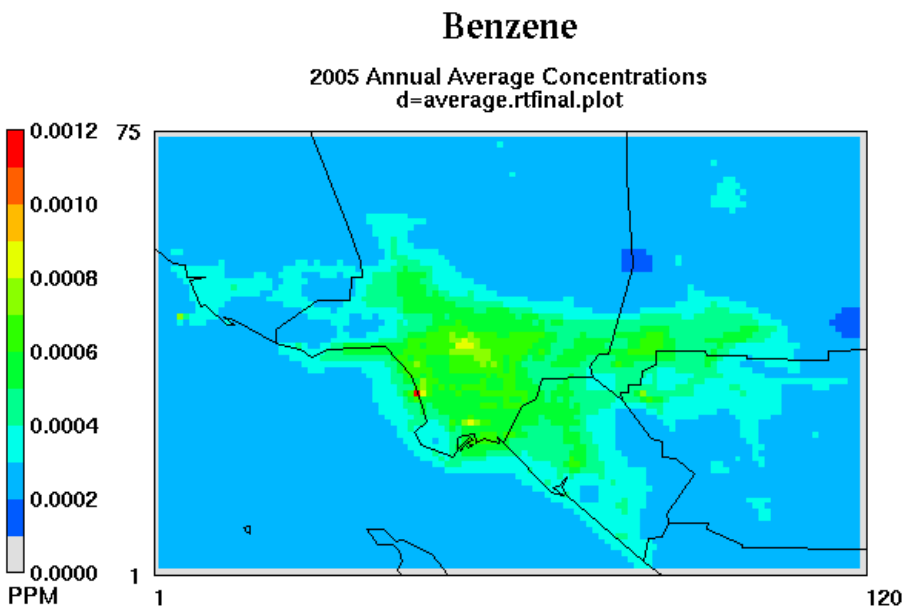

FIGURE IX-13h
CAMx simulated 2005 annual average Benzene.

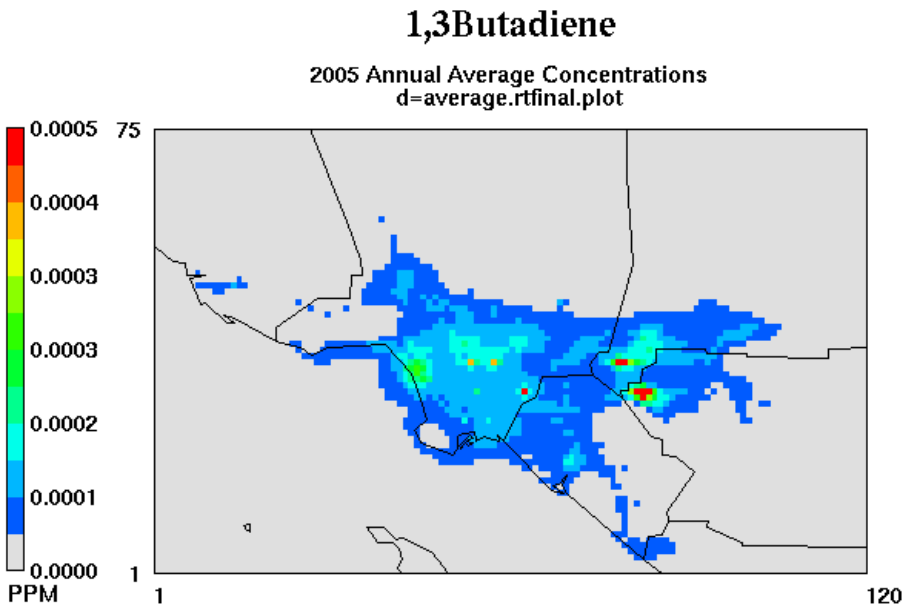

FIGURE IX-13i
CAMx simulated 2005 annual average 1,3 Butadiene.

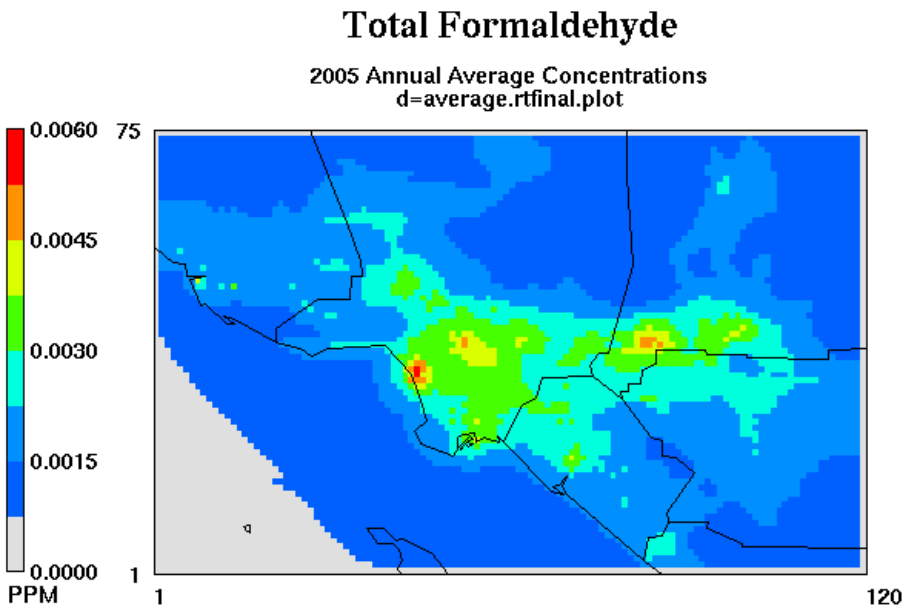

FIGURE IX-13j
CAMx simulated 2005 annual average for Total Formaldehyde.

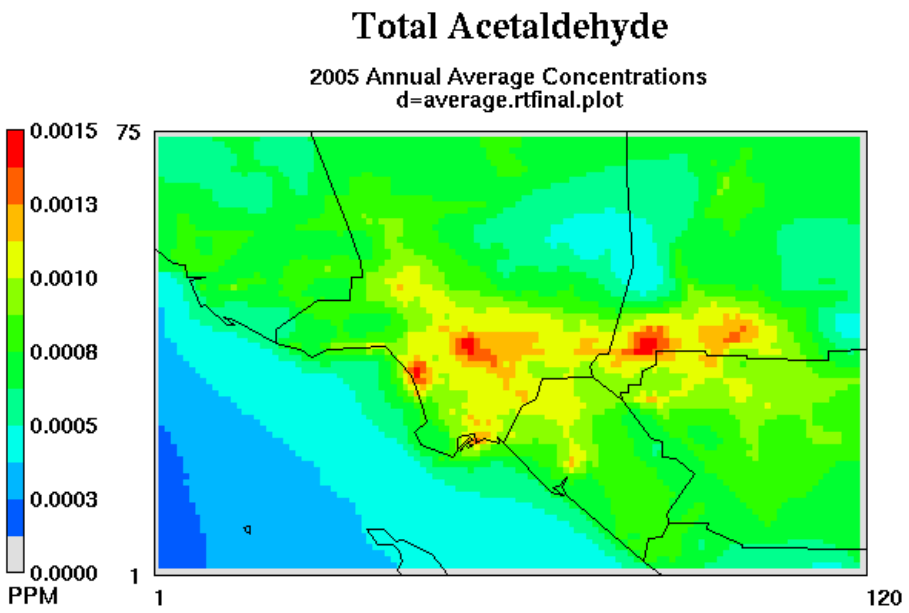

FIGURE IX-13k
CAMx simulated 2005 annual average Acetaldehyde.

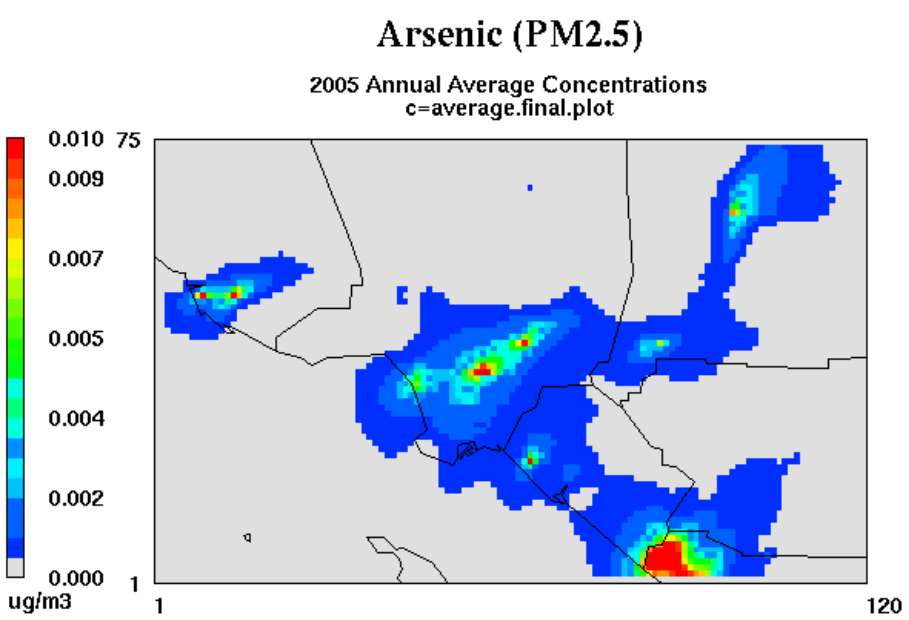

FIGURE IX-13l
CAMx simulated 2005 annual average Arsenic $PM_{2.5}$.

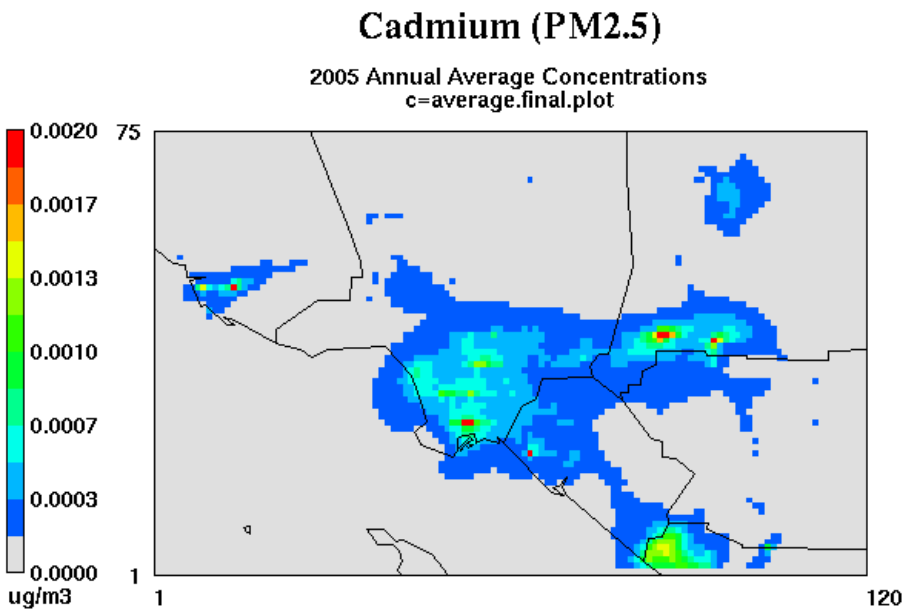

FIGURE IX-13m
CAMx simulated 2005 annual average Cadmium $PM_{2.5}$.

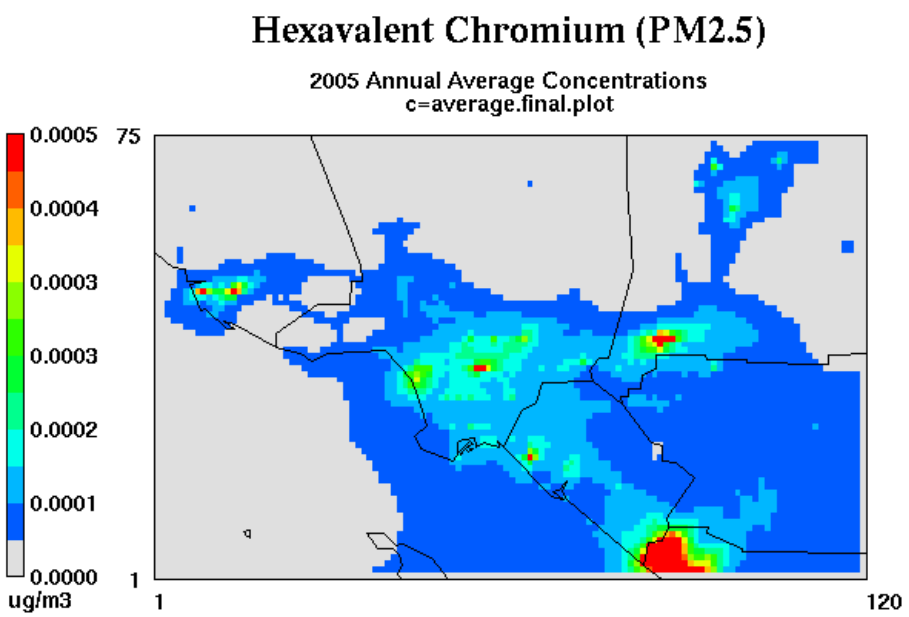

FIGURE IX-13n
CAMx simulated 2005 annual average Chromium $PM_{2.5}$.

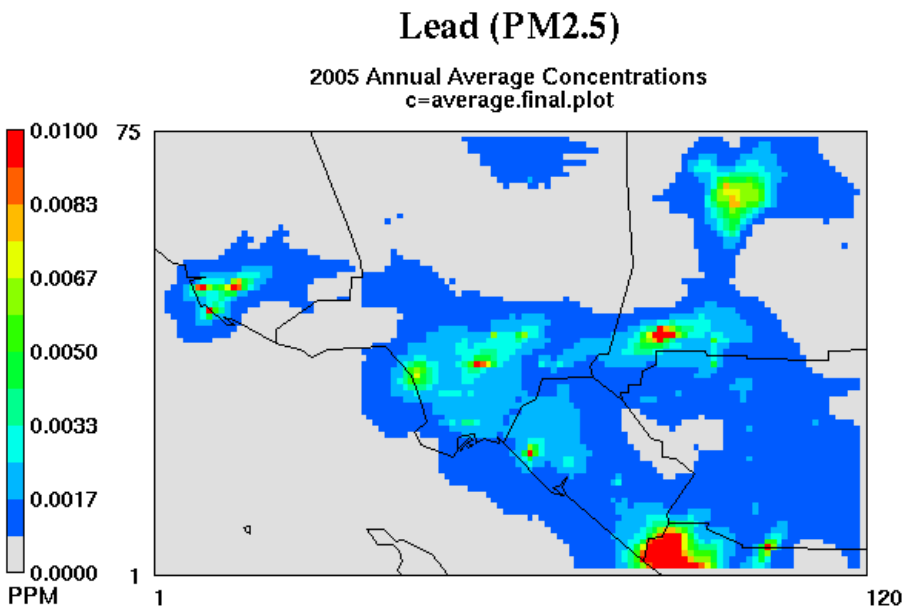

FIGURE IX-13o
CAMx simulated 2005 annual average Lead $PM_{2.5}$.

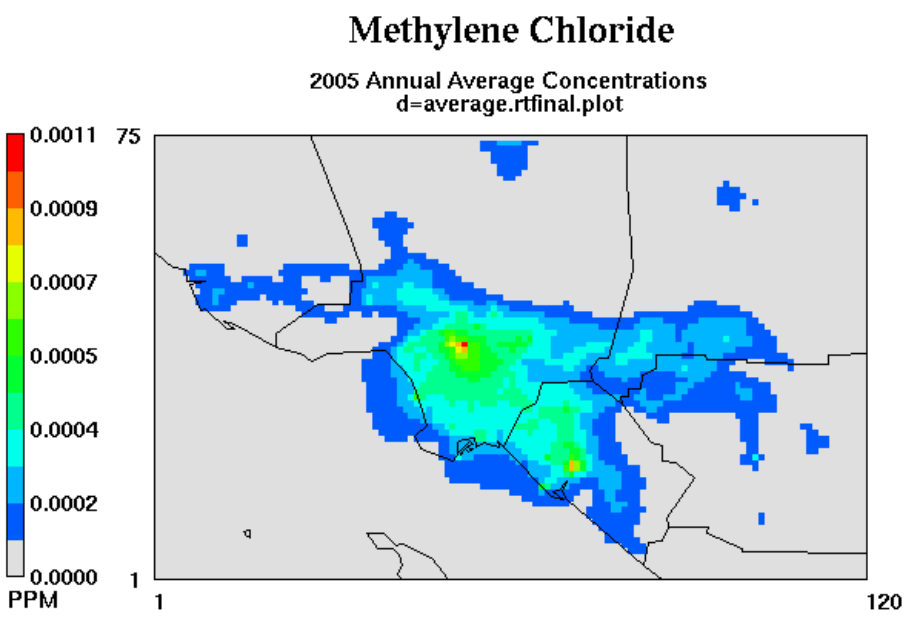

FIGURE IX-13p
CAMx simulated 2005 annual average Methylene Chloride.

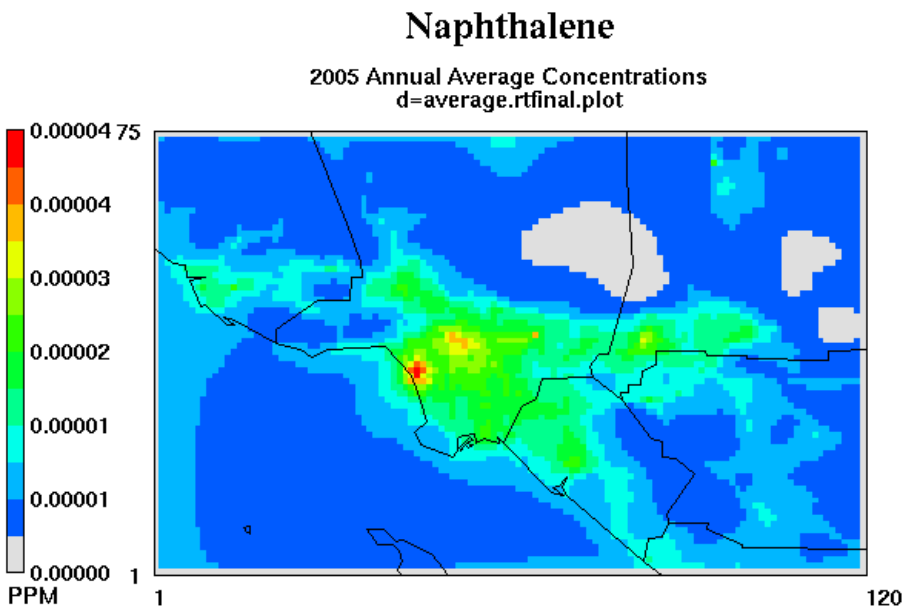

FIGURE IX-13q
CAMx simulated 2005 annual average Naphthalene.

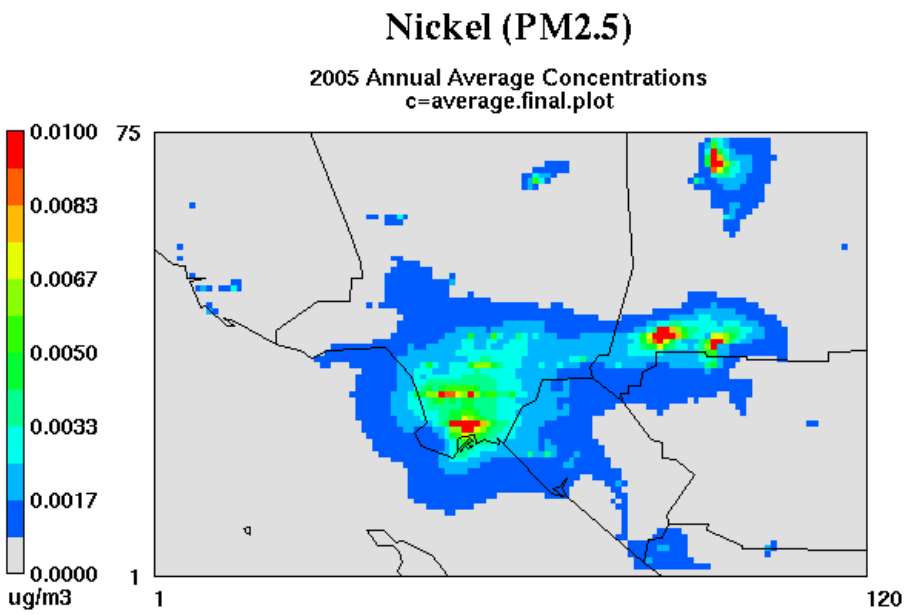

FIGURE IX-13r
CAMx simulated 2005 annual average Nickel $PM_{2.5}$.

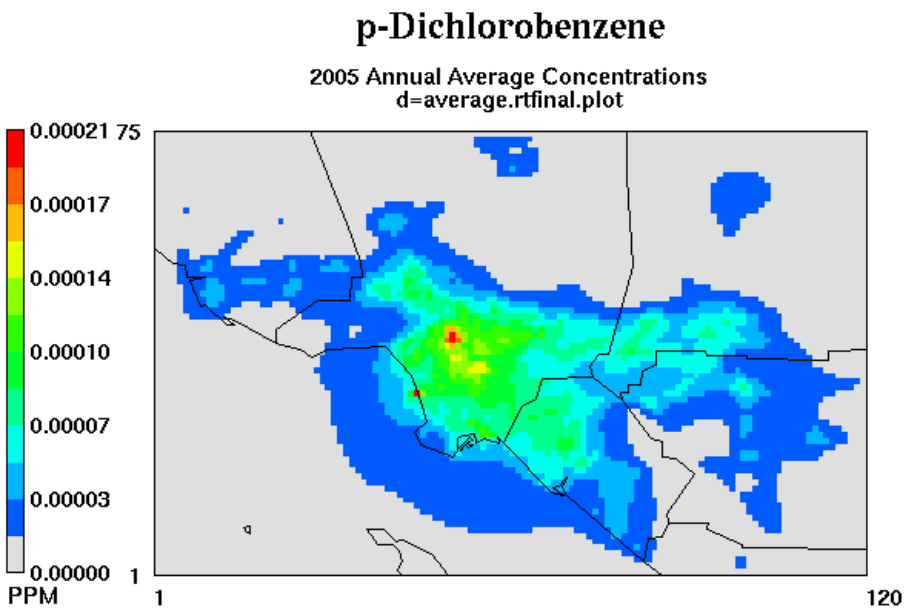

FIGURE IX-13s
CAMx simulated 2005 annual average p-Dichlorobenzene.

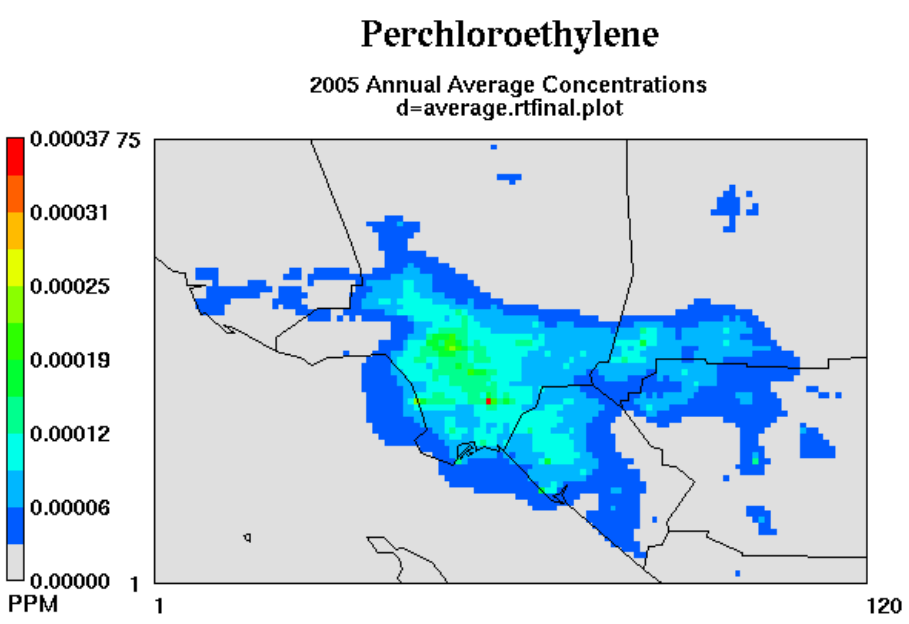

FIGURE IX-13t
CAMx simulated 2005 annual average Perchloroethylene.

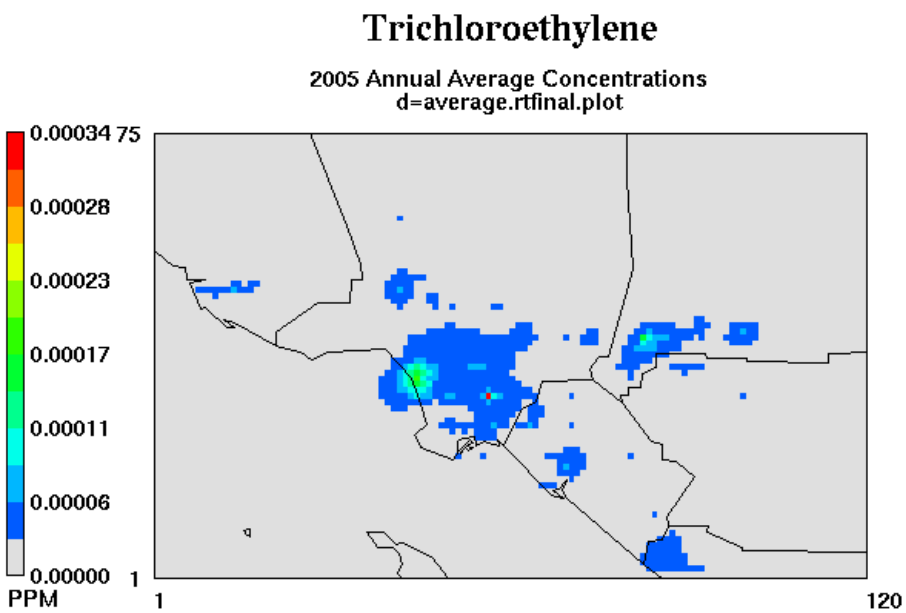

FIGURE IX-13u
CAMx simulated 2005 annual average Trichloroethylene.

Estimation of Risk

Figure IX-14 depicts the distribution of risk estimated from the predicted annual average concentrations of the key toxic compounds. (Figure IX-14 is presented twice, first in shaded black and white, then in color). Risk is calculated for each grid cell as follows:

$$\text{Risk}_{i,j} = \Sigma\ \text{Concentration}_{i,j,k} \text{ X Risk Factor}_{i,j,k}$$

Where $_{i,j}$ is the grid cell (easting, northing) and k is the toxic compound.

The grid cell having the maximum simulated risk of 3,693 was located in the Ports of Los Angeles and Long Beach. More specifically, the grids having the top 25 estimated risk values in 2005 were located in cells around the ports area. The cell having the highest risk outside of the port area occurred in South Los Angeles as part of a cluster of grids that extended from Central Los Angeles to the southeast, following Interstate 5. Other elevated areas included the eastern Basin near the communities of Colton, Inland Valley San Bernardino, and San Bernardino. As with the MATES II analysis, areas projected to have higher risk followed transportation corridors, including freeways and railways.

Figure IX-15 provides the CAMx RTRAC simulated risk for the 1998-99 period (using back-cast 1998 emissions and 1998-99 MM5 generated meteorological data fields). Figure IX-16 depicts the 1998-99 to 2005 change in risk estimated from the CAMx RTRAC simulations. The greatest increase in risk occurred in the port area. Overall, air toxics risk improves to varying levels in

most of the Basin with the exceptions of the areas directly downwind of the Ports and those areas heavily impacted by activities associated with goods movement. Risk increases of more than 800 in a million between the two periods were noted in the immediate areas encompassing the ports.

The 2005 Basin average population weighted risk summed for the toxic components yielded a lifetime estimated cancer risk of 853 in a million. (The Basin average risk included all populated over-land cells that reside within the Basin portion of the modeling domain). The MATES III Basin population weighted average risk is approximately 87% of the MATES II Basin average risk (981 per million) determined from the UAMTOX modeling analysis. However, when Basin population weighted average risk is recalculated for the 1998-99 MATES II period based on the CAMx RTRAC simulations the comparable Basin average risk is 931 per million. A direct comparison of Basin population weighted risk calculated using the CAMx RTRAC simulations shows an 8% improvement between 1998-99 and 2005. The 8% reduction in Basin risk can be attributed to several factors most notably changes in quantity and spatial allocation of emissions between 1998 and 2005. While weather profile between the two monitoring periods varied, no appreciable difference was observed in the meteorological dispersion potential.

Figures IX-17a through IX-17f depict risk associated with diesel and its specific emissions categories. Figure I-17 provides the Basin risk excluding the contribution of diesel particulates. (Again, Figures IX-16a through IX-17 are presented twice, first in shaded black and white, then in color). On and off-road diesel impacts are spread throughout the Basin following the transportation corridors and off-road facilities such as the intermodal transfer sites. The shipping impacts are concentrated in the vicinity of the Ports of Los Angeles and Long Beach and the adjacent downwind communities. The shipping lanes to the northwest and southeast following the coastline and Asia-bound are clearly depicted. Risk impacts from rail travel/transport and stationary sources range from over 200 to 500 in one million respectively.

Regional risk from nondiesel sources (Figure IX-18) is also uniformly distributed throughout the Basin, with values typically ranging from 100 to 300 in one million. Several elevated grid cells are apparent with risk estimated upwards of 400 in one million in the coastal plain encompassing Los Angeles International Airport and the heavily industrialized areas of south of Downtown Los Angeles. Selected elevated grid cells are also evident in the east Basin with localized risk values of up to 1,000 in one million.

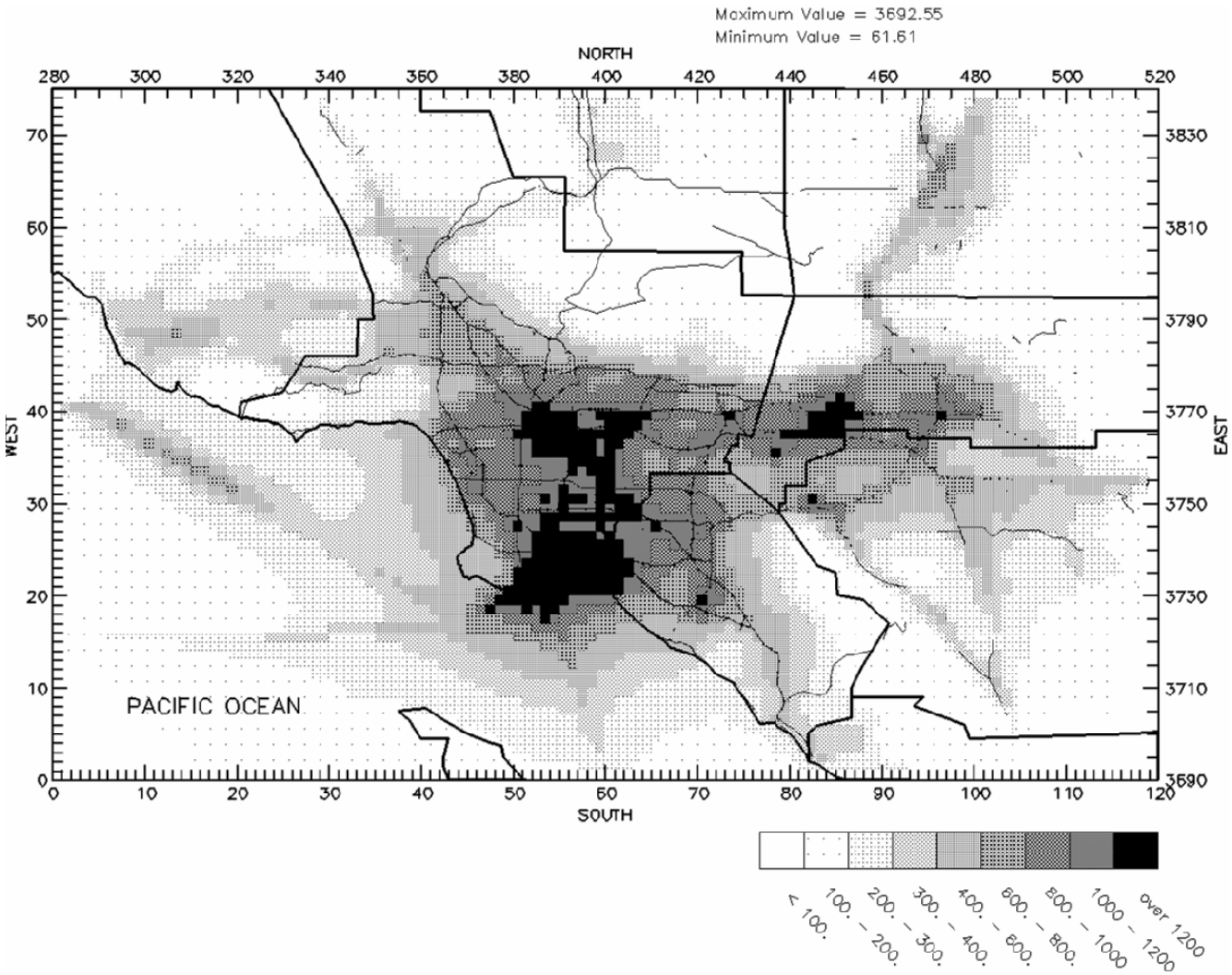

FIGURE IX-14
2005 MATES III CAMx RTRAC Simulated Air Toxic Risk.

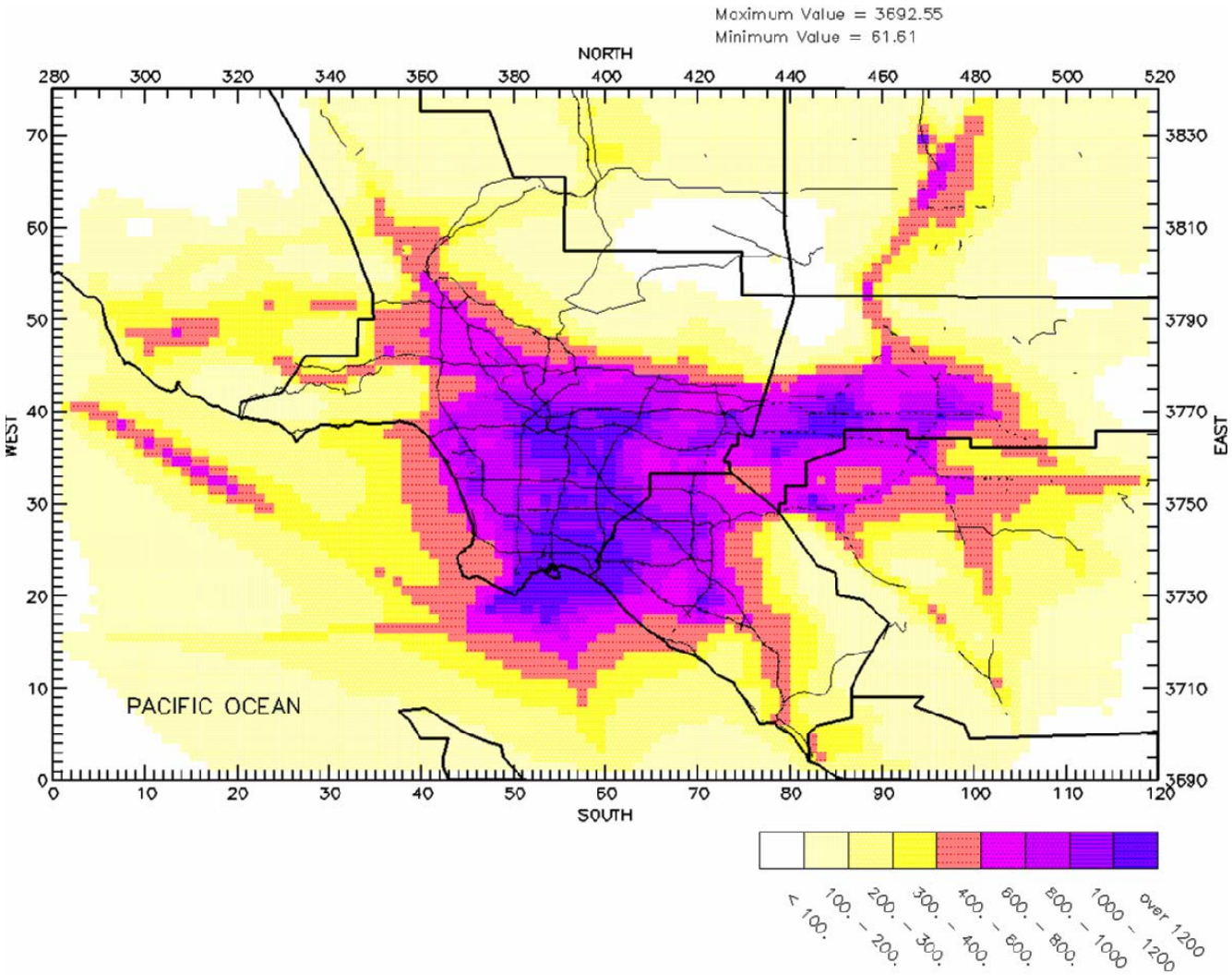

FIGURE IX-14 (Repeated)
2005 MATES III CAMx RTRAC Simulated Air Toxic Risk.

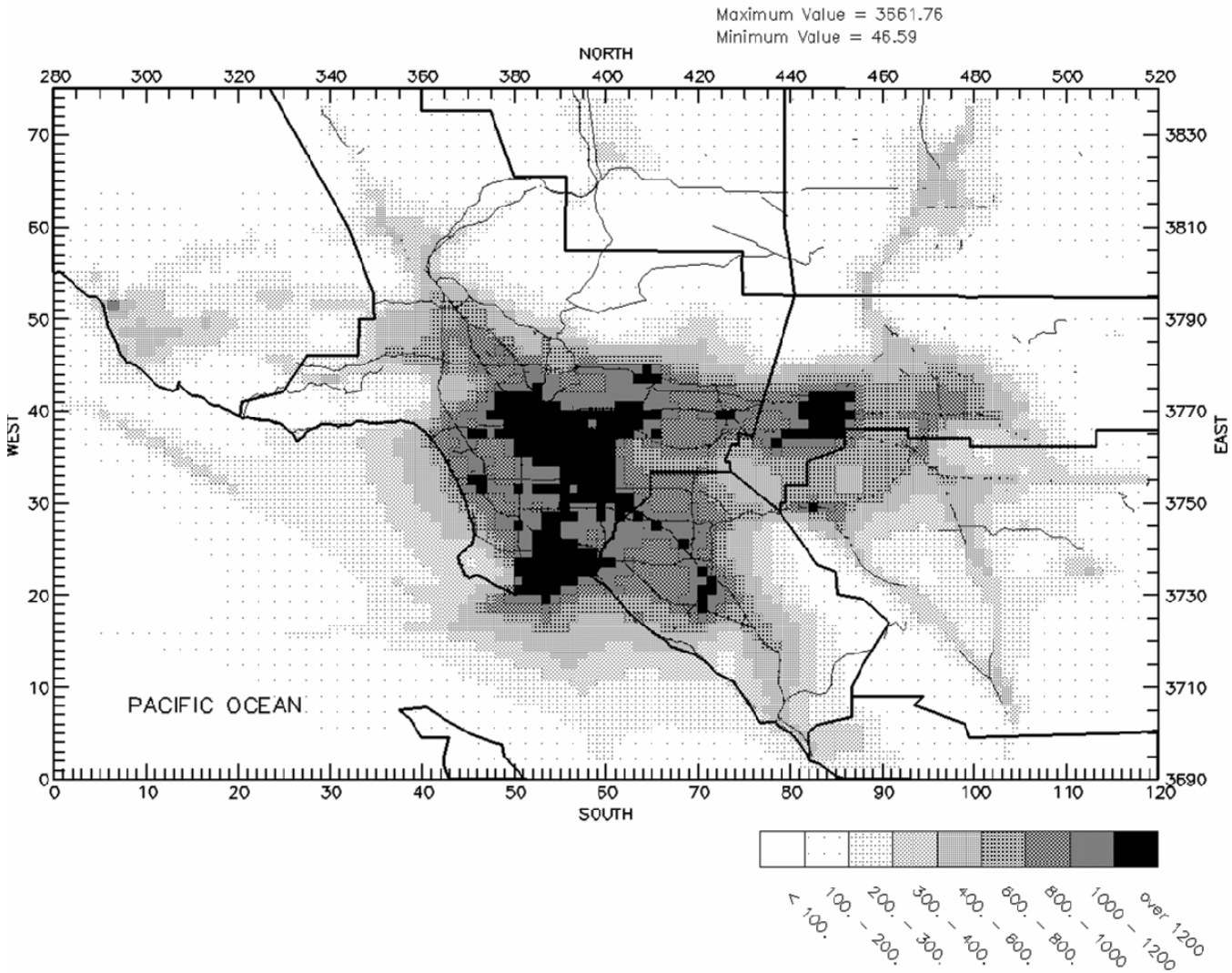

FIGURE IX-15
1998-99 CAMx RTRAC Simulated Air Toxic Risk.

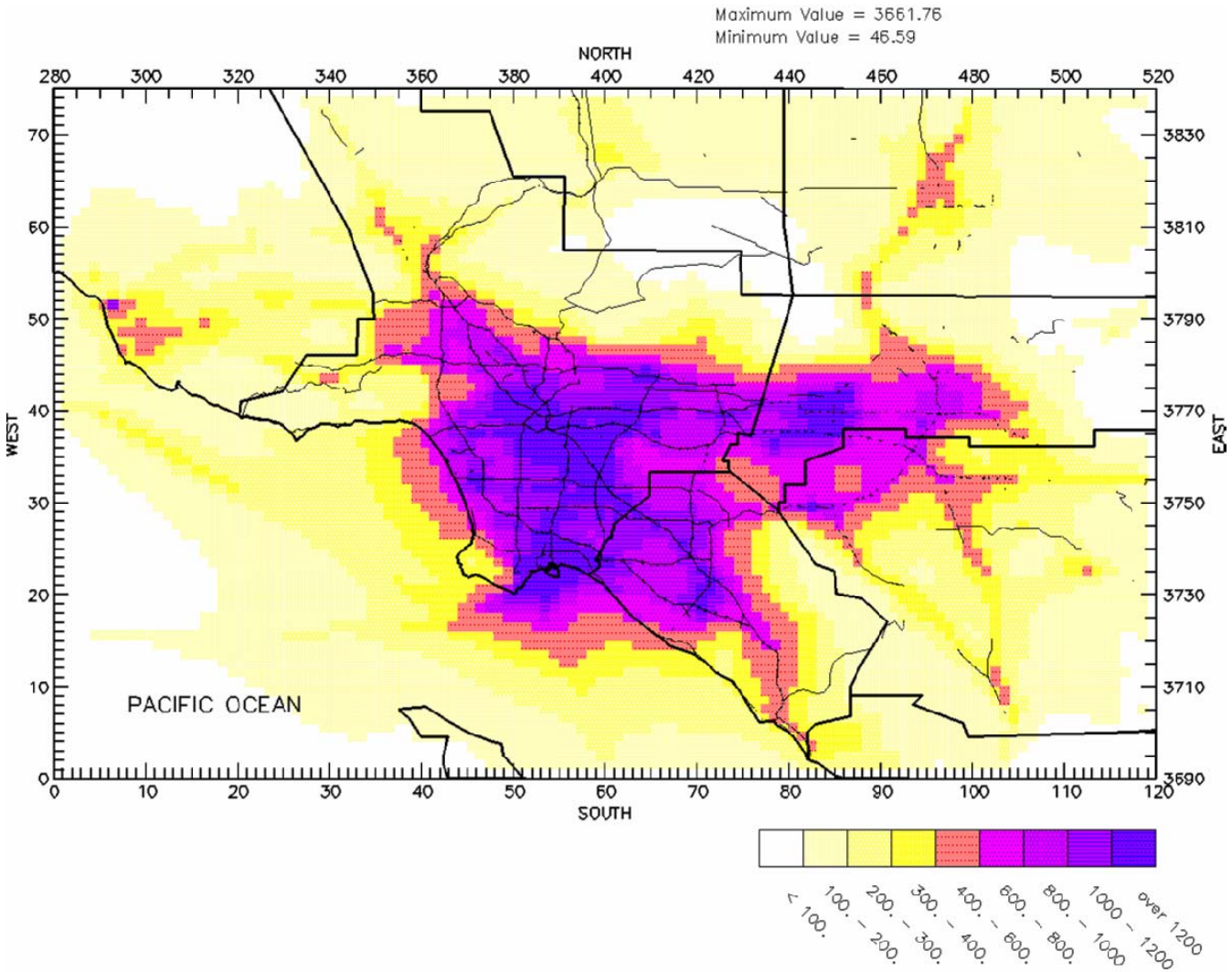

FIGURE IX-15 (Repeated)
1998-99 CAMx RTRAC Simulated Air Toxic Risk.

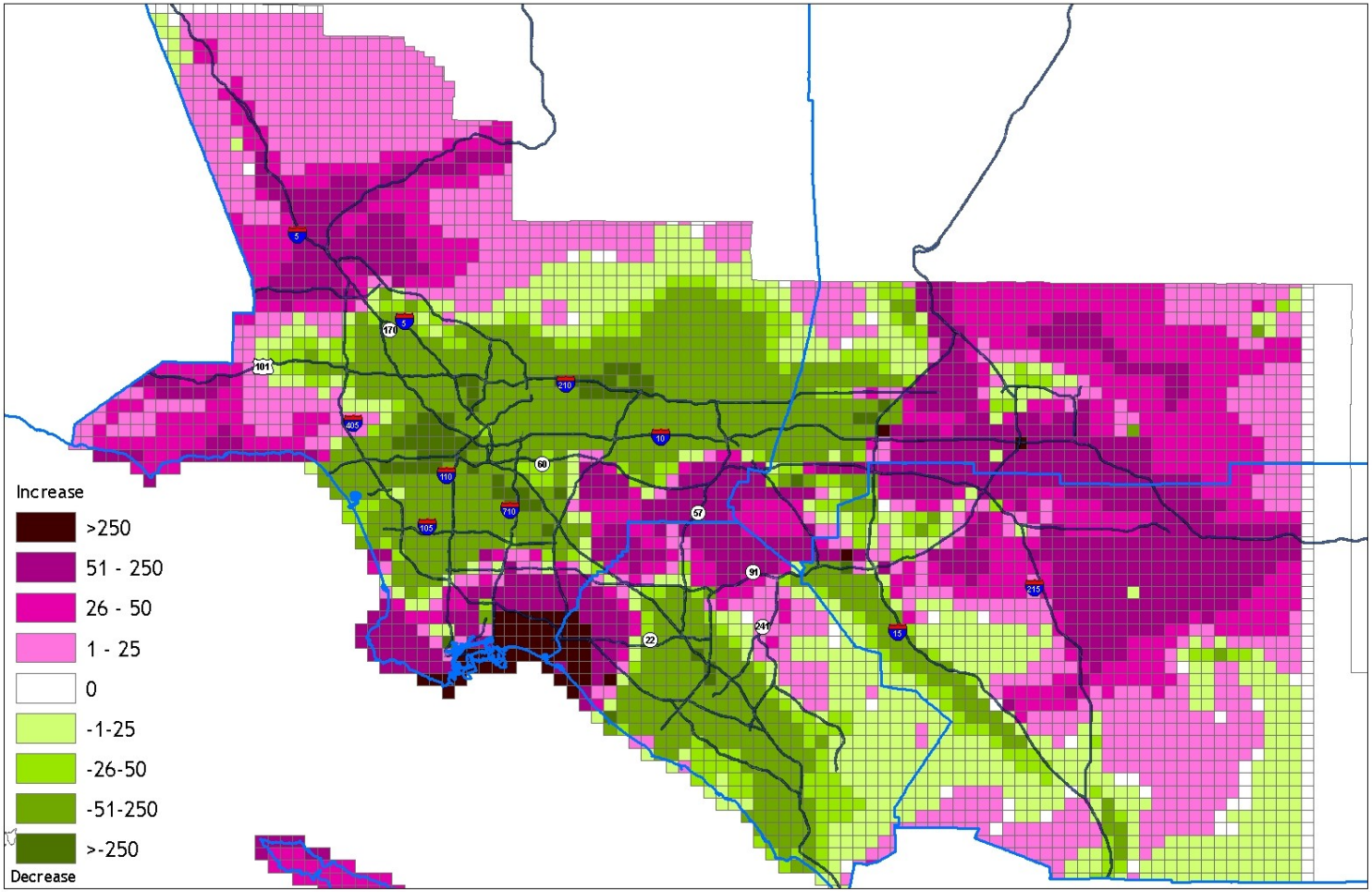

FIGURE IX-16
Change in CAMx RTRAC simulated risk from the 1998-99 to 2005
(using back-cast 1998 emissions and 1998-99 MM5 generated meteorological data fields).

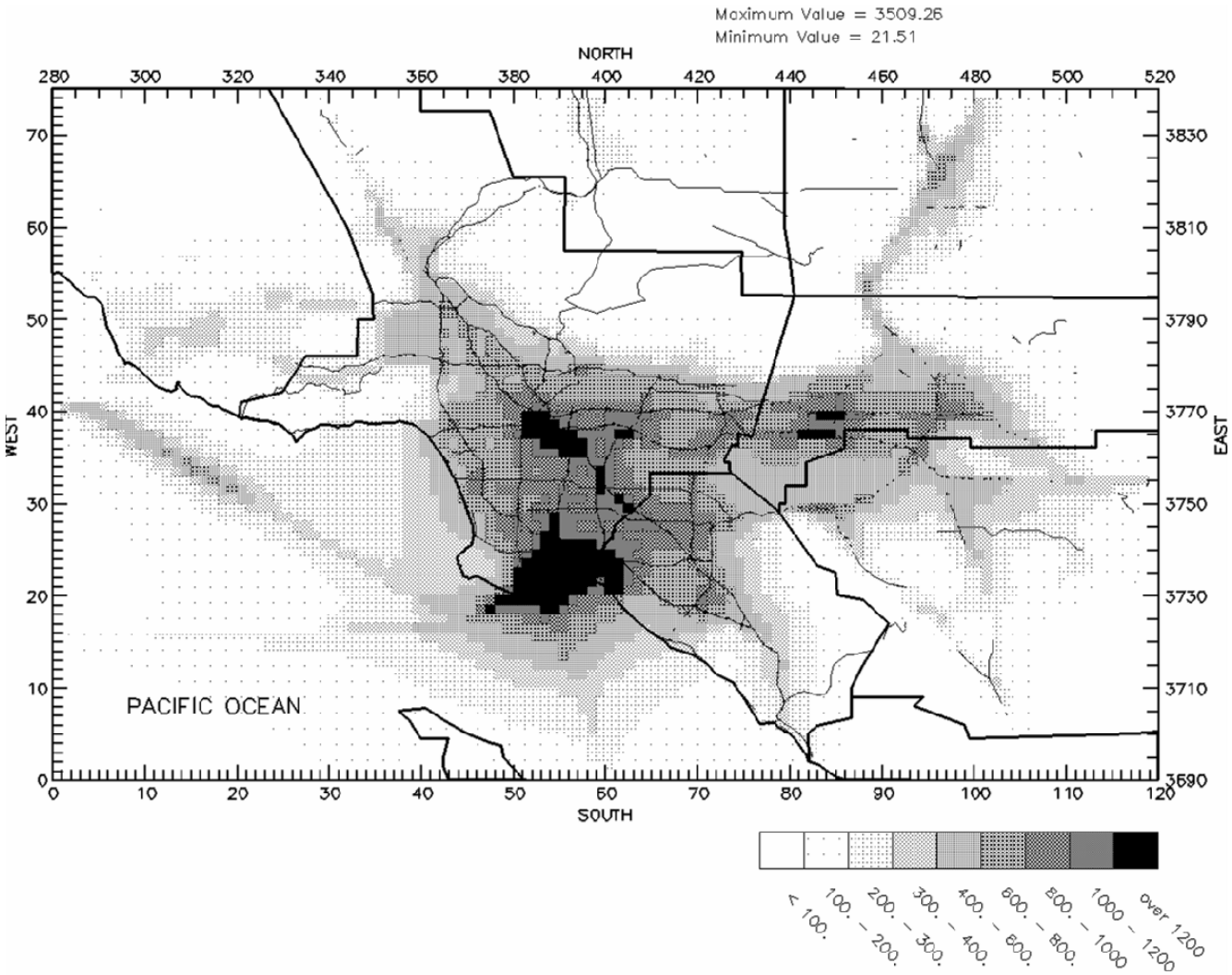

FIGURE IX-17a
MATES III Risk from Diesel.

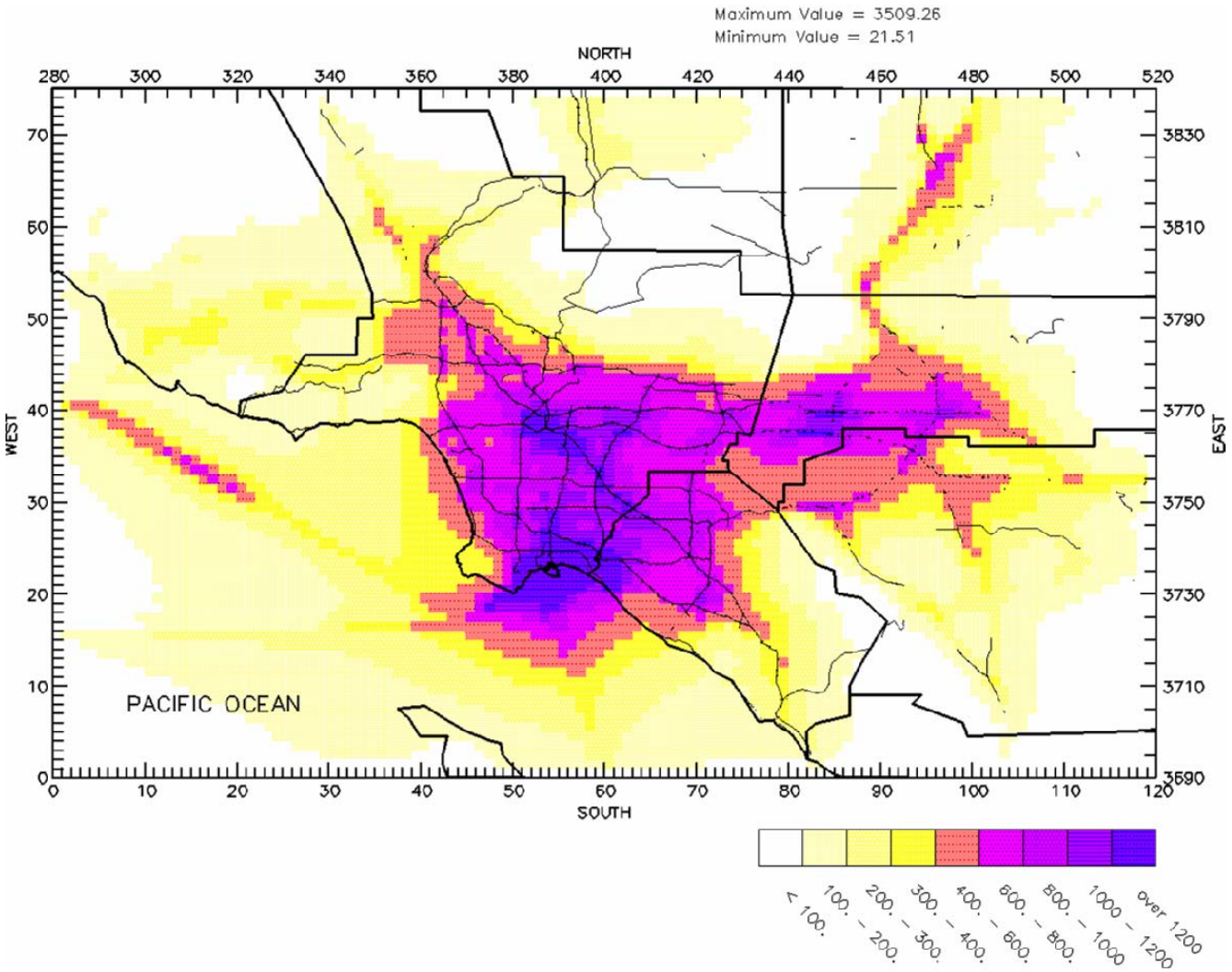

FIGURE IX-17a (Repeated)
MATES III Risk from Diesel.

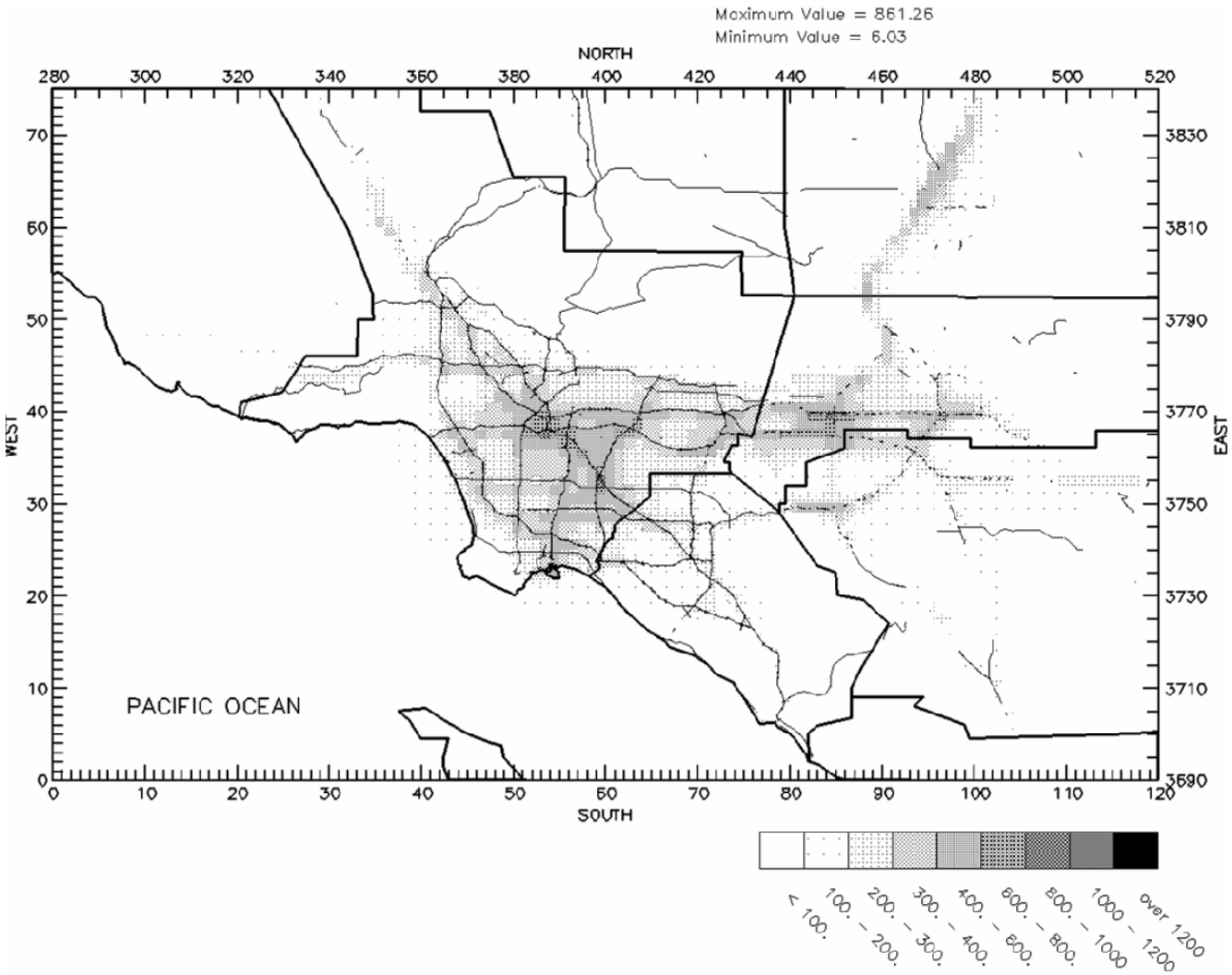

FIGURE IX-17b
MATES III Simulated Risk from On-Road Diesel.

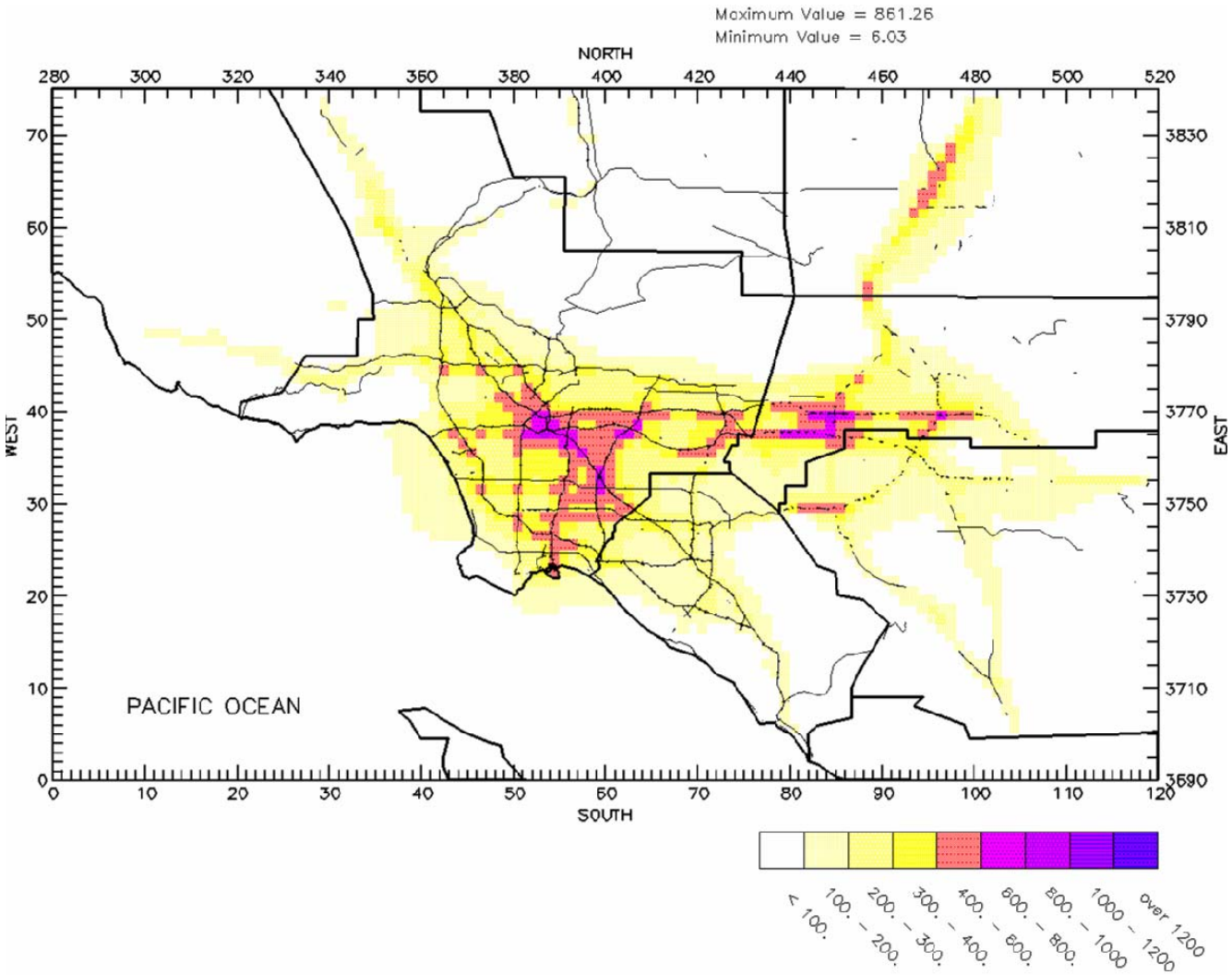

FIGURE IX-17b (Repeated)
MATES III Simulated Risk from On-Road Diesel.

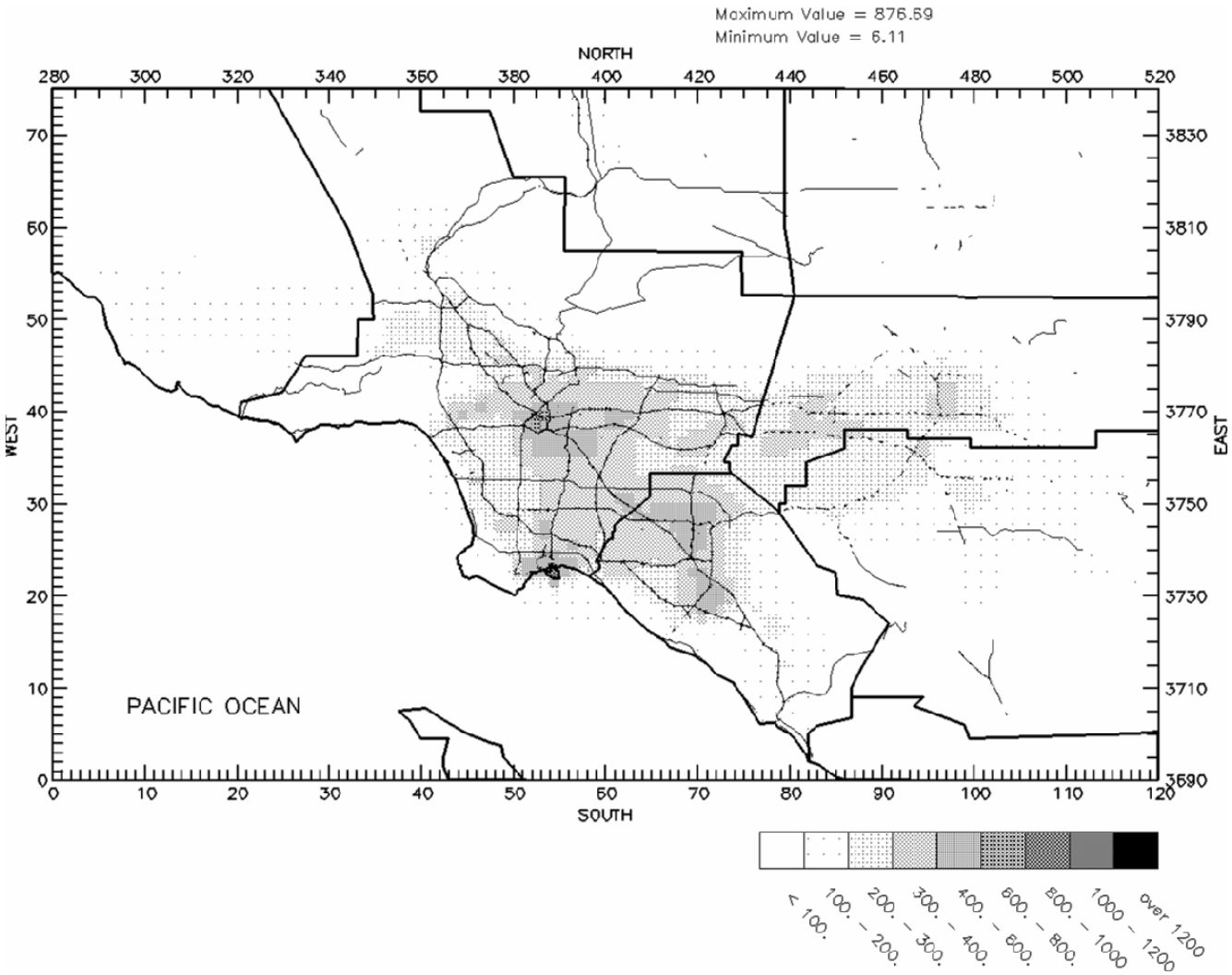

FIGURE IX-17c
MATES III Simulated Risk from Off-road Diesel (including rail yards but excluding trains and ships).

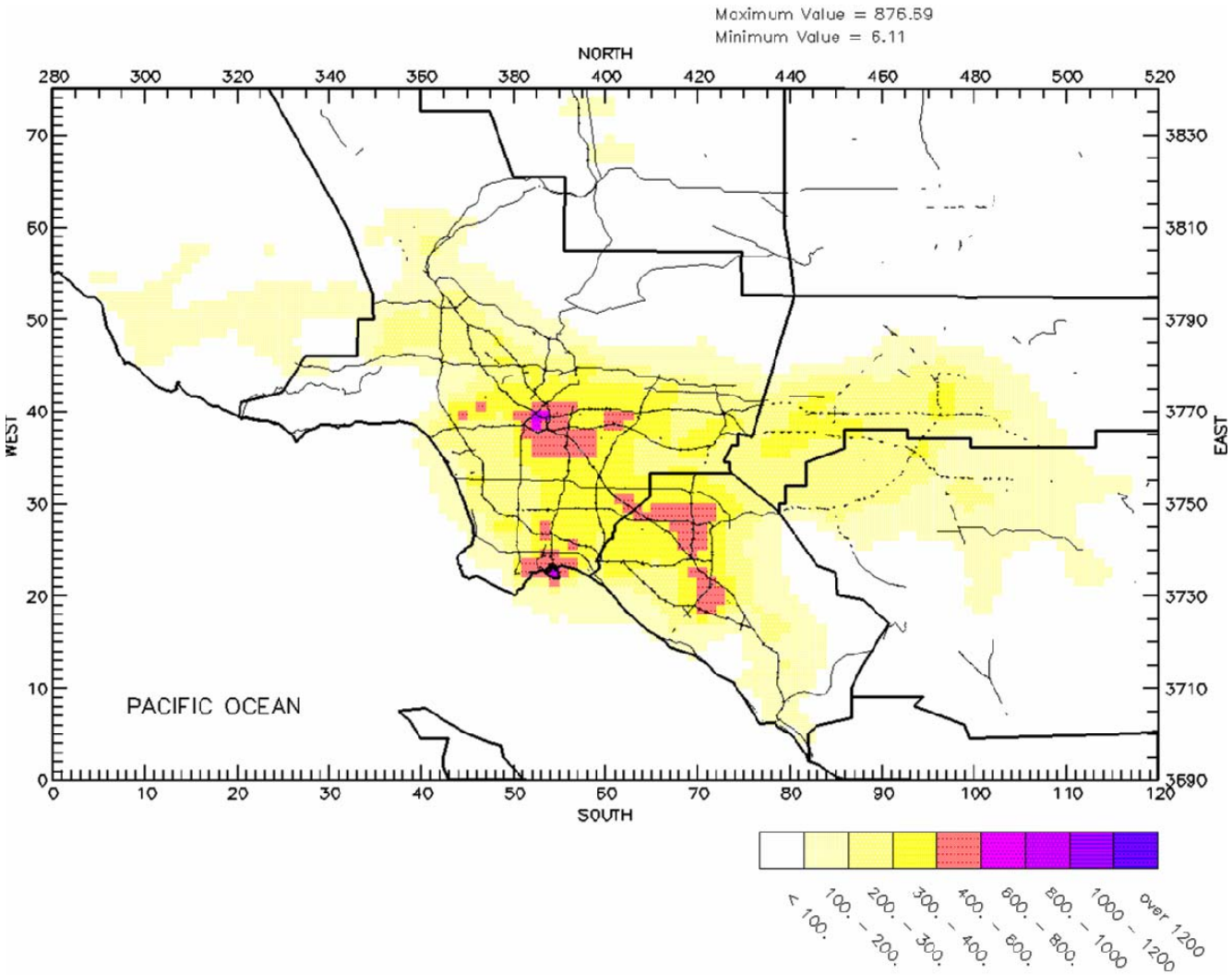

FIGURE IX-17c (Repeated)
MATES III Simulated Risk from Off-road Diesel (including rail yards but excluding trains and ships).

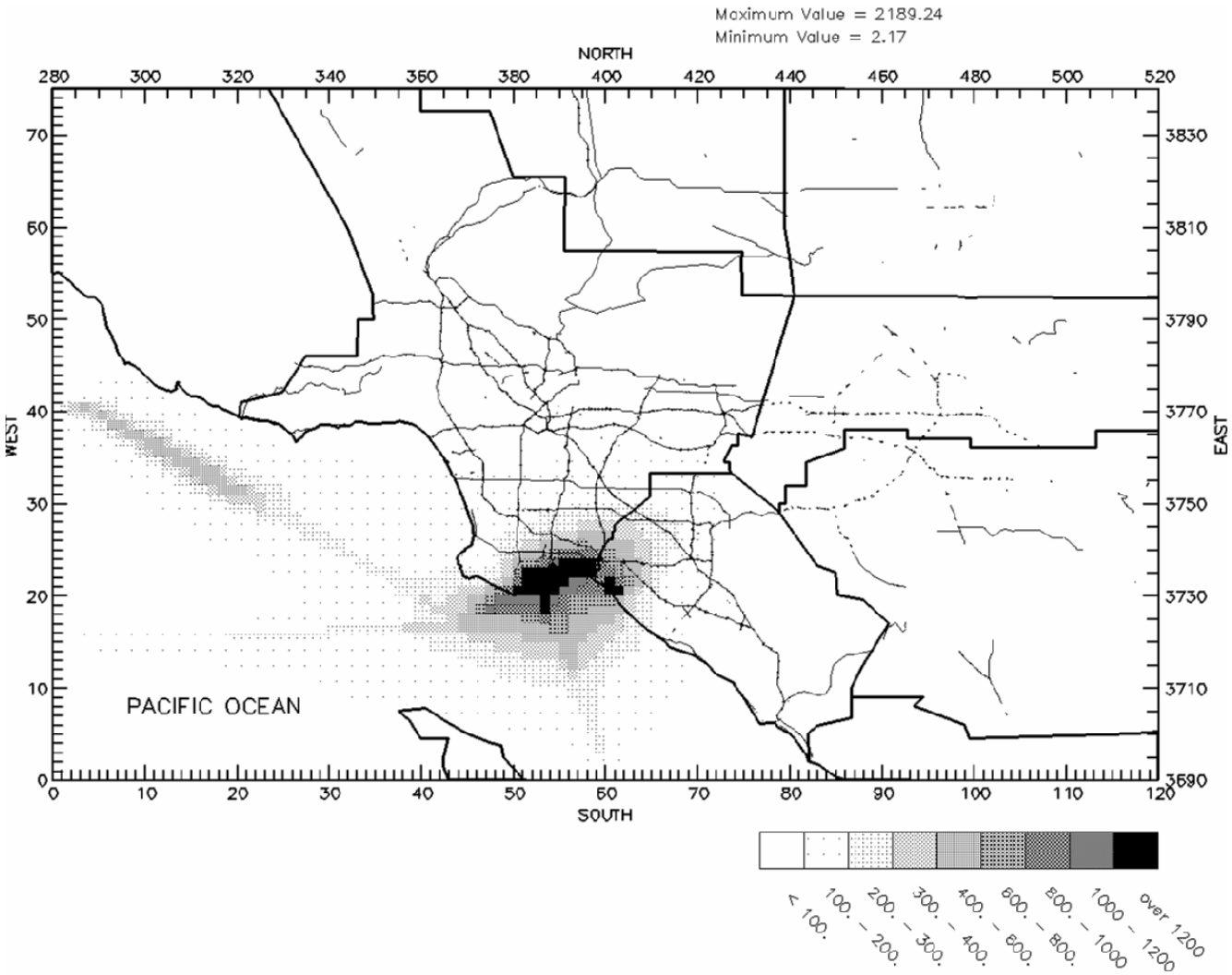

FIGURE IX-17d
MATES III Simulated Risk from Ship Diesel.

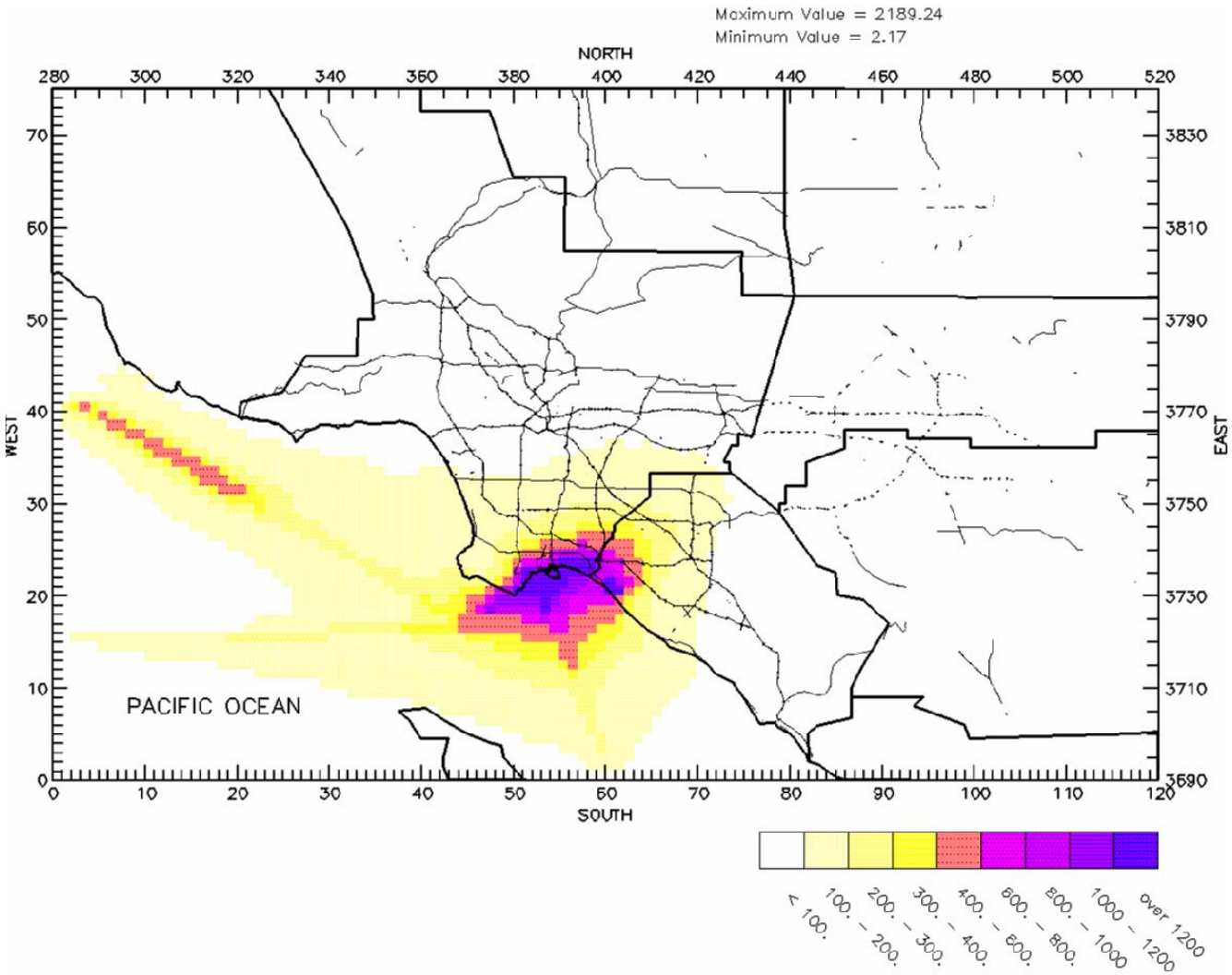

FIGURE IX-17d (Repeated)
MATES III Simulated Risk from Ship Diesel.

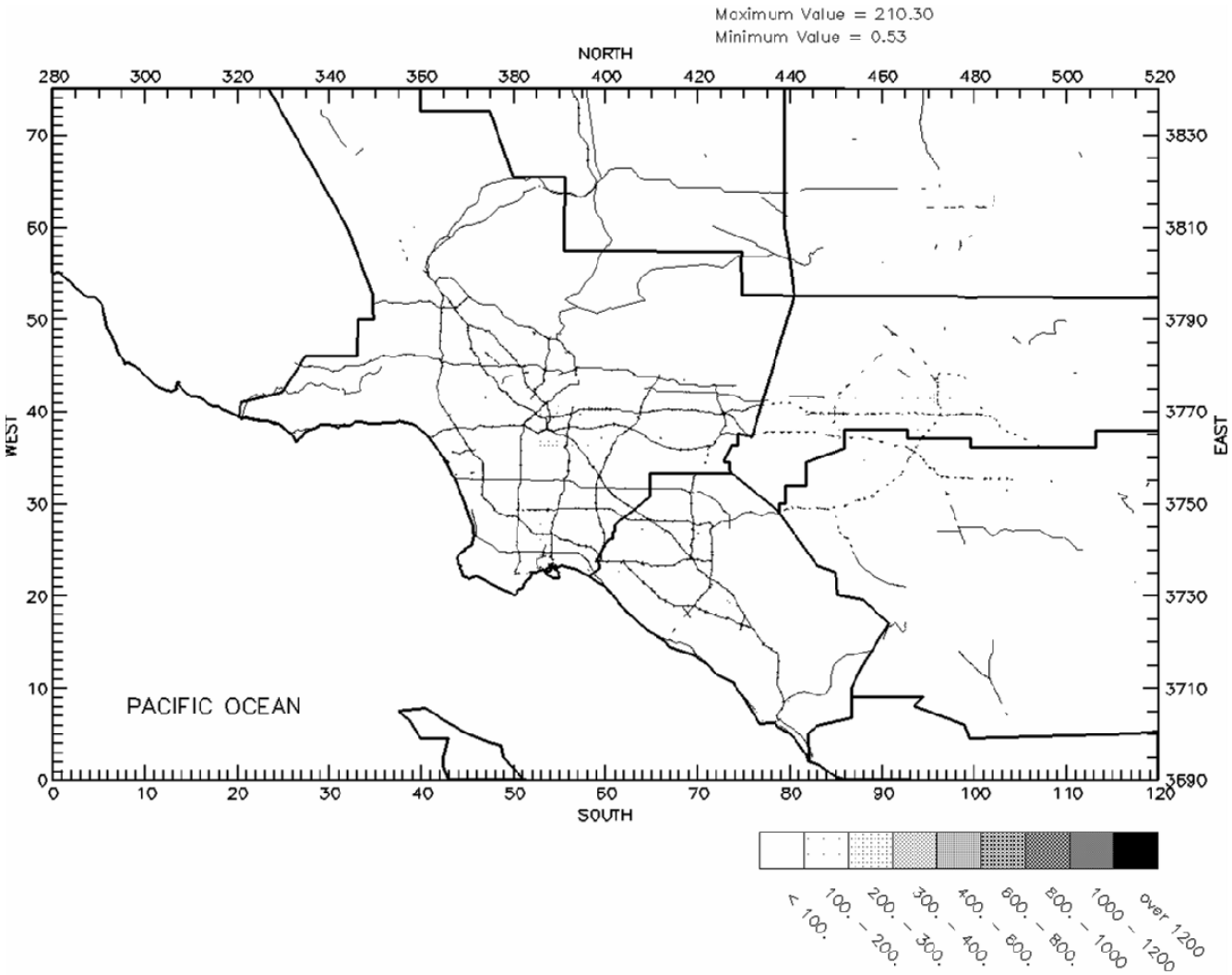

FIGURE IX-17e
MATES III Simulated Risk from Trains (Excluding Rail Yards).

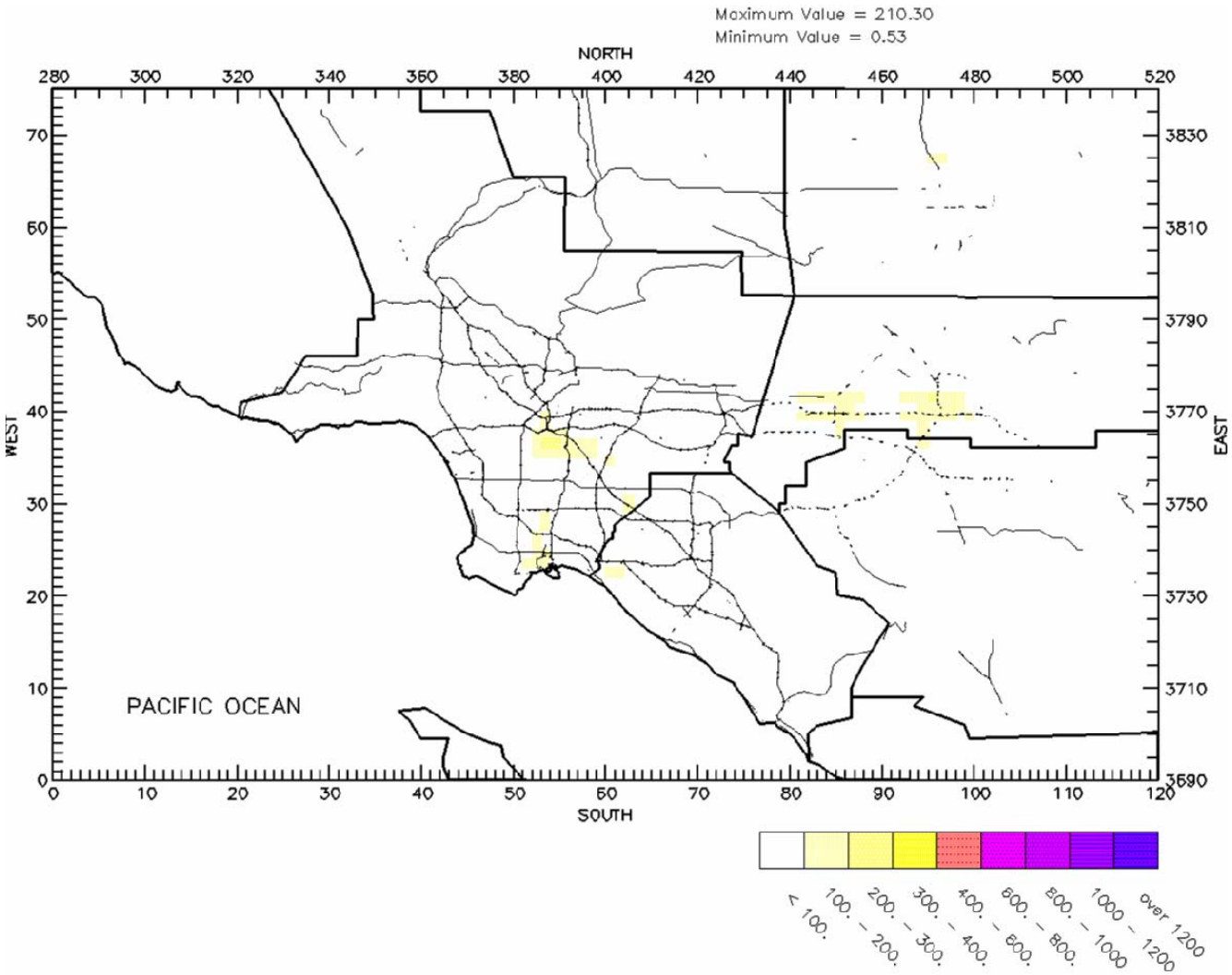

FIGURE IX-17e (Repeated)
MATES III Simulated Risk from Trains (Excluding Rail Yards).

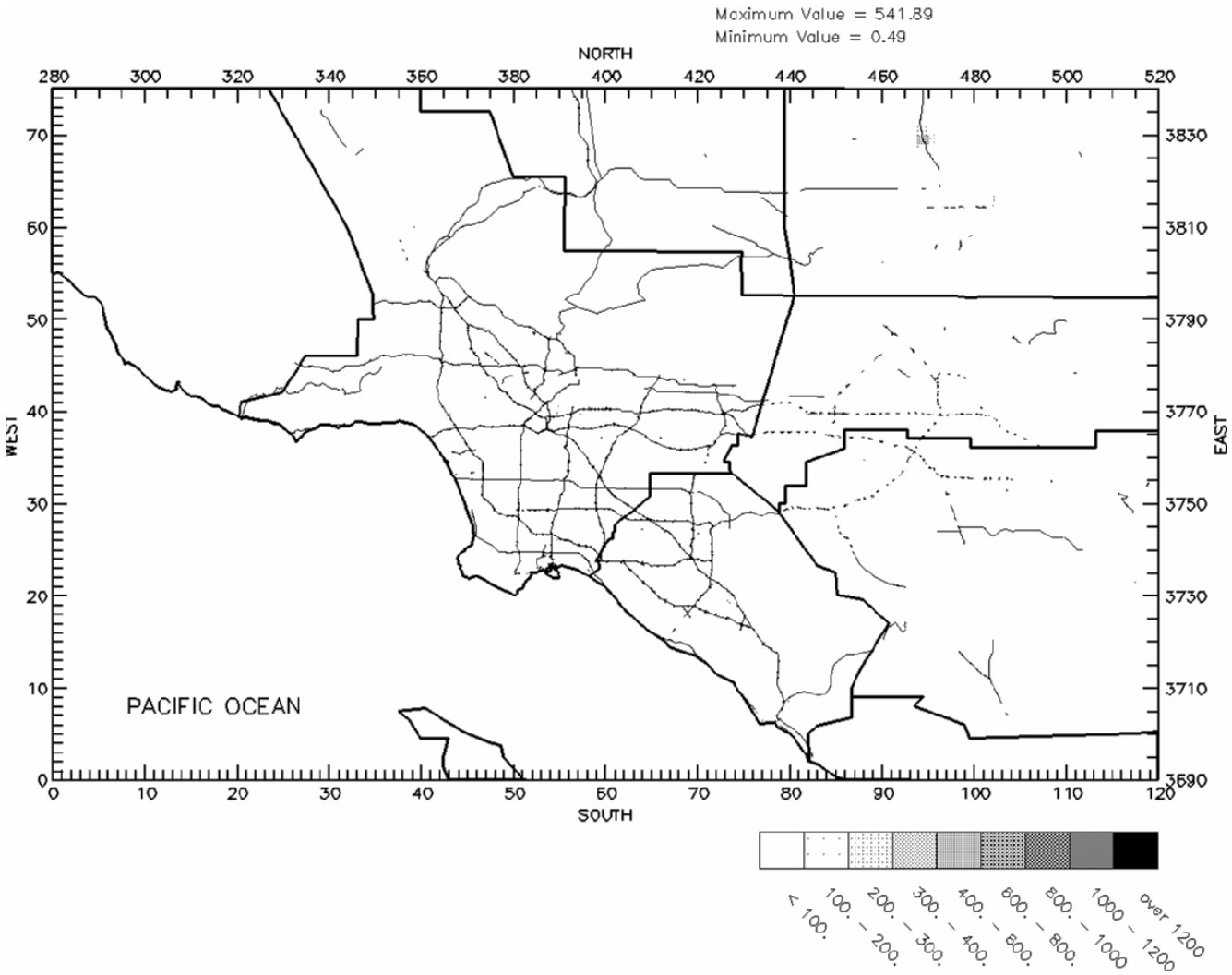

FIGURE IX-17f
MATES III Simulated Risk from Stationary Diesel.

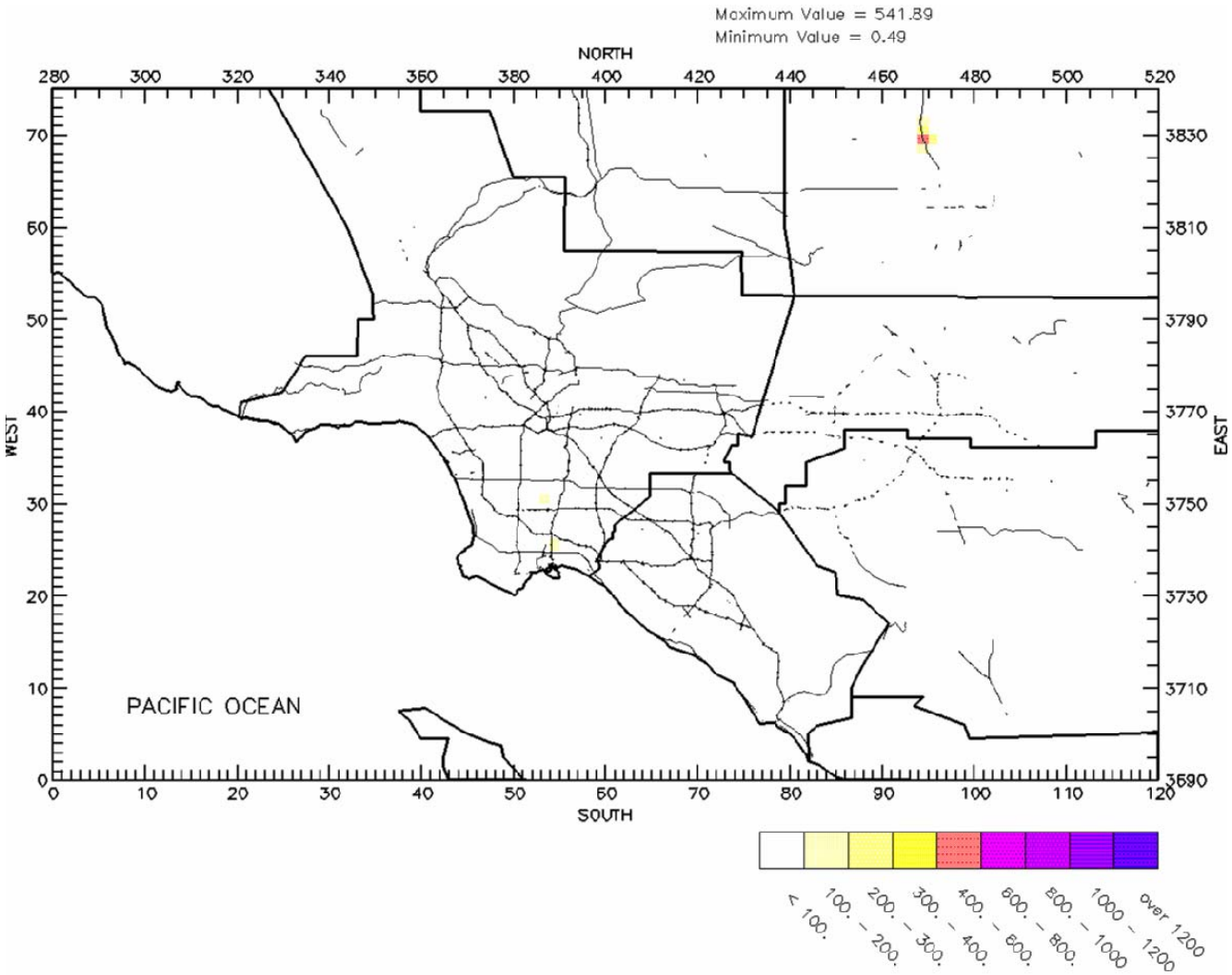

FIGURE IX-17f (Repeated)
MATES III Simulated Risk from Stationary Diesel.

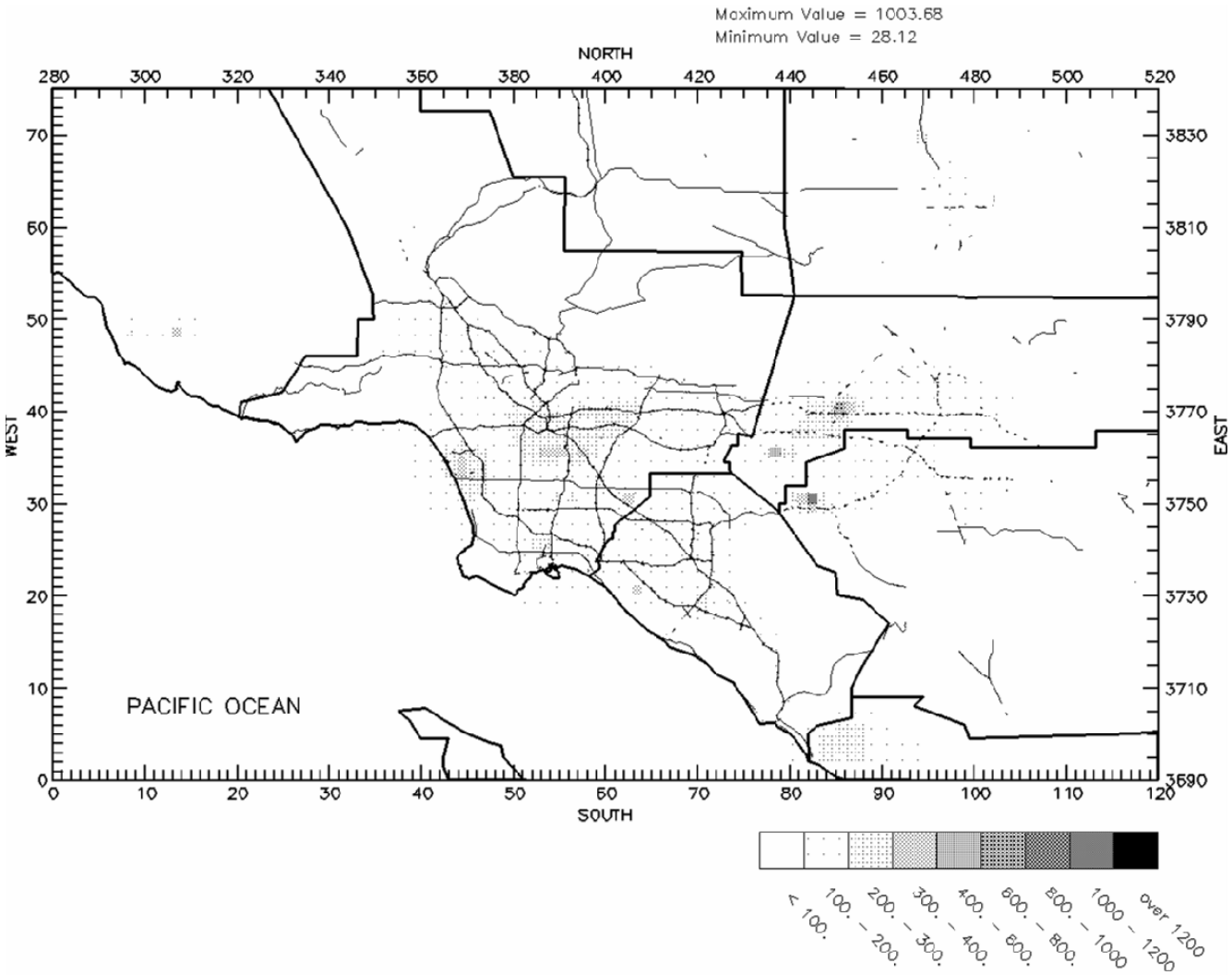

FIGURE IX-18
MATES III Simulated Risk No-Diesel.

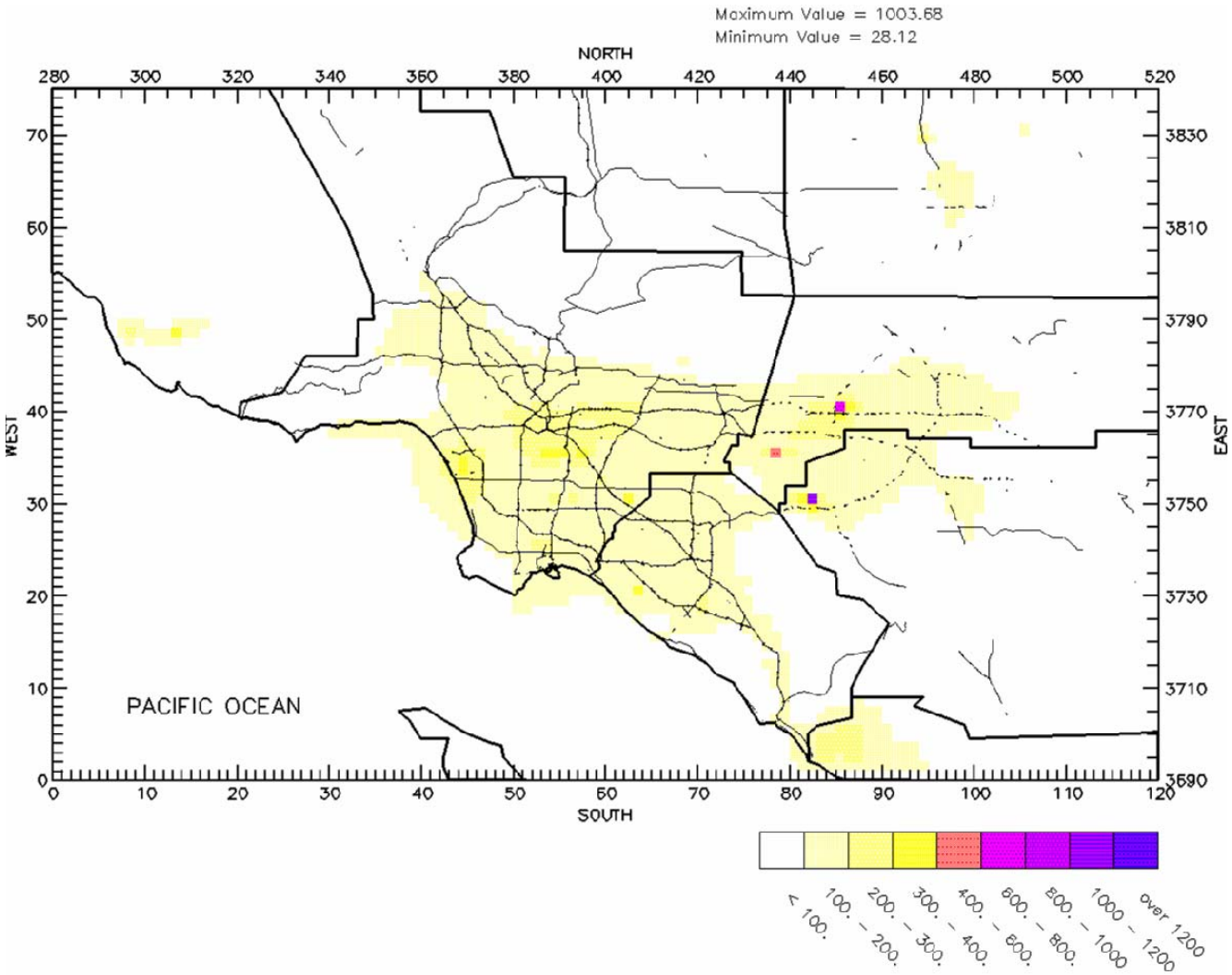

FIGURE IX-18 (Repeated)
MATES III Simulated Risk No-Diesel.

Figure IX-19 provides a focused 2005 estimated air toxics risk in the Ports area. Table IX-12 provides a summary risk estimated for the Basin, for the Ports area, and for the Basin excluding the Ports area. For this assessment, the Ports area includes the populated cells roughly bounded by the Interstate 405 to the north, San Pedro to the west, Balboa Harbor to the east and Pt. Fermin to the south. The 2005 average population weighted air toxics risk in the Ports area (as defined above) was 1,415 in one million. The Basin average population weighted air toxics risk, excluding the grid cells in the Ports area, valued 816 in one million. (It is important to note that the downwind impacts resulting from Port area activities are reflected in the air toxics risk estimates for the grid cells categorized as "Basin excluding Ports"). A similar calculation based on the CAMx RTRAC simulations for 1998-99 indicated that the Ports area air toxics risk was 1,208; and the Basin, minus the Ports area, was 912 in one million. Overall, the Ports area experienced an approximate 17% increase in risk, while the average population weighted risk in other areas of the Basin decreased by about 11%.

As a sensitivity analysis, simulations were generated to examine the hypothesis "what would the Basin toxics risk profile in 2005 be if no-growth occurred in the goods movement sector from 1998?" To attempt to answer this question, heavy-duty truck transport, shipping, port and rail operation activity levels associated with goods movement were held at 1998 levels. The impacts of fleet turnover and control measure implementation were allowed to go forward through 2005 to develop the hypothetical emissions inventory. The results of the sensitivity test indicated that the Ports area, Basin, and Basin excluding the Ports areas would experience lower air toxic risk levels by 6.2%, 14.8%, and 15.4% respectively.

Figures IX-20 through IX-23 provide close up depictions of air toxics risk to Central Los Angeles, Mira Loma/Colton, Central Orange County and West Los Angeles areas, respectively.

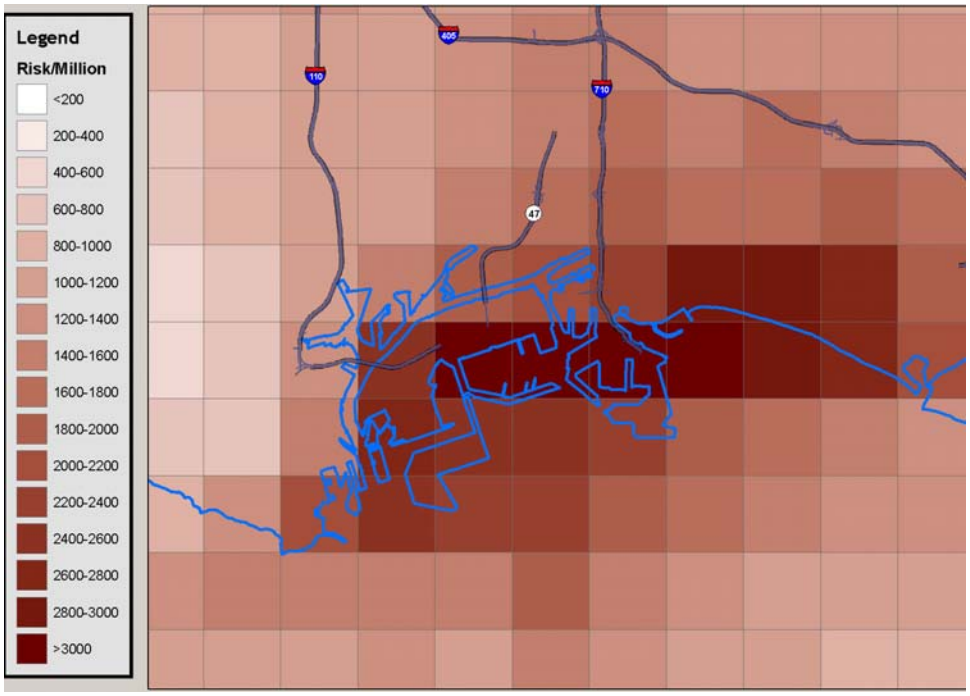

Figure IX-19
2005 Ports area MATES III Simulated Air Toxic Risk.

Table IX-12
Basin and Port Area Population Weighted Risk

Region	MATES III		MATES II*		Average Percentage Change in Risk
	2005 Population	Average Risk (Per Million)	1998 Population	Average Risk (Per Million)	
Basin	15,662,620	853	14,404,993	931	-8
Ports Area	959,761	1,415	911,834	1207	17
Basin Excluding Ports Area	14,702,859	816	13,493,159	912	-11

**** CAMx RTRAC Simulations***

County Risk Assessment

Table IX-13 provides the county breakdown of air toxics risk to the affected population for 2005 MATES III and the 1998-99 MATES II CAMx RTRAC simulations. As presented in the spatial distribution, Los Angeles County bears the greatest average risk at 951 per one million person population. Orange County has the second highest number of projected risk at 781 per one million person population. Risk in the Eastern Basin is lower. The estimated risk for San Bernardino is 712 per million, and Riverside was estimated to have the lowest population weighted risk at 485. It should be noted that these are county-wide averages and individual communities could have higher risks than the average if they are near emissions sources, such as rail yards or intermodal facilities.

Comparison of the county-wide population weighted air toxics risk shows that the greatest reduction occurred in Los Angeles County. Reductions in emissions from mobile sources including benzene, 1,3 butadiene, and diesel particulate have contributed to the improved county-wide risk. A similar profile is evident in Orange County. Despite across-the-board improvements in measured toxic air quality from MATES II (with the sole exception of hexavalent chromium at Rubidoux), population growth in the Eastern Basin and associated increases in mobile source emissions have resulted in a nominal increase in population-weighted risk for Riverside County. Similarly, San Bernardino County risk levels improved only marginally.

Table IX-13
County-Wide Population Weighted Air Toxic Risk

Region	MATES III		MATES II CAMx RTRAC Simulations		Average Percentage Change in Risk
	2005 Population	Average Risk (Per Million)	1998 Population	Average Risk (Per Million)	
Los Angeles	9,887,127	951	9,305,726	1,047	-9
Orange	2,764,620	781	2,579,794	833	-6
Riverside	1,548,031	485	1,249,554	478	2
San Bernardino	1,462,842	712	1,269,919	725	-2
SCAB	15,662,620	853	14,404,993	931	-8

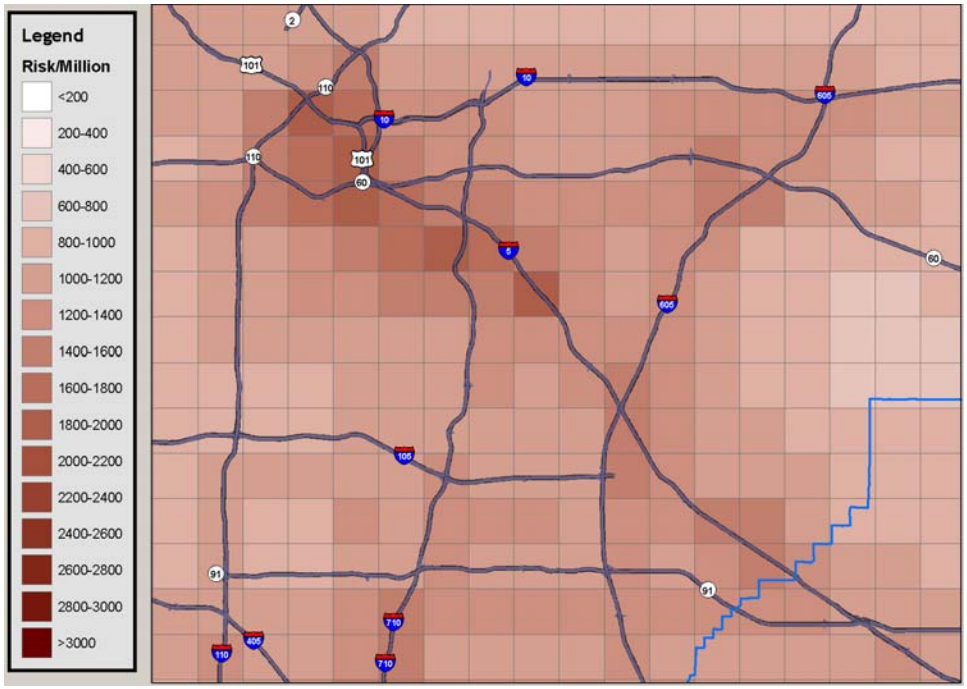

Figure IX-20
2005 Central Los Angeles MATES III Simulated Air Toxic Risk.

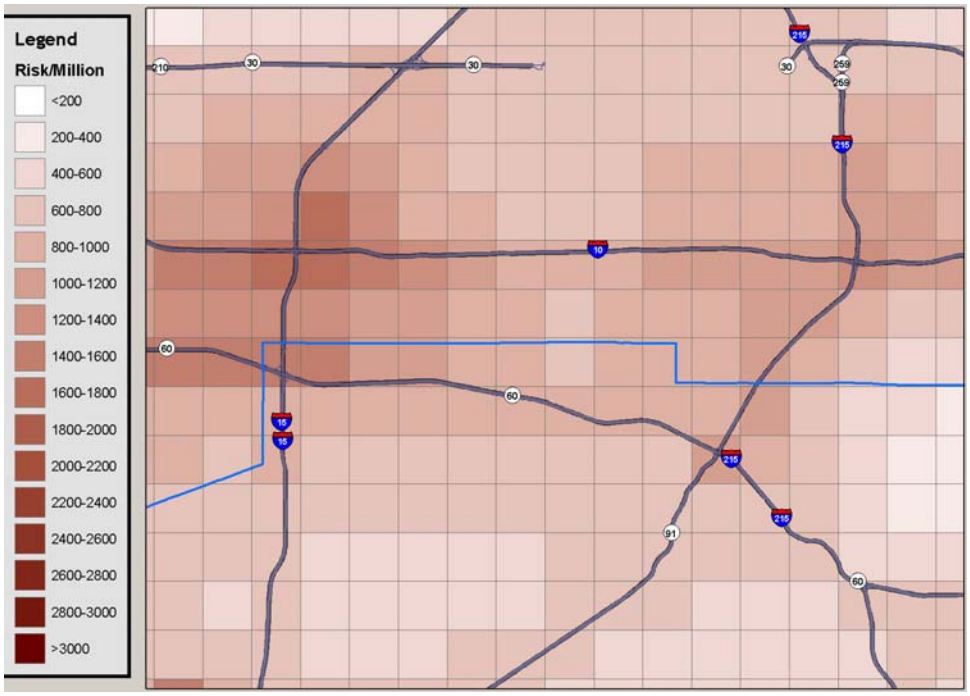

Figure IX-21
2005 Mira Loma/Colton MATES III Simulated Air Toxic Risk.

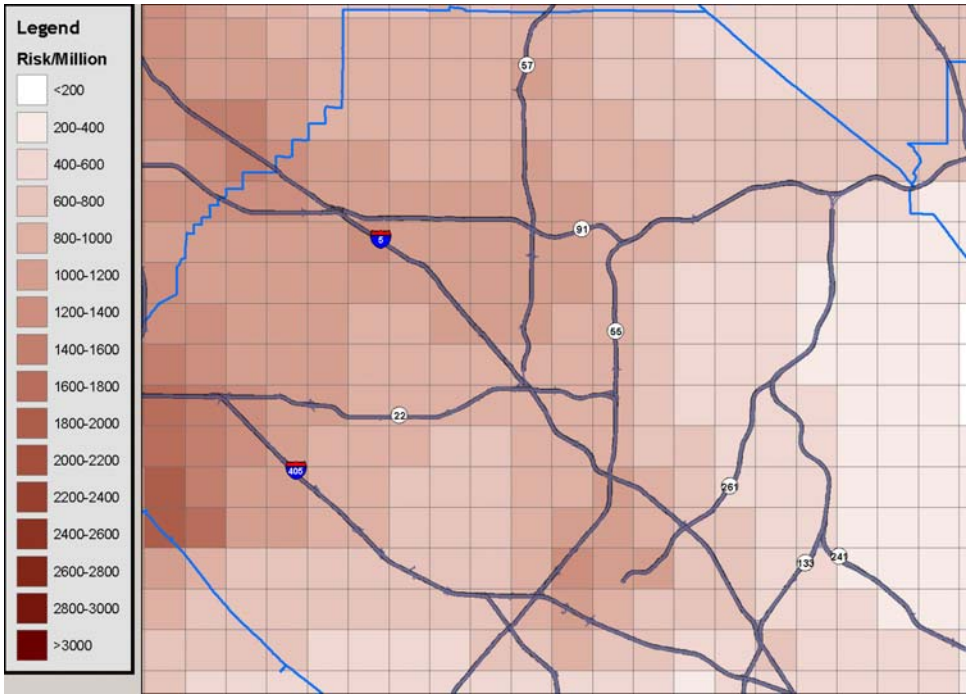

Figure IX-22
2005 Central Orange County MATES III Simulated Air Toxic Risk.

Figure IX-23
2005 West Los Angeles MATES III Simulated Air Toxic Risk.

Risk from Key Compounds

Table IX-14 provides the Basin average breakdown of risk associated with each of the key compounds simulated in the analysis. Diesel particulate ranked highest as the toxic compound contributing to the overall risk to the population. The next three highest contributors included benzene, 1,3 butadiene, and hexavalent chromium. Formaldehyde, acetaldehyde and arsenic each contribute approximately 1% of the risk while the remaining compounds combined accounted for less than 3% of the total.

Network Risk Evaluation

Table IX-15 provides the CAMx RTRAC simulated risk at each of the eight stations for the three main toxic compounds and the remaining aggregate based on the regional modeling. Risk is calculated using the predicted concentrations of each toxic component for the specific monitoring station location (based on a nine-cell weighted average concentration). The summary also provides the comparison between simulated average risk for the eight stations combined and the average risk calculated using the annual toxic compound measurements and the estimated diesel concentrations at those sites.

Table IX-14
2005 MATES III Risk from Simulated Individual Toxic Compounds

Compound	Risk Factor (μg/m^3)	Highest Grid Cell Concentration	Population Weighted Annual Average Concentration	Units	Population Weighted Risk (per million)	Percent Contribution
Diesel	3.00E-04	11.70	2.35	μg/m^3	703.76	82.5
Benzene	2.90E-05	1.15	0.48	ppb	44.53	5.2
1,3 Butadiene	1.70E-04	2.32	0.081	ppb	30.45	3.6
Hexavalent Chromium	1.50E-01	0.003	0.00016	μg/m^3	23.41	2.7
Primary Formaldehyde	6.00E-06	4.89	1.60	ppb	11.78	1.4
Secondary Formaldehyde	6.00E-06	1.60	1.30	ppb	9.61	1.1
Arsenic	3.30E-03	0.022	0.0024	μg/m^3	7.97	0.9
p-Dichlorobenzene	1.10E-05	0.208	0.076	ppb	5.01	0.6
Secondary Acetaldehyde	2.70E-06	0.766	0.67	ppb	3.25	0.4
Perchloroethylene	5.90E-06	0.370	0.92	ppb	3.67	0.4
Napthalene	3.40E-05	0.046	0.017	ppb	3.10	0.4
Cadmium	4.20E-03	0.009	0.00054	μg/m^3	2.28	0.2
Primary Acetaldehyde	2.70E-06	0.917	0.35	ppb	1.72	0.2
Methylene Chloride	1.00E-06	1.062	0.29	ppb	1.02	0.1
Nickel	2.60E-04	0.298	0.0035	μg/m^3	0.90	0.1
Trichloroethylene	2.00E-06	0.340	0.029	ppb	0.31	< 0.1
Lead	1.20E-05	0.104	0.0075	μg/m^3	0.09	<0.1

The highest simulated risk was estimated for West Long Beach followed by Los Angeles, North Long Beach and Compton. The lowest modeled risk was simulated at Burbank. As previously discussed, simulation performance at Burbank showed a tendency for underprediction, and this feature appears to be translated to the risk calculation.

The nondiesel portion of the simulated risk can be directly compared to risk calculated from the toxic compound measurements. Figure IX-24 presents a comparison of the model simulated and measurement estimated nondiesel risk at each monitoring site as well as the eight-station average. Simulated nondiesel risk is within 30% of measurements at all stations with the sole exception of Burbank. In general, there appears to be no geographical bias in model

performance and the simulated eight-station average risk is essentially equal to the risk estimated from the measurements.

Simulated total risk includes the contribution of diesel particulates; and, taken as an eight-station average, the modeled risk is 1,166 in a million. The eight-station average simulated risk is approximately 6% lower than the risk calculated from the measured toxic compound concentrations, and the estimates of diesel concentrations using the emissions based factor (1.95) applied to the $EC_{2.5}$ average concentration. When the model simulated risk is compared to the measurement calculated risk including the range of CMB estimated diesel concentrations, the eight-station average risk was nominally less than the lower projection of the range based on measurement data. The eight-station simulated risk based on the CAMx RTRAC analyses was approximately 10% lower than the average of the CMB estimated diesel risk based on the two source profiles.

Table IX-15
Comparison of Network Averaged CAMX RTRAC 2005 Modeled Risk to Measured Risk at the Eight MATES III Sites

Location	2005 MATES III CAMX RTRAC Simulation				
	Benzene	1,3 Butadiene	Others	Diesel	Total
Anaheim	47	31	75	900	1,054
Burbank	44	25	64	613	746
Compton	52	54	94	950	1,150
Inland Valley San Bernardino	41	25	121	734	922
North Long Beach	53	36	84	1,282	1,455
Central Los Angeles	64	47	115	1,256	1,482
Rubidoux	42	33	70	700	845
West Long Beach	55	30	86	1,501	1,672
Simulated 8-Station Average	50	35	89	992	1,166
8-Station MATES III Average Measured ($EC_{2.5}$ * 1.95 for Diesel)	53	34	83	1,070	1,240
8-Station Average Measured (with range of CMB Diesel risk)	53	34	83	1,004–1,120	1,174 – 1,290
8-Station Average Measured (average of CMB Diesel risk)	53	34	83	1,062	1,232

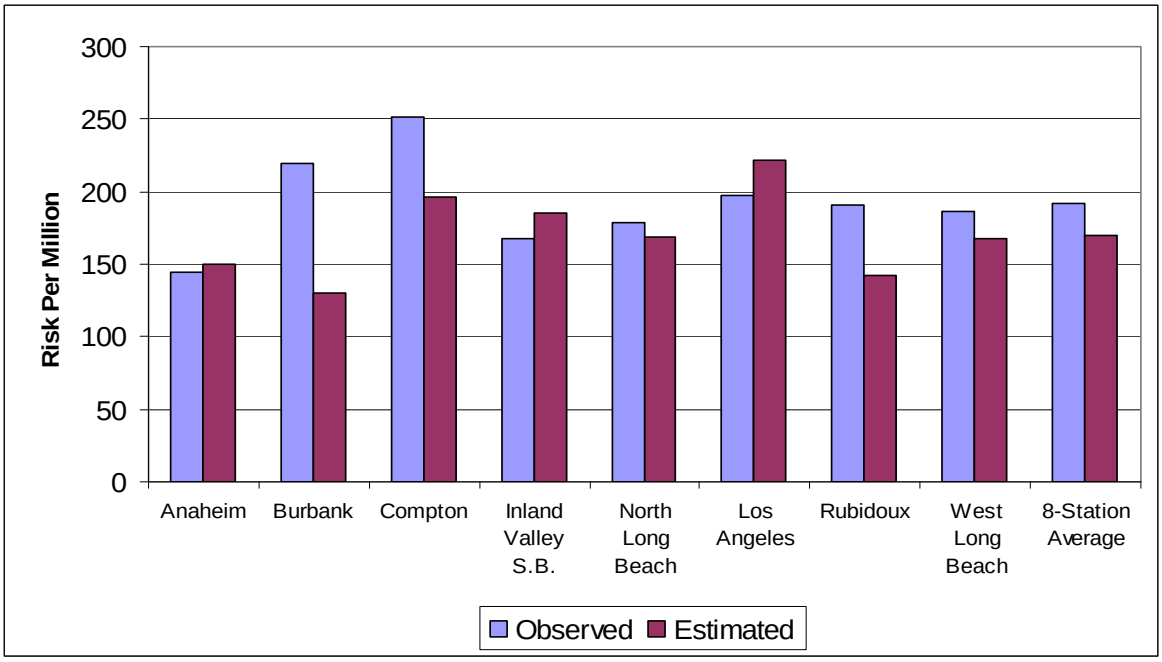

Figure IX-24
2005 MATES III Simulated Vs. Measured Compounds NonDiesel Air Toxics Risk.

Evaluation

The population weighted average Basin air toxic risk (853 per million) simulated using CAMx RTRAC for the 2005 MATES III period was estimated to be 8% lower than that estimated for 1998-99 (931 in a million) when the same modeling platforms and year-specific meteorology are evaluated. This is loosely compared to a 13% reduction in average population weighted risk estimated for the 1998-99 MATES II analysis (981 in a million) using the UAMTOX modeling platform. The areas of the Basin having maximum risk continued to be the Ports of Los Angeles and Long Beach with a secondary maximum occurring in an area starting in South Los Angeles and extending towards southeastern Los Angeles.

The average simulated Basin risk for the 2005 MATES III data is 8% lower than the comparable average risk estimated for the 1998 MATES II analysis. Using the 2007 AQMP inventory back-cast methodology, the percentage reduction in diesel mass emissions from 1998 to 2005 is approximately 5%. However, emissions reductions of benzene (36%), 1,3-butadiene (31%), arsenic (20%) and hexavalent chromium (85%) contribute greatly to the overall reduction in 2005 simulated risk. A general assessment of the observed meteorological profile suggests that the two monitoring periods were comparable in dispersion potential.

References

ENVIRON, Inc., 2008, CAMx User's Guide Version 4.5. ENVIRON. Novato, CA 94945

ENVIRON, Inc., 2005, "METSTAT software for MM5 version 3 (02/11/05)," ENVIRON. Novato, CA 94945, http://www.camx.com/down/support.php

ENVIRON, Inc., 2006, "KVPATCH software for CAMx," ENVIRON. Novato, CA 94945, http://www.camx.com/down/support.php

J.J. O'Brien, 1970, A note on the vertical structure of the eddy exchange coefficient in the planetary boundary layer. J. Atmos. Sci., 27, 1213-1215

PSU/NCAR Mesoscale Model (MM5) 2004, http://www.mmm.ucar.edu/mm5/mm5-home.html

WRAP, 2007, Western Regional Air Partnership, Technical Support System, Emissions Method, Offshore Emissions, http://vista.cira.colostate.edu/

U.S. EPA, 2006," Guidance on Use of Modeled and Other Analyses for Demonstrating Attainment of Air Quality Goals for Ozone, $PM_{2.5}$ and Regional Haze NAAQS," U.S. EPA, Office of Air Quality Planning and Standards, Emissions, Monitoring, and Analysis Division, Air Quality Modeling Group, Research Triangle Park, North Carolina, September, 2006